Republic of Iraq

Ministry of Higher Education and Scientific Research

University of Kerbala

College of Engineering

Civil Engineering Department

Behavior of Reinforced Green Concrete Piers of Bridge Using Different Types of Reinforcement

A thesis

Submitted to the Civil Engineering Department /College of Engineering /University of Kerbala in Partial Fulfillment of the Requirements for the Degree of Master of Science in Civil Engineering-Infrastructure

BY

Hajir Ahmad Salman

(BSc in Civil Engineering-2013)

Supervised by

Assist. Prof. Dr. Ali Hameed Naser

Dr. Wajde Shober Saheb Alyhya

2019 A.D 1440 A.H

وَاللَّهُ أَخْرَجَكُمْ مِنْ بُطُونِ أُمَّهَاتِكُمْ لا تَعْلَمُونَ شَيْئاً وَجَعَلَ لَكُمُ السَّمْعَ وَالْأَبْصَارَ وَالْأَفْئِدَةَ لَعَلَّكُمْ تَشْكُرُونَ

صدق الله العلي العظيم

(سورة النحل - الآية 78)

Acknowledgements

Firstly, my great thanks to ***ALLAH,*** *who gave me the power to finish my work.*

I would like to express my gratitude and thanks to my supervisors, ***Assist. Prof. Dr. Ali Hameed Naser*** *and* ***Dr. Wajde Shober Saheb*** *for their great assistance, guidance and valuable suggestions throughout the research period.*

A special thank and gratitude are due to my family, especially ***my husband****,* ***my father, my mother, my brothers, my sisters, and my uncle*** *for their care, patience and encouragement throughout the research period.*

Thanks are also due to the head and staff of the civil engineering department, the construction materials laboratory and all those who stood with me to finish this work.

Finally, I would like to express my extreme love and appreciation to everyone who has supported this work.

Hajir A. Alhussainy

Supervisor Certificate

We certify that this thesis entitled **"Behavior of Reinforced Green Concrete Piers of Bridge Using Different Types of Reinforcement"**, which is prepared by "Hajir Ahmed Salman", is under our supervision at University of Kerbala in partial fulfillment of the requirements for the degree of Master of Science in Civil Engineering (Infrastructure Engineering).

Signature:

Name: Asst. Prof. Dr. Ali Hameed Naser

(Supervisor)

Date: / / 2019

Signature:

Name: Dr. Wajde Shaker Saheb Alyh

(Supervisor)

Date: 24 / 6 / 2019

EXAMINATION COMMITTEE CERTIFICATION

We certify that we have read the thesis entitled "BEHAVIOR OF REINFORCED GREEN CONCRETE PIERS OF BRIDGE USING DIFFERENT TYPES OF REINFORCEMENT" and as an examining committee, we examined the student "Hajir Ahmad Salman" in its content and in what is connected with it, and that in our opinion it is adequate as a thesis for degree of Master of Science in Civil Engineering (Infrastructure Engineering).

Signature: .....

Name: Asst. Prof. Dr. Ali Hameed Naser

Date: 17 / 6 / 2019

(Supervisor)

Signature: .....

Name: Dr. Wajde Shober Saheb Alyhya

Date: 18 / 6 / 2019

(Supervisor)

Signature: .....

Name: Assist. Prof. Dr. Haitham Ali Bady

Date: 17 / 6 / 2019

(Member)

Signature: .....

Name: Assist. Prof. Dr. Hussam Ali Mohammed

Date: 18 / 6 / 2019

(Member)

Signature: .....

Name: Asst.Prof Dr. Laith Shakir Rasheed

Date: 11 / 6 / 2019

(Chairman)

University Of Kerbala
Dean Office
College Of Engineering

Approval of Department of Civil Engineering

Signature: .....

Name: Prof. Dr. Waqed H. Hassan

(Head of Dept. of Civil Engineering

Date: 18 / 6 / 2019

Approval of Deanery of the College of Engineering -University of Kerbala

Signature: .....

Name: Prof. Dr. Basim Khlail Nile

(Dean of the College of Engineering)

Date: 25 / 6 / 2019

Abstract

Rapid industrial development causes serious problems all over the world such as the depletion of natural aggregates and creates an enormous amount of waste material from construction and demolition activities. One of the ways to reduce this problem is to utilize recycled concrete aggregate (RCA) in the production of concrete. The present study involves an experimental work and numerical application for the behavior of reinforced concrete piers using recycled aggregate concrete as green concrete. The experimental work included a test of thirteen reinforced concrete piers with different types of mix and reinforcement. Each pier has the same dimensions of (200 mm width, 400 mm height, and 600 mm total length) with column dimensions of 200×300 mm and 200 mm for depth. The experimental parameters were: concrete mix types, using recycled aggregate as green concrete (GC) at 50% replacement ratio instead of normal concrete (NC), recycled steel fiber with 2% volumetric ratio to be added to the GC mix in different areas of the pier and using of green high strength in different areas of the pier. The study involves using carbon fiber reinforced polymer (CFRP) bars and glass fiber reinforced polymer (GFRP) bars for reinforcing pier cap and the top two layers of pier cap. The load was applied to each pier by two points of loading, and the deflection was measured under the load and the average value was taken.

The results showed that using green concrete with 50% replacement ratio decreases the ultimate load by 2.41% and increases deflection by 18.5 %. The ultimate carrying capacity of GC pier has been increased when adding recycled steel fiber to the green concrete mix as it led to an

increase in the ultimate load at rate reach to 8.95% than the ultimate load of GC. It was also found that using green high strength concrete mix has improved the ultimate load at rate reach to 36.76% than GC pier specimen. Furthermore, changing the reinforcement type with CFRP has a positive influence on pier characteristics as it led to an increase in the ultimate load at rate reach to 6.86 as compared with GC pier. Using of GFRP bar led to a decrease in the ultimate load to 6.96% as compared with GC pier specimen. Moreover, the use of GFRP as stirrups for pier cap has led to an increase in the ultimate load by 0.95.

Three-dimensional finite element analysis by ANSYS program (version 17.2) was used to investigate the behaviour of reinforced concrete piers. Fully bonding was assumed between concrete and steel reinforcement. Concrete was represented by SOLID65, and the reinforcement by LINK180, while the steel plates of loading and supports were represented by SOLID185. The results of the numerical application showed an acceptable degree of variation with the experimental results.

List of Contents

List of Figures

List of Plates

List of Tables

Notation

Symbol	Description
E	Modulus of Elasticity (GPa)
f_c'	Cylinder compressive strength of concrete (MPa)
f_r	Flexural strength of concrete (modulus of rupture) (MPa)
f_{ct}	Indirect tensile strength (splitting tensile strength) (MPa)
Fy	Yield stress of steel (MPa)
P_{cr}	Cracking load (kN)
Pu	Ultimate load (kN)
W/C	Water /Cement Ratio
Ø	Bar Size (mm)
Є	Strain (mm/mm)

Abbreviation

Symbol	Description
ACI	American Concrete Institute
ANSYS	Analysis System Program
ASTM	American Society for Testing and Materials
AASHTO	American Association of State Highway and Transportation Officials
CFRP	Carbon Fiber Reinforcement Polymer
Exp.	Experimental
GFRP	Glass Fiber Reinforcement Polymer
IQS	Iraqi Specification
MPa	Mega Pascal (N/mm^2)
RAC	Recycled Aggregate Concrete

Chapter One

Chapter One
Introduction

1.1 General

Pier of the bridge is usually used as a general term for any type of substructure located between horizontal spans and foundations. Pier gives vertical supports for spans at intermediate points and performs two main functions. These functions are transferring superstructure vertical loads to the foundations and resisting horizontal forces acting on the bridge. There are many pier types that are used in bridge construction. The simplest may be pile bent piers where a reinforced concrete cap is placed on piling. The other pier type is a cap and column pier in which the column supports on individual footings that support a common cap. There are some factors could be affected on the spacing of columns such as the type of superstructure, the superstructure beam spacing, and the size of the columns **(AASHTO, 2007)**.

1.2 Types of Piers

The most usually used highway bridge piers are those made from reinforced concrete. There are several ways of defining pier types. One is by its structural connectivity to the superstructure (monolithic or cantilevered). Another is by its sectional shape: solid or hollow; round, octagonal, hexagonal, or rectangular. Pier can be also distinguished by its framing configuration: single or multiple column bents; hammerhead or pier wall **(Chen *et al.*,, 2000)**.

1.2.1 Single-Column Piers

ingle-column piers are often found in urban areas where space limitation is a concern. It can increase the clearance under the bridge, .single piers can be rectangular, circular, oval-shaped, form for round end, cutting-

edge-shaped, according to the cross-sectional shapes**.(LI Juan et al.,2013)**. It is also called as solid shaft piers. It have a single solid concrete cross section that support the cap. In this pier, it is seen that the major axis of the pier and the direction of steam flow is approximately same. It is recommended to use circular or small rectangular cross section when the flow is not in the same direction as the major axis. Spread footings are generally used for this type of piers. plate(1.1)show this type of piers.

Plate 1. 1Single-Column Piers (Fu, 2013)

1.2.2 Multi-Column Piers

Multi-column piers or bents are often selected when space is available. A minimum of three columns should be provided to ensure redundancy when a vehicular collision occurs. Multi-column piers are also used for stream crossings. They are suitable where a long pier is required to provide support for a wide bridge or for a bridge with a severe skew angle. Two- or three-column systems may be the most popular piers as shown in Plate (1.2).

The columns also may have different cross-sections. Multi-column piers are apparently more stable in comparison with single-column piers. When there are three or more columns, there is a significant amount of redundancy built into the system. For example, if one of the columns is damaged, the system may still be stable and failure would not occur, which will allow for replacement or repair **(Fu, 2013)**.

Plate 1. 2 Multi-Column Piers (Fu, 2013)

1.2.3 Wall Piers

A wall pier is used for most stream crossings to avoid collecting of debris and floating ices between columns. A wall type pier consisting of a single row of piles, especially H-piles, encased with concrete to form a wall provides more resistance to ice and debris and allows debris to pass through as shown in plate (1.3) ***(Francisco, 2015)***.

Plate 1. 3 Wall Piers (Francisco, 2015)

1.3 Design of Piers

Piers should be designed to fulfill the strength and serviceability requirements in a similar way of designing other structural components. They should be able to withstand overturning and sliding forces applied from superstructure as well as the forces applied to substructures. Indeed, the piers need to be able to prevent the collapse of the structure during extreme events, which may be accompanied by some damage. A pier, as a structural component, is subjected to combined forces of axial, bending, and shear. For a pier, the bending strength is dependent upon the axial force. In the plastic hinge zone of a pier, the shear strength is also influenced by bending superstructure if the constraint is provided by the pier to the superstructure **(Chen et al., 2000)**.

Design of piers should be carried out with at least the loads below according to the AASHTO design specifications as shown in Figure 1.1:

1. Self-weight load of the pier

2. Loads applied from bridge superstructure and transmitted to the pier

3. Earth load on the pier

4. Earthquake loads as a result of ground motion.

5. Wind load.

6. Impact load

In general, the design needs to be investigated for the load combination producing the most severe condition to the structure.

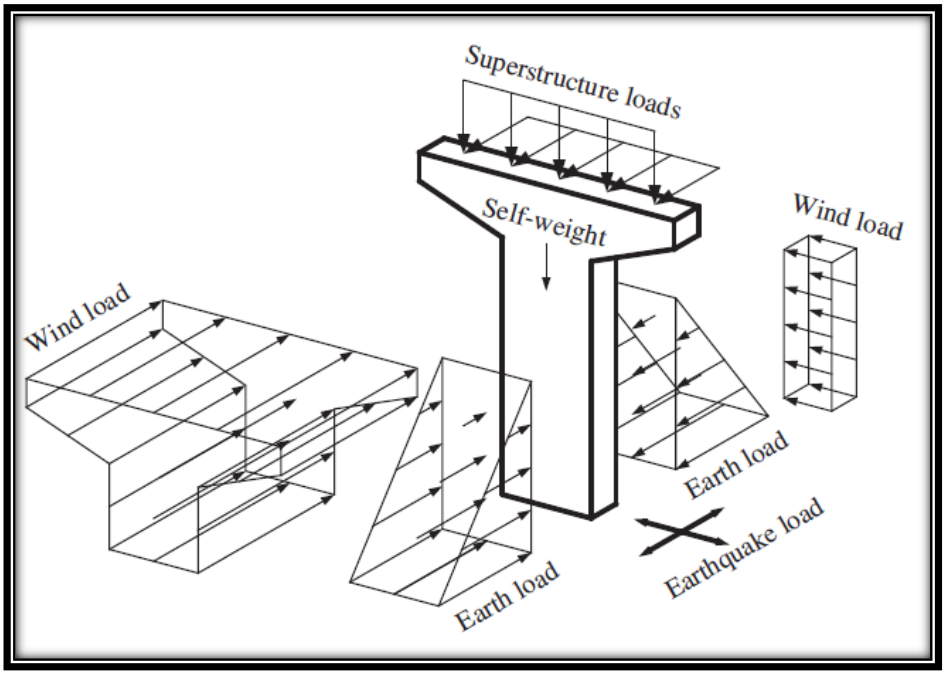

Figure 1. 1 Various Loads on a Pier ***(Fu, 2013)***

There are three design methods for the pier cap:

1. AASHTO (1992) Corbel Provisions

2. ACI 318-89 Deep Beam Provisions

3. Strut-and-Tie Method

The corbel and deep beam provisions are very conservative in predicting the capacity of the pier cap because they only consider concrete capacity in shear. However, these two methods underestimate the pier strength by

a factor of 3 to 4. The strut-and-tie method is much more accurate than conventional design methods **(Denio et al., 1995)**.

1.4 Green Concrete

Green concrete is defined as a concrete which uses waste material as at least one of its components, or its production process does not lead to environmental destruction **(Obla. K.H,2009)**. It should also have high performance and life cycle sustainability. In other words, green concrete is an environment friendly concrete. Green concrete improves the three pillars of sustainability: environmental, economic, and social impacts. The key factors that are used to identify whether the concrete is green are : amount of portland cement replacement materials, manufacturing process and methods, performance and life cycle sustainability impacts. Green concrete should follow reduce, reuse and recycle technique or any two process in the concrete technology. The three major objective behind green concept in concrete is to reduce green house gas emission (carbon dioxide emission from cement industry); to reduce the use of natural resources such as limestone, shale, clay, natural river sand, natural rocks that are being consume for the development of human mankind that are not given back to the earth; and the use of waste materials in concrete that results in the air, land and water pollution. This objective behind green concrete will result in the sustainable development without destruction natural resources **(Bambang,2014)**

1.5 Recycled Aggregate Concrete

Concrete has been proved to be a leading construction material for more than a century. Previously, almost all materials used in the construction industry were entirely natural and all waste from demolished buildings was disposed to landfills and partially in unauthorized places. Rapid industrial development caused serious problems all over the world such

as the scarcity of natural aggregates resources and the depletion of the existing landfills. One of the ways to reduce this problem is to encourage the use of construction and demolition waste as a source of aggregates in the production of new recycled aggregate (RA) **(Yong and Teo, 2009)**. The utilization of recycled aggregate created from processing construction and demolition waste in new construction has become more important over the last two decades. Several factors contributing to this utilization such as the availability of new material, the damage caused by natural aggregate (NA) quarrying and the increased disposal costs of waste materials. The advances in the manufacturing of crushing machinery and recycling processes made it easier to scale or crush down large masses of construction and demolition waste into smaller particles to produce recycled aggregate at an acceptable cost **(Abukersh, 2009)**. The effects of using recycled aggregate as a partial or total replacement of normal aggregate in concrete were well understood and extensively documented **(Mirza and Brant, 2009)**.

1.6 steel fiber

Steel fiber is a metal reinforcement. Steel fiber for reinforcing concrete is defined as short, discrete lengths of steel fibers with an aspect ratio (ratio of length to diameter) from about 20 to 100, with different cross-sections, and that are sufficiently small to be randomly dispersed in an unhardened concrete mixture using the usual mixing procedures. A certain amount of steel fiber in concrete can cause qualitative changes in concrete's physical property, greatly increasing resistance to cracking, impact, fatigue, and bending, tenacity, durability, and other properties. Basically, steel fiber can be categorized into five groups, depending on the manufacturing process and its shape and/or section: cold drawn wire,

cut sheet, melt-extracted, mill cut, and modified cold-drawn wire(Wen SH,2003)

1.7 Fiber Reinforcement Polymer (FRP)

Fiber reinforcement polymer (FRP) composites were composed of fibers and polymer resin. The fibers are the main load-carrying element that has high strength and the polymer resin is used to tie up those fibers. FRP composites were often manufactured in several forms such as plates, laminates, or bars. Typically, it is used to strengthen structural members or rehabilitate their deteriorations. There are different types of fibers that are used in FRP composites such as; carbon, aramid, and glass. The mechanical properties and chemical compositions of these fibers types were different. A comparison among several types of FRP composites with steel reinforcement bars and steel tendons in term of stress-strain relationships are schematically presented in Figure 1.2 **(Carolin, 2003)**.

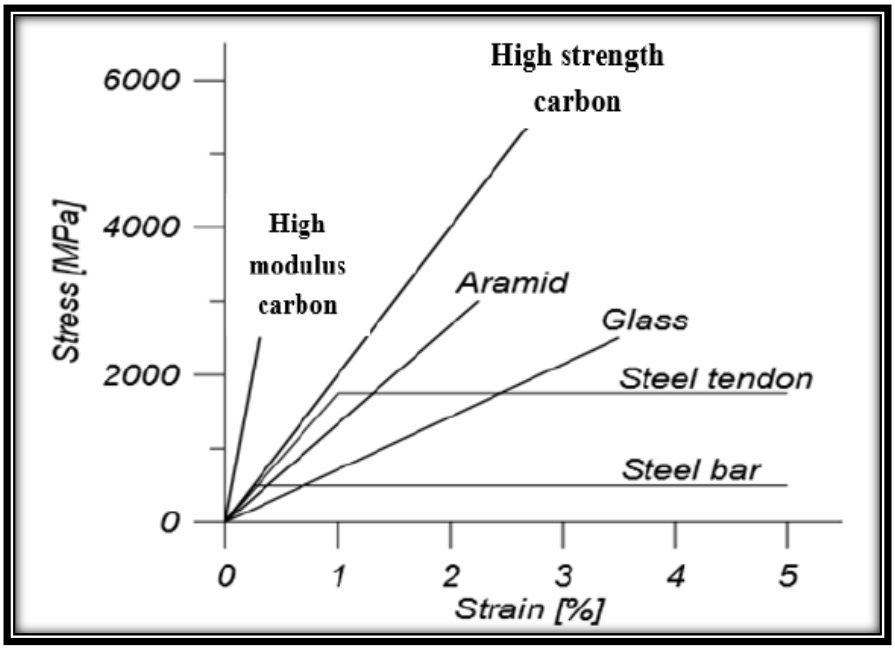

Figure 1. 2 Stress-Strain Relationships for Several FRP Composites and Steel Reinforcement Bars and Tendons ***(Carolin, 2003)***

1.8 Aim of the Study

The main aim of this study is to investigate the structural behavior of piers produced from green concrete mixes reinforced with different types of reinforcement. The objectives could be summarized in the following points:

1. Studying the behavior of the piers under a point load on their cantilever parts using recycled aggregate, at a specific replacement level, with various types of reinforcement.
2. Determining the use of recycled aggregate as a construction material in structural members.
3. Studying the effect of recycled steel fiber at different parts of pier.
4. Comparing the predicted responses of the piers using the non-linear finite element program "ANSYS" with the measured responses from the experimental tests.

1.9 Layout of the Thesis

The current thesis was presented through six chapters, as follows: **Chapter one** presents the fundamental information and general introduction regarding bridge pier, green concrete, recycled aggregate, steel fiber, and fiber reinforced polymer. **Chapter two** reviewed a background on the applications and the documents that are related to piers. Indeed, the literature review for the research and experimental studies about green concrete were also given. While the materials used in the present study and the test results of these materials, details of concrete mixing and casting procedures used for concrete piers were displayed in **Chapter three. Chapter four** devoted to the experimental results of the study such as the effect of various parameters that have been investigated on the ultimate load and deflection of the

studied piers as well as the discussion concerning the effect of these parameters. **Chapter five** revealed the numerical result using three-dimensional finite element analysis (ANSYS computer program version 17.2) as well as a comparison with the experimental results. Finally, **Chapter six** summarizes the overall findings and the main conclusions of the research program. Recommendations for future studies are also presented.

Chapter Two

Chapter Two
Literature Review

2.1 Introduction

Bridges are essential part of a road network which not only provide free flow conditions for travelling of vehicles but also connect areas separated by water, human and /or geological obstructions. These characteristics make bridges the most sensitive element of a transportation network **(Elnashai et al., 2004)**. It generally consists of two parts. The first part, which is known as superstructure includes bearings, girders or beams, reinforced concrete deck, joints, pavement layers, security barriers, and drainage system. The second part, which is called substructure includes foundations, abutments, piers, and piers caps **(Naser and Zonglin, 2011)**.

Piers are the vertical loadbearing member such as an intermediate support for adjacent ends of two bridge spans. In foundations for large buildings, piers are usually cylindrical concrete shafts, cast in prepared holes, while in bridges they take the form of caissons, which are sunk into position. Piers serve the same purpose as piles but are not installed by hammers and, if based on a stable substrate, will support a greater load than a pile **(J. Moon et al.,2016)**.In the United States, nearly two-thirds of all the existed bridges are over 20 feet (6 m) long and are constructed from concrete. Many of these are ageing and deteriorating, and 18% are currently structurally deficient or functionally obsolete. These bridges may have fatigue, deterioration or corrosion problems due to capacity problems resulting from the increase in loading, clearance or geometry problems owing to a change in standards or use **(Milde *et al.*, 2005)**. Replacement is usually not an option due to economic reasons, and recent available advances in strengthening techniques that have made repairing

very attractive. Fiber reinforced polymers (FRP) have emerged in recent years as a popular method for strengthening or retrofitting reinforced concrete structures**(Milde *et al.*, 2005)**. FRP materials are thus increasingly being used to enhance or restore the load-carrying capacity, ductility, and seismic resistance of a wide range of structures **(M. N. S. Hadi 2007)**.The use of fiber-reinforced polymer (FRP) to retrofit and strengthen existing deteriorating concrete or masonry structures is attractive as these light weight materials improve tensile strength, durability, and flexibility, are easy to handle, and incur low installation and maintenance costs (Balsamo et al., 2012).

2.2 Experimental Studies on Pier Cap

A survey of the literature review was carried out to identify previous studies with experimental results pertinent to the current investigation. Despite the lack of highly relevant data, several studies have specifically performed to determine the strength of pier caps. A brief description of the specimens testing, results, and conclusions of each of these studies were provided below. These results were used to create the experimental database used in this investigation. In addition, the recommendations of these studies were also included. The first noted experimental study on pier was performed by Ferguson (1964) at the University of Texas. The study included testing experimentally thirty-six in. deep pier cap overhang specimens. Variables associated with the specimens included shear span, bar anchorage length, the grade of steel reinforcement, amount of flexural reinforcement, amount of shear reinforcement, the presence of horizontal skin steel, and cap width. All specimens were tested to failure in which the failure load and type of failure was reported for all specimens. Only qualitative data was provided on the appearance of cracks. One key finding of the study was that vertical stirrups placed at

standard spacing had little to no effect on the shear capacity of the overhangs. This is because the cracks in the overhang were at very steep angles and did not cross many stirrups. Ferguson also suggested that placing horizontal skin steel in the pier caps could alleviate this problem. The horizontal bars would cross the cracks in more places providing greater shear strength along with reducing crack widths. Furthermore, the study has determined that the bond failure would not occur if at least nine inches of reinforcing bar extended past the location of the applied load in the overhang. Indeed, it has been concluded that the crack widths were larger in caps designed using grade sixty reinforcing bars than in caps using intermediate grade reinforcement. Ferguson recommended that a service stress limit of 165-180 MPa in the tensile flexural reinforcement be used to control crack widths **(Ferguson, 1964)**. (Sami 1990) carried out an experimental investigation, which involves testing six reinforced concrete pier caps. Parameters that were varied in these specimens included: the geometry of the pier caps, the amount and distribution of uniformly distributed reinforcement, and the anchorage details of this reinforcement. The following conclusions and recommendations were made: After yielding the main tension reinforcement, yielding was spread to the distributed reinforcement. The uniformly distributed reinforcement contributed significantly to the strength and played a key role in controlling cracks. The uniformly distributed horizontal reinforcement may be provided in the form of U shaped stirrups and properly lap spliced over the central region of the pier cap. The uniformly distributed vertical reinforcement may be provided in the form of closed stirrups or lap-spliced U-shaped stirrups. The column reinforcement, which was extended into the pier cap, provided additional horizontal (column ties) and vertical reinforcement in the central region of the pier cap. This

additional reinforcement controlled cracks and provided some confinement for the lap splices of the uniformly distributed horizontal reinforcement **(Sami, 1990)**.

Young et al., (2004) carried out an experimental study involved sixteen pier cap specimens. All specimens were thirty-six in. deep, thirty-three in. wide and had a shear span of fifty-four in. The study investigated reinforcing details to reduce the widths of flexure and flexure-shear cracks in the specimens at loads similar to bridge service loads. Design alterations considered varying the amount and spacing of tensile steel, the amount and spacing of horizontal skin steel, and the amount of transverse steel. The specimens were instrumented with strain gages on the longitudinal and transverse reinforcement. Each specimen was loaded in 180 kN increments with crack widths and propagation measured at every increment until the specimen failed. All specimens failed in shear. The reported results provided a very detailed description of the crack propagation in the pier cap overhang specimens. The study also found that the first flexural cracks appeared in the caps with stresses of 28-48 MPa in the flexural tensile reinforcing steel. The horizontal distribution of this steel, within reasonable limits, was found to have a little effect on crack widths. Contrary to the findings of Ferguson, the study has determined that increasing the amount of transverse steel was effective in reducing the widths of flexure-shear cracks. The study recommended that pier cap overhangs should be designed using the center of the column as the critical section instead of the column face. This will cause the pier cap to be overdesigned at the face of the column and accordingly reduce the stress levels in the steel at service loads. To limit the widths of flexure-shear cracks, the study suggested designing pier cap overhangs to have sufficient shear strength to develop flexural over strength at the column

face as well as meet the shear demand **(Gonzalez and Moo-Young, 2004)**.

2.3 Recycled Concrete Aggregate (Green Concrete)

Recycled aggregate is derived from crushing construction and demolition waste. It may be classified as a recycled concrete aggregate (RCA) when consisting primarily of crushed concrete or more general recycled aggregate (RA) or it contains substantial quantities of materials other than crushed concrete **(Standard, 2006)**. From construction and demolition waste management in Malaysia, old concrete and aggregate materials constitute more than 65% of the site construction waste. Approximately, around 73% of these materials were recycled as shown in Fig. (2.3) (Nitivattananon and Borongan, 2007).

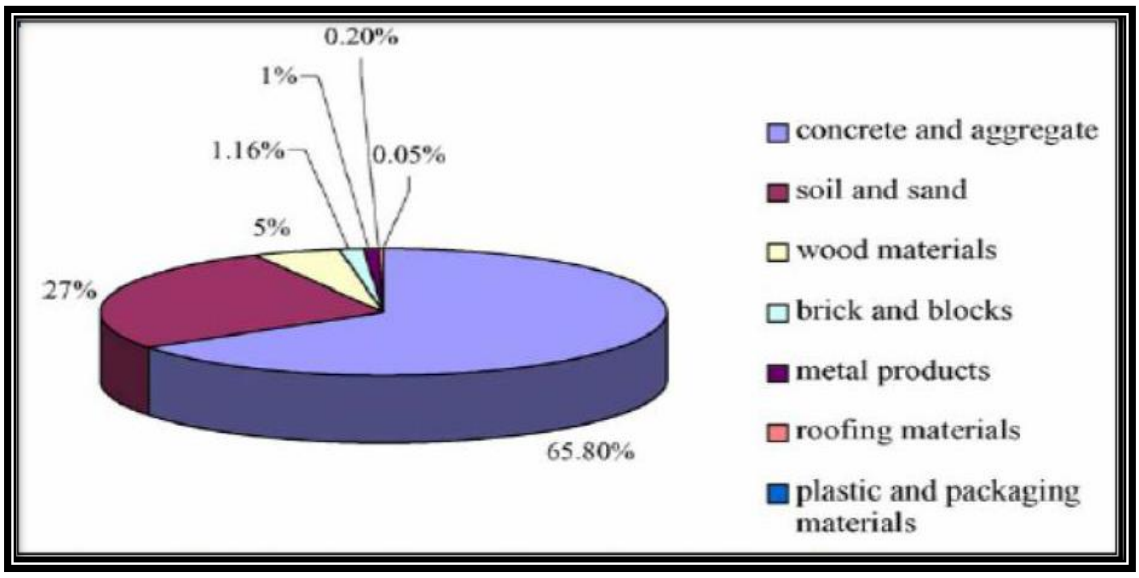

Figure 2. 1 Composition of Generated Construction Waste Materials (Nitivattananon & Borongan, 2007)

Recycled aggregates obtained from the construction and demolition waste has currently received increasing attention, due to its potential to be used in environmentally friendly concrete structures. Furthermore, the deficiency of natural aggregates, shortage of dumping sites, increase in transport cost and environmental pollution lead to the use of recycled

aggregate as a substitute material in the production of concrete in many countries **(Rao *et al.*, 2010)**.

2.4 Historical Background of Recycled Concrete Aggregate

The idea of using waste concrete as recycled concrete aggregate in the construction industry is not new. Attempts to utilize concrete demolition wastes as a recycled aggregate for producing new concrete were made when an urgent rebuilding need was faced in Europe after world war II. There was a massive job of recycling waste material, especially building rubble, into new concrete construction with generally good success. As soon as the need for this action was satisfied, such recycling was generally abandoned **(Buck, 1977)**.

The construction industry worldwide is using natural resources and disposing of construction and demolition waste to landfill in very large quantities. Both practices are damaging to the environment and are no longer considered sustainable at their current levels. Therefore, many governments throughout the world are actively promoting policies aimed at reducing the use of primary resources and increasing reuse and recycling. One of the most environmentally responsible and economically viable ways of meeting the challenges of sustainability within the construction industry is the use of recycled concrete and demolition waste as aggregate in new construction**(Dhir et al., 1998)**.

The rapid development in research on the use of RCA for the production of new concrete has also led to the production of concrete of high performance. It should be noted that the use of coarse RCA (up to 30%) is normally recommended but the addition of superplasticizer is inevitable **(Limbachiya et al., 2000)**. In Australia, over three million tons of waste rubble-largely concrete-are produced annually. Approximately

50% of the material is recycled as an RCA and the remainder is sent to landfills **(Shayan and Xu, 2003)**.

Every year, roughly 2-10% of the estimated 3480 million cubic meters of ready-mixed concrete produced in the USA (estimation in 2006) is returned to the concrete plant. This material is different from crushed concrete aggregates as construction debris tends to have a high level of contaminations (rebar, oils, deicing salts etc.). Crushed concrete aggregates, on the other hand, is prepared from concrete that has never been in service and thus likely to contain much lower levels of contamination or none **(Kim, 2009)**.

2.5 Recycled Concrete Aggregate Properties(RCA)

It is critical to be able to accurately define the properties of RCA. This is because the properties of any concrete made with RCA are very dependent upon the quality of the RCA used **(Limbachiya *et al*., 2012)**. It is generally thought that if there is less mortar surrounding the RCA, the quality and effectiveness of the RCA will increase. The basis of this thought is the assumption that the RCA will exhibit properties similar to the original virgin aggregate used in the RCA source material **(Garber *et al.*, 2011)**. Further, the better the source material used, the better the final concrete produced. Even if the RCA source concrete is not of the highest quality, it is still possible that the RAC could be used effectively in new concrete.

2.5.1 Fresh Concrete Properties

Three of the most important properties of fresh concrete are workability, air content, and density. Previous research has shown that RCA has an influence on each of these properties **(Mjelde, 2013)**.

2.5.1.1 Density

The density of concrete mixtures incorporating RCA is typically lower than that of concrete made with only natural aggregates. The mortar portion of the RCA has an entrained air structure that is less dense than the rock it is adhered to. Therefore, as more RCA is incorporated into a concrete mixture, the resulting concrete density will be lower **(Anderson and Uhlmeyer, 2009)**.

2.6.1.2 Workability

Concrete mixes made with RCA are typically less workable than those with only natural aggregates. This decrease in workability comes from two sources. First, the adhered mortar portion of the aggregate has higher water absorption, which can reduce the effective water of mix, thus making the mix harsher and less workable **(Garber *et al.*, 2011)**. Second, RAC has a more angular shape than natural aggregates, which increases the friction between aggregates **(Amorim *et al.*, 2012)**. This is due to the crushing processes used in producing RAC. The decreased workability of RCA mixtures can be mitigated by adding more water to the mix design or by adding a water-reducing admixture.

2.6.1.3 Air Content

Concrete mixes incorporating RCA tend to have slightly higher air contents than concrete mixtures with only natural aggregates. This is due to the entrained air of the adhered mortar portion of the RCA **(Anderson and Uhlmeyer, 2009)**. In an attempt to counter this issue, it is recommended to remove as much mortar from the RCA before incorporating it into a concrete mixture.

2.6.2 Hardened Concrete Properties

Incorporating RCA can have several effects on hardened concrete properties. Five of these properties are compressive strength, modulus of rupture, the coefficient of thermal expansion, drying shrinkage, and durability. One study found that up to a 30% substitution of RCA has no significant negative effects on hardened concrete properties **(Limbachiya *et al*., 2012)**.

2.6.2.1 Compressive Strength

Conclusions on the effects of RCA on compressive strength fall into two camps. Some researchers concluded that there is no difference in compressive strengths between normal and RCA concretes **(Amorim *et al.*, 2012).** It is speculated that the stronger interfacial transition zone between the more angular aggregates and the new cement paste accounted for the lack of a reduction in compressive strength. However, other research indicated that the compressive strength of concretes made incorporating RCA is typically lower than those with only natural aggregate **(Anderson and Uhlmeyer, 2009)**. Several factors have been suggested as contributing to causing the reduction in strength. RCA concretes typically require a higher water-cement ratio to achieve needed workability. An increase in the water-cement ratio has the effect of lowering the compressive strength of concrete. Further, RCA concretes usually have higher air content, which can cause lower compressive strengths **(Mjelde, 2013)**.

2.6.2.2 Modulus of Rupture

Modulus of rupture is defined as the flexural tensile strength of concrete when subjected to a flexural loading. Similar to the compressive strength, the modulus of rupture of concrete incorporating RCA has been reported

to be lower than that of concrete with just natural aggregate. One study found that the flexural strength of RCA concrete can be up to eight per cent lower than concrete with only natural coarse aggregate **(Anderson and Uhlmeyer, 2009)**. This reduction in strength may be a result of the relatively weaker bond strength between the new cement paste and the mortar adhered to the RCA **(Limbachiya *et al.*, 2012).** Further, as with the compressive strength, the higher water-cement ratio and air content of RCA concretes may contribute to the reduced flexural strength

2.6.2.3 Drying Shrinkage

The drying shrinkage of hardened concrete depends upon the ability of the aggregates to restrain the paste from shrinking. Since RCA has mortar adhered to the aggregate, there is less aggregate to restrain the drying shrinkage. Therefore, RCA concretes have typically higher drying shrinkage **(Anderson and Uhlmeyer, 2009).**

2.6.2.4 Coefficient of Thermal Expansion

The coefficient of thermal expansion is a material property that is used to define the expected length change of a material when subjected to a temperature loading. Ordinary concrete has typically a coefficient of thermal expansion ranging from 3.2 to 7.0 millionths per degree Fahrenheit. The coefficient of thermal expansion of concrete is influenced by many factors such as the aggregate type, which has the most effect**.** One report indicated that incorporating RCA decreases the coefficient of thermal expansion of hardened concrete **(Smith and Hendy, 2009).**

2.7. Concluding Remarks

From the previous review of studies related to reinforced concrete piers and recycled aggregate concrete described in this chapter, several points had been concluded:

1. In pier cap design, the use of sixty-grade reinforcing bars led to make the crack width larger than intermediate grade reinforcement.
2. The column pier reinforcement controls the cracks and provides some confinement for the lap splices of the uniformly distributed horizontal reinforcement.
3. The horizontal distribution of steel, within reasonable limits, have a little effect on crack widths.
4. The best way for design pier cap is by using strut and tie model.
5. The density of concrete mixes incorporating recycled aggregate was lower than that of concrete made with only natural aggregates.
6. Recycled Aggregate concrete has usually higher air content, which is the reason behind the decrease in the compressive strength.

Chapter Three

Chapter Three
Experimental Work

3.1 Introduction

This chapter contains the properties of the material used in the experimental program, details of specimens**,** design mix, casting, and curing of specimens. The specimens were cast using a rotary mixer in which its fresh properties has been investigated using the slump test that has been implemented for all mixes to measure its consistency. After the curing period, hardened concrete tests were performed to determine the concrete properties such as the compressive strength, the splitting tensile strength, and the density. In addition, the details of specimens, instrumentation and testing setup are illustrated in this chapter. All tests were carried out in the structural laboratory in the civil engineering department/college of engineering/ University of Kerbala.

3.2 Materials

Various materials were used in this research to prepare concrete mixes such as sulfate-resisting Portland cement, fine aggregate, recycled aggregate (RA), natural coarse aggregate (NA), steel reinforcement, glass fiber reinforced polymer (GFRP), carbon fiber reinforced polymer (CFRP), and recycled steel fiber (RSF). Details of all materials are given below:

3.2.1 Cement

The type of used cement was the sulfate resistant Portland cement Type V, which is known commercially as Al-JESR. This type was found to be

confirmed to the limits of Iraqi Specification No. 5/1984. Test results of the chemical and physical properties are given in Tables (3.1) and (3.2).

Table 3. 1 Chemical Properties of Cement

Test	Results	Limits of the IQS NO. 5 /1984
Cao	61.3	-----
SiO_2	20.1	-----
Al_2O_3	6.2	-----
Fe_2O_3	3.2	-----
SO_3	2.3	≤ 2.8
MgO	4.4	≤ 5.0
L.O.I (Loss on ignition)	1.75	≤ 4.0
I.R.(Insoluble residue)	0.6	≤ 1.5
L.S.F.(Lime saturation factor)	0.88	0.66-1.02

Table 3. 2 Physical Properties of Cement

Test		Results	Limits of the IQS NO. 5 /1984
Initial Settling Time (Minutes)		130	>45
Final Settling Time (Hours)		4.2	<10
Fineness (cm^2/gm) by Blaine Method		3400	>2500
Compressive Strength	**3 days(MPa)**	25	≥ 15
	7 days (MPa)	32	≥ 23

3.2.2 Fine Aggregate

The fine aggregate used in this research work was a local well-graded natural fine aggregate from Al-Ukhaydir region. The chemical and physical tests that were carried out showed that it meets the requirements

of the Iraqi specification (IQS No. 45/1984) as tabulated in Tables (3.3) and (3.4). Figure (3.1) shows the comparison of the sieve analysis of the fine aggregate with the limits of the Iraqi specifications.

Table 3. 3 Grading of Natural Sand

Sieve Size (mm)	**Cumulative** Passing%	**Limits of IQS No. 45/1984/Zone 2**
10	100	100
4.75	98	90-100
2.36	77	75-100
1.18	59	55-90
0.6	46	35-59
0.3	17	8-30
0.15	5	0-10

Table 3. 4 Chemical Properties of Sand

Property	**Result**	**Limits of Iraqi Specification No. 45/1984**
Absorption	0.7%	-----
Sulfate Content	0.107	≤ 0.5 %
Material Passing 75 µm Sieve	2.80	< 5
Specific Gravity	2.6	-----

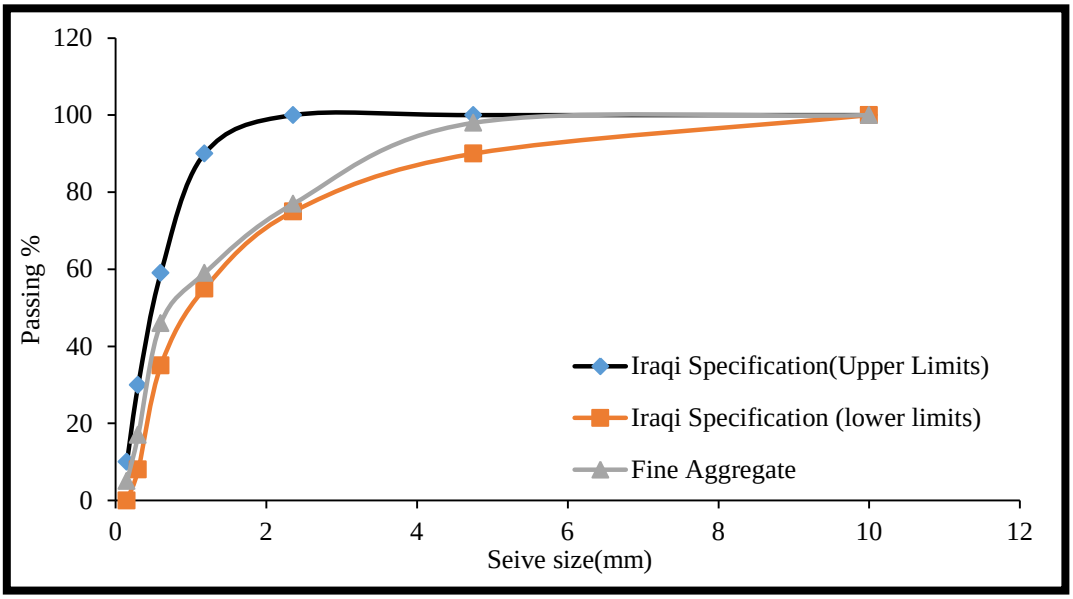

Figure 3. 1 Grading of Fine Aggregate in Comparison with the IQS Limits

3.2.3 Coarse Aggregate

The coarse aggregate that has been used in this work in all mixes was white crushed stones with 19 mm maximum size. Table (3.5) and Figure (3.2) shows that the test results of this aggregate, which have found to meet the Iraqi specification (IQS No. 45/ 1984).

Table 3. 5 Test Results of Coarse Aggregate

	Sieve Size (mm)	**Passing %**	**Limits IQS No. 45/1984**
Grading	19.5	98	95 – 100
	9.5	35	60 – 30
	4.75	1	0 – 10
Specific Gravity	2.65		------
Sulfate Content, SO_3 %	0.046		0.1 (Max.)

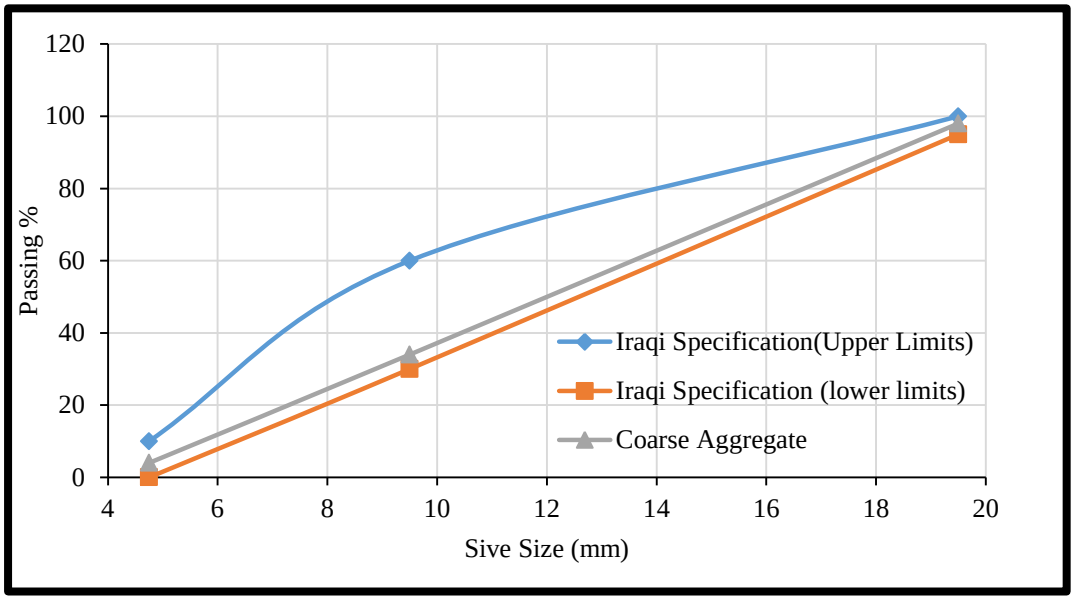

Figure 3. 2 Grading of Coarse Aggregates

3.2.4 Recycled Coarse Aggregate

Old cubes and cylinders concrete samples, which are available in the laboratory of concrete- engineering college- university of Kerbala, were collected to be used as a recycled coarse aggregate (RCA). These samples were broken down into small size particles by hand hummer to be taken then to the sieving process to be within the Iraqi Specifications No. 45 /1984. Test results of the recycled aggregate are given in Table (3.6) and it has been prepared to be acceptable to the IQS No. 45/1984.

Table 3. 6 Test Results of Recycled Coarse Aggregate

	Sieve Size (mm)	Passing %	Limits of IQS No. 45/1984
Grading	19.5	98	95 – 100
	9.5	34	60 – 30
	4.75	4	0 – 10
Specific Gravity	2.65		-----
Sulfate Content, SO_3 %	0.074		0.1 (Max.)

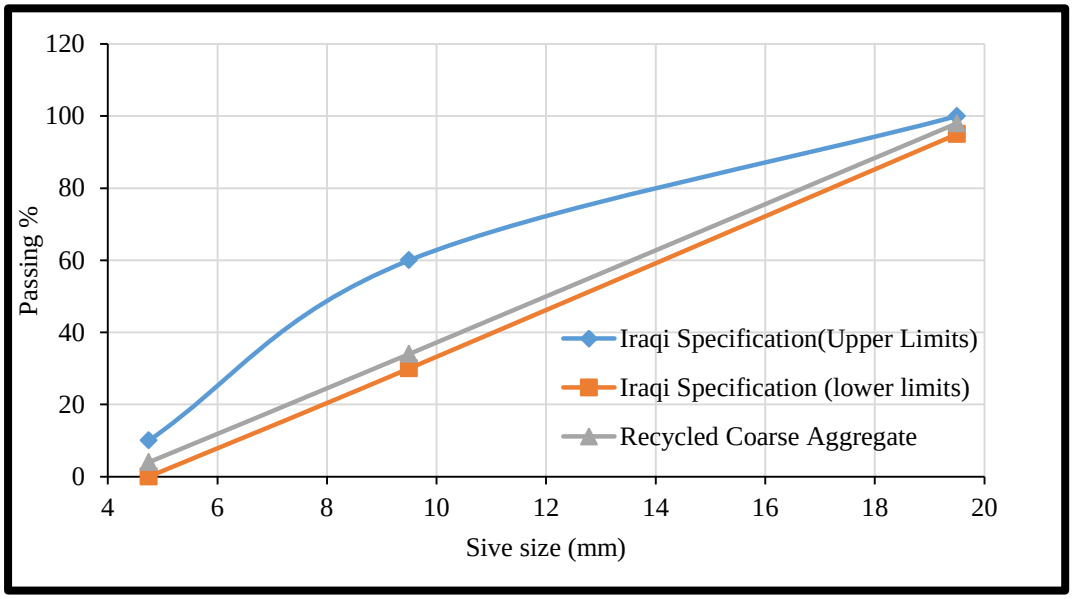

Figure 3. 3 Gradient of the Recycled Coarse Aggregates and the Comparison with the Limits of IQS No.45/1984

3.2.5 Water

Ordinary tap water was used for mixing and curing of all concrete samples and piers.

3.2.6 Superplasticizer

High-range water reducing admixture was used in this research work for producing high strength concrete (HSC) mix only. It was supplied by Sika company, which is known commercially by SikaViscoCrete®-5930. This admixture has the ability to reduce the water content by up to 30 %. Indeed, it has several advantages besides reducing water content in the mixture such as; improve shrinkage, enhance creep behaviour, increase high early strength, and density (plate 3.1). The characteristics of this type of superplasticizer are shown in Table (3.7), and it was found to be confirmed to ASTM-C494-99 types G and F.

Table 3. 7 Technical Data of Sika ViscoCrete®-5930*

Property	Description or Value
Basis	An aqueous solution of modified polycarboxylate
Appearance	Turbid liquid
Density (kg /lt)	1.095
Boiling	100 °C
PH	7-9
Recommended	0.2-0.8 % litter by weight of cement for NC

***From supplier**

Plate 3. 1 Superplasticizer used in the Present Work

3.2.7 Steel Reinforcement

Two sizes of the common deformed steel bars were used in the present study. A bar size of (Ø 10 mm) used to be as a longitudinal reinforcement, in addition to a bar size of (Ø 6 mm) was used as stirrups. Tensile tests on three samples for each bar size have been carried out according to ASTM A- 615-05. The yield and ultimate stresses for these bars are listed in Table (3.8). This test was carried out in the laboratory of the mechanical engineering department/ Kerbala University using the tensile testing machine as shown in Plate (3.2).

Table 3. 8 Properties of Steel Reinforcement Bars

Property		**Ø 10**	**Ø 6**
Diameter (mm)	**Nominal**	10	6
	Actual	9.852	5.963
Yield Stress, *fy* (MPa)	**Result**	541.8	583.3
Tensile Strength, *fu* (MPa)	**Result**	669.7	597.1
Area (mm^2)		77.0	28.3
Mass (kg/m)		0.598	0.219
Elongation (%)		19.6	9.6

Plate 3. 2 Tensile Testing Machine of Steel Reinforcement

3.2.8 FRP Reinforcement

Two types of FRP bars were used to achieve the desired aims of the research. Aslan 200 CFRP and GFRP bars with nominal diameters of (6 mm) and (10 mm). CFRP bars have greater tensile strength and modulus of elasticity as compared with steel and GFRP bars as well as the weight of these bars was about 20 % of steel reinforcing bars(Brothers, 2010).

Table (3.9) shows the properties of these types as supplied from the manufacturer. The results were acceptable according to the standard specification ASTM D 7205.

Table 3. 9 Properties of Aslan 200 CFRP and GFRP Bars

Type / Properties	GFRP (6mm)	GFRP (10mm)	CFRP (6mm)	CFRP (10mm)
Nominal Diameter (mm)	6	10	6	10
Nominal Area (mm)	31.67	71.26	31.67	71.26
Ultimate Tensile Load (KN)	28	59	71	154
Guaranteed Tensile strength (MPa)	896	827	2241	2172
Modulus of Elasticity (GPa)	46	46	124	124
Weight (g/m)	77.4	159	-----	-----
Transverse Shear Strength (MPa)	150	150	-----	-----

3.2.9 Recycled Steel Fiber

The steel fiber used in this investigation was a recycled one produced and extracted from old cars tires. The tires were burned and the steel fiber was extracted to be then cut into small pieces of 2 cm length (see Plate 3.3). Some physical properties have been measured in the laboratory such as the diameter and the density, which were found to be equal to 1 mm, and 6740 (kg/m^3) respectively.

Plate 3. 3 Recycled Steel Fiber

3.3 Concrete Mixes

All specimens have been cast by using a rotary mixer. Mixes were designed according to ACI method to get (28 MPa) compressive strength at 28-days age and a slump range of (100-80) mm using (19 mm) maximum size of aggregate. The mix proportions were [1:1.4:2.2 (cement: sand: gravel)] and [1:0.97:1.23 (cement: sand: gravel)] with w/c ratios equal to 0.43 and 0.38 for normal (NC) and green high strength concrete (HSC) respectively. Different concrete mixes were produced based on the replacements of natural aggregate with recycled aggregate, which were (25%,50%,75% and 100%)of normal coarse aggregate. Many trail mixes had been carried out for each of them to find the best mix of concrete according to the results that were obtained from the laboratory tests including slump test and compressive strength at age 7,14, and 28 days. The selected mixes for each concrete case were stated after that many trail mixes are presented in Table (3.10).

Table 3. 10 Properties of Trail Mixes

Materials (kg/m^3) / Mixes		Cement	Fine Aggregate	Coarse Aggregate	Recycled Coarse Aggregate	w/c	SP* %	Slump Test (mm)
NC		465	651	1023	0	0.43	0	125
Recycled Aggregate Concrete	25% of Coarse Agg. Weight	465	651	767.25	225.75	0.43	0	100
	50% of Coarse Agg. Weight	465	651	511.5	511.5	0.43	0	80
	75% of Coarse Agg. Weight	465	651	225.75	767.25	0.43	0	65
	100% of Coarse Agg. Weight	465	651	0	1023	0.43	0	55
HSC		500	485	615	615	0.38	1	75

***superplasticizer**

Although the concrete mix with a replacement ratio of 25% gave better results than the mix of a 50% substitution ratio in terms of the compressive strength, the mix of 50% substitution ratio was adopted for economic considerations. The compressive strengths were determined from the results of testing three standard cylinders of 100 mm in diameter by 200 mm in length as shown in Plate (3.4).

Plate 3. 4 The specimens of cylinders

According to (ASTM/C31/C31M, 2003), Mixing of the specimens has been carried out. The coarse aggregate, fine aggregate, and recycled coarse aggregate were placed into the mixer to be mixed in the dry condition for two minutes. A portion of the total mix water was added at this stage in order to facilitate absorbing water by aggregates and also to reduce dust from the mixing process. The mixer was then run until the aggregates were well blended. Keeping the mixer running, the cementations materials were added into the mixer. All of the remaining water was then added into the mixer. The mixer continues to run until there was a well-blended and homogeneous concrete mix. The mixer was then stopped, and the slump was measured. After this, the concrete was ready to be cast into the moulds for the hardened concrete tests.

3.4 Design Method

The design of pier reinforcement was conduct using strut and tie method as follows :

Fy = 400 MPa

Fc=28 MPa

P= 281.5 kN

Cover= 20mm

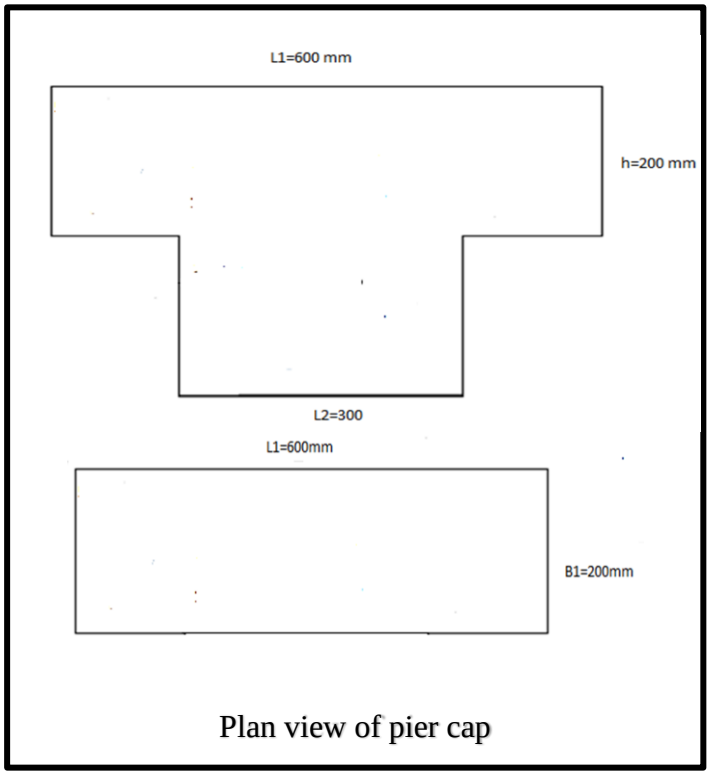

Figure 3.4 Pier cap geometry

Size the base plate

Pu = 450.kn

Ø= 0.7 for bearing

P n = nominal bearing strength

Pn required = Pu/Ø = 643.4 kn

Pn = 0.85 fc' A1(A2/A1)$^{0.5}$

A1 = base plate area

A2 = surrounding area of concrete

, taken as the area of a square

=0.85*28*40000*(57600/40000)$^{0.5}$

=856.8 kn >pn required ok

Base plate size =150*150mm

w/b=150/240=0.625

Size C5 and find the location of its resultant

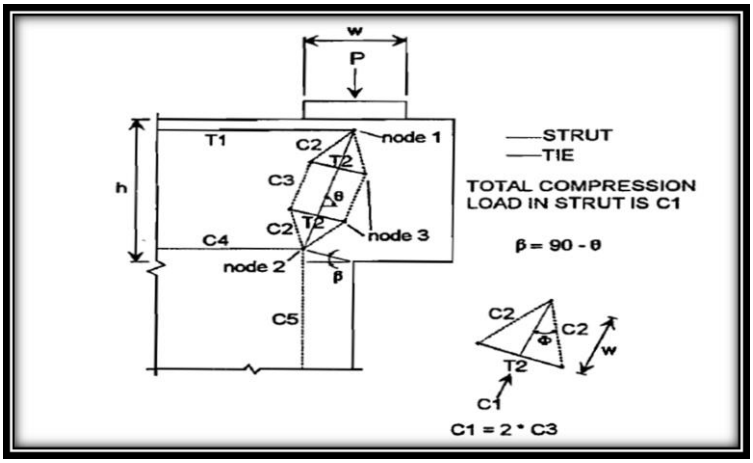

Figure 3.5 Strut and tie model

Pu = 450kN

Ø= 0.9

Pn = Pu/Ø = 500.4kn = required pier cap strength

Knowing Pn, the centroid ofC5 can be found because C5 = Pn.

F_{cd}= concrete design strength = ufc' for all struts in the model

where u = 0.8

Fcd=ufc' = 22.4

AC5 = area of strut C5 = C5/fc^{-} = 22341.3mm^2

WC= AC5/B2= 111.7mm the width of strut C5.

The centroid of AC5 is then found,

Xcg = WC/2= 55.9mm

Find the inclination angle of the bottle strut

d=h-cover-db/2

Assuming a ø10 bar in the top layer, db = 10mm

so d = 240-20-5 = 195mm

Θ = 0.5 asin [2Xg/d] = 72.5

Knowing Θ, check Tl and assumed d

Tl = Pn/tan Θ = 158.0kn

AT1 = area of steel for T1 = Tl/fy = 395.0mm

use 4 ø10 and 6ø6 bars, with As = 483.7mm^2

=> this implies that 2 layers of steel will be needed

2 ø 10 and 3 ø6 for each layer .

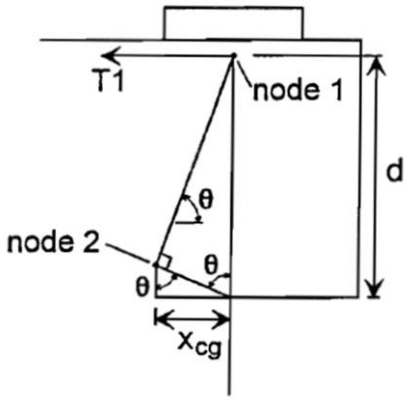

Recalculate Θ using two layers of steel for T1

For 2 layers of steel, use a clear spacing of $2d_b$ = 20mm for ø 10 bar

d = h - cover - d_b - clear spacing/2 = 155mm

so new Θ = 0.5 asin [2Xq/d] = 66.9

Check T1 using the new Θ

T1 = Pn/tan Θ = 2130/tan 71.8 = 213.5 kN

AT1 = Tl/fy = 533.7 mm^2 < 785.0 mm^2 provided, OK

For the components of T2, horizontal and vertical stirrups are used. Since there are two ties T2 in the bottle strut, steel must be provided to resist 2*T2. Since steel will be distributed on each face of the pier, the steel required for T2 is provided on each face of the pier cap.

T2= 0.5*C1*tan (Ɵ) =75.2, where (C1= pn/sin(Ɵ)) =544.1

T2 horiz = T2*(sin Ɵ)= 69.2 kN

A T2horiz. = T2hori/fy = 173 mm^2on one face of the cap

for T2horiz. use 3 ø10 bars, As =235.6mm^2

The horizontal stirrups for T2 are evenly spaced across the depth of the pier cap

T2vert =T2 *cos(Ɵ)= 29.5 kN

A T2vert = *T2vert/fy* = 73.8mm^2on one face of the cap

for T2vert use 3 ø6 bars, As =84.8 mm^2

The vertical stirrups for T2 are spaced across the width of the compression strut.

3.5 Description of Test Specimens

Thirteen reinforced concrete piers have been tested to represent the experimental variables of the research plan. All specimens have identical geometry and reinforcement pattern as shown in Figure (3.6). The specimens have a total pier cap length of 600 mm with a cantilever part of 150 mm from the face of the supporting column, which has dimensions of 300 × 200 × 200 mm (width, length, height). The details of all specimens are shown in Table (3.11) .

Table 3. 11Description of Tested Pier Specimens

Name	Type of Concrete in Pier Cap	Type of Concrete in Pier Column	Type of Reinforcement in the Pier Cap	Type of Reinforcement in the Pier Column	Stirrups
NC	Normal	Normal	Steel	Steel	Steel
GC	Green	Green	Steel	Steel	Steel
TRSF	Green +2% vol. ratio of RSF	Green concrete	Steel	Steel	Steel
HRSF	Green +2% vol. ratio of RSF	(½ Green +2% vol. ratio of RSF)+ Green concrete	Steel	Steel	Steel
ARSF	Green +2% vol. ratio of RSF	Green +2% vol. ratio of RSF	Steel	Steel	Steel
THSC	Green high strength	Green concrete	Steel	Steel	Steel
HHSC	Green high strength	1/2 green high strength +1/2 green concrete	Steel	Steel	Steel
AHSC	Green high strength	Green High strength	Steel reinforcement	Steel	Steel
TCFRP	Green concrete	Green concrete	CFRP	Steel	Steel
T1CFRP	Green concrete	Green concrete	CFRP for two upper layers+ steel	Steel	Steel
TGFRP	Green concrete	Green concrete	GFRP	Steel	Steel
T1GFRP	Green concrete	Green concrete	GFRP for two upper layers+ steel	Steel	Steel
SGFRP	Green concrete	Green concrete	Steel	Steel	GFRP

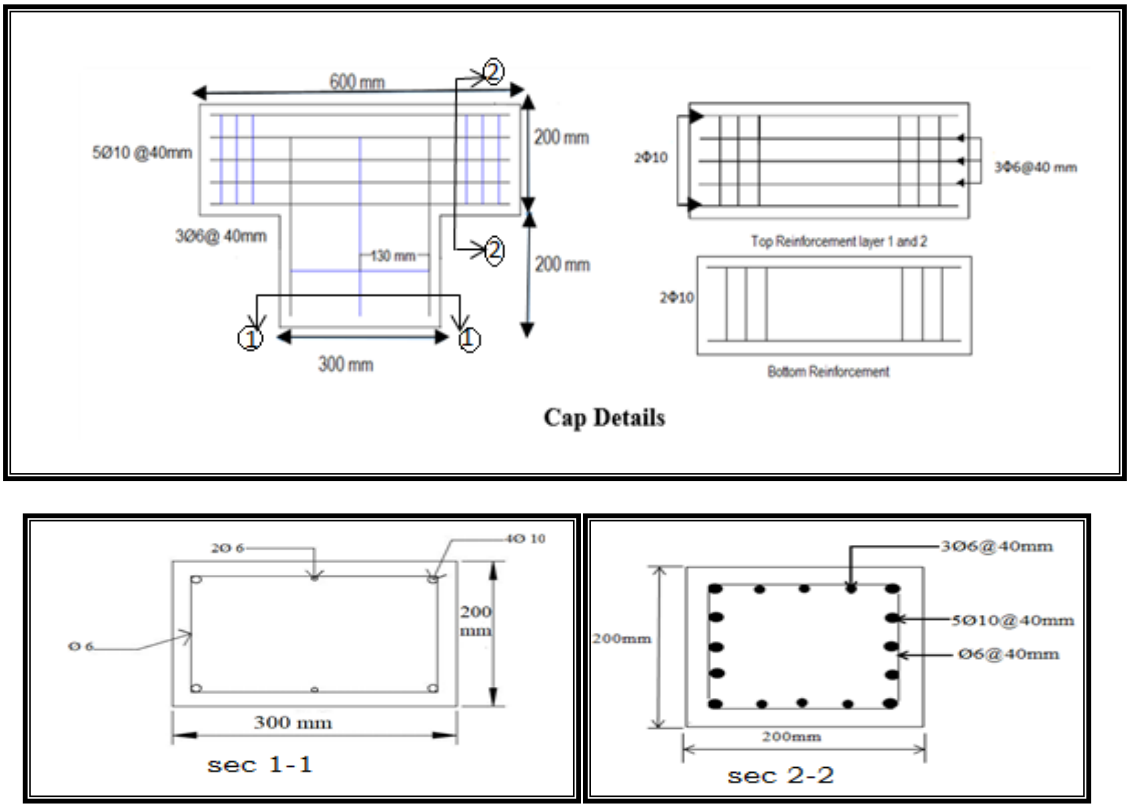

Figure 3. 6 Details of the reinforced concrete piers specimens

Specimen No. 1 (NC)

This case represents a reference pier that was cast using normal concrete (NC) and reinforced with ordinary steel reinforcement as shown in Figure (3.6).

Specimen No. 2 (GC)

This case investigates the effect of using a concrete known as a green concrete (GC), which is produced by replacing 50% of the natural aggregate (NA) by recycled coarse aggregate (RCA). This pier used also the same ordinary steel reinforcement as in the reference pier model.

Specimen No. 3 (TRSF)

This case aims at investigating the effect of a recycled steel fiber (RSF), which is added to the GC mix at 2% volumetric ratio in the pier cap only, while the column part cast with GC only. This specimen was reinforced with steel reinforcement as shown in Figure (3.7).

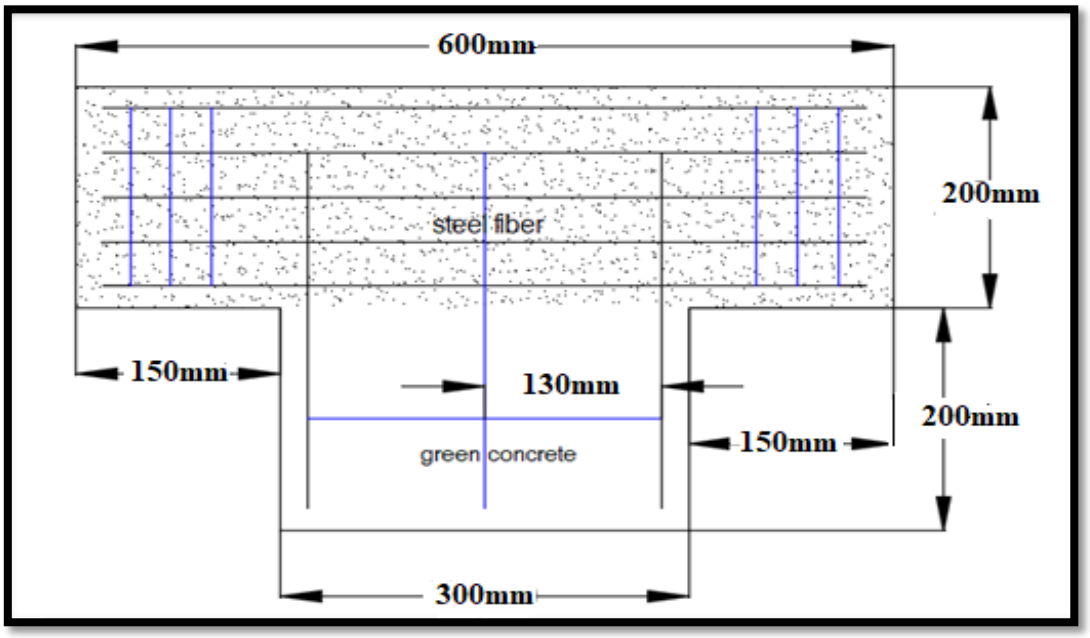

Figure 3. 7 Details of TRSF Pier Specimen

Specimen No. 4 (HRSF)

This case investigates the effect of using GC in casting this pier as well as a recycled steel fiber (RSF) at the pier cap and half of the column pier, while the other part of column cast with GC only. Ordinary steel reinforcement was used in this specimen as shown in Figure (3.8).

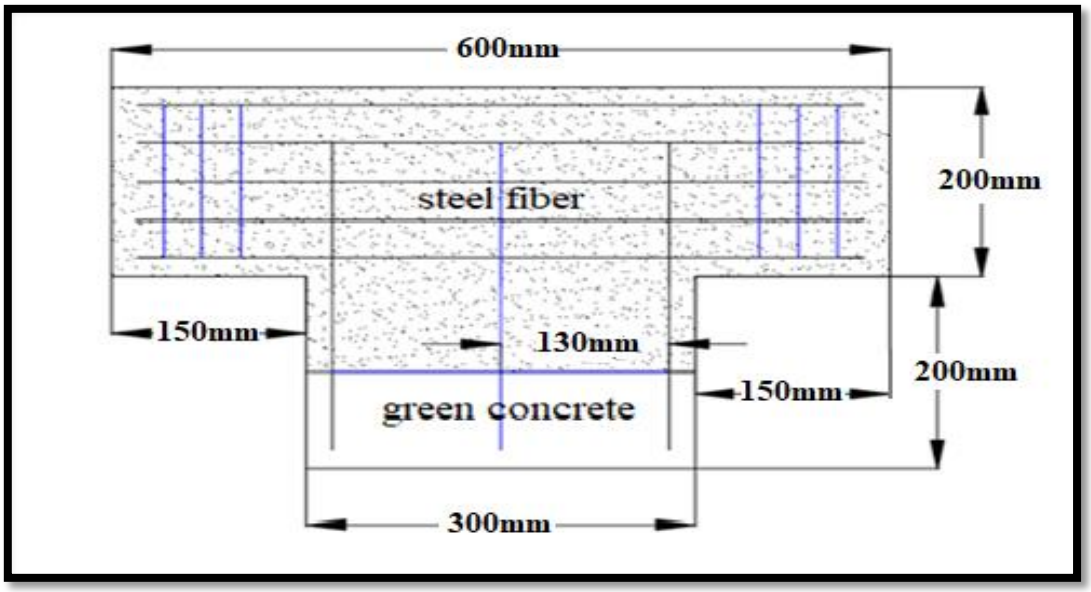

Figure 3. 8Details of HRSF pier specimen

Specimen No. 5 (ARSF)

This case investigates the effect of using a recycled steel fiber (RSF) for the whole pier specimen as well as using an ordinary steel reinforcement as a reinforcement as shown in Figure (3.9).

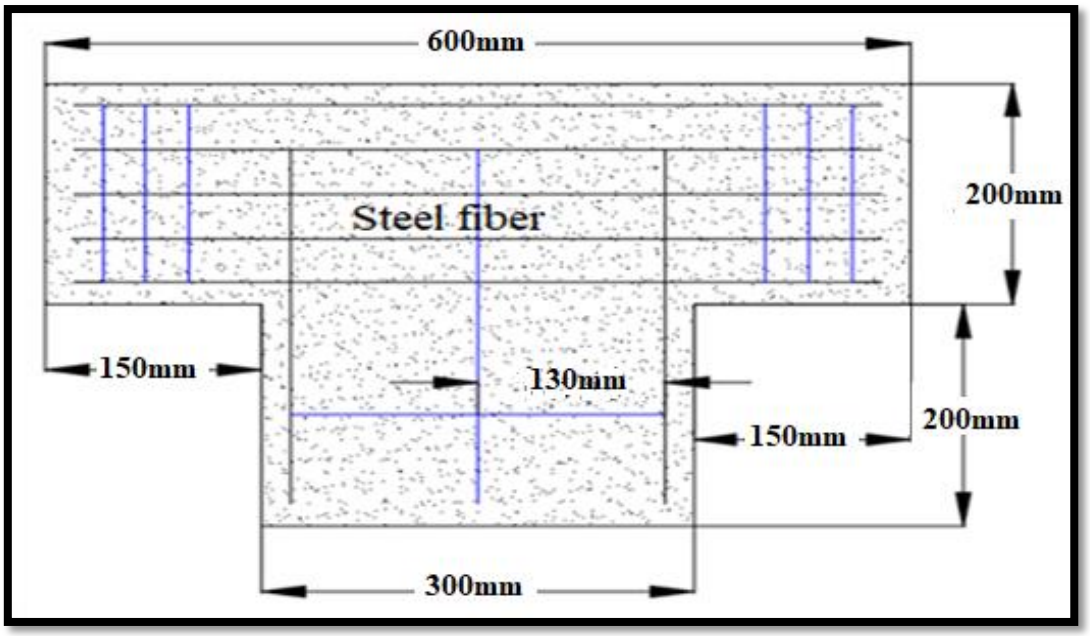

Figure 3. 9 Details of ARSF pier specimen

Specimen No. 6 (THSC)

This case includes using high strength concrete (HSC) in casting the pier cap to investigate its effect on pier behavior. The column pier was cast with GC. Ordinary steel reinforcement was used to reinforce this specimen as shown in Figure (3.10).

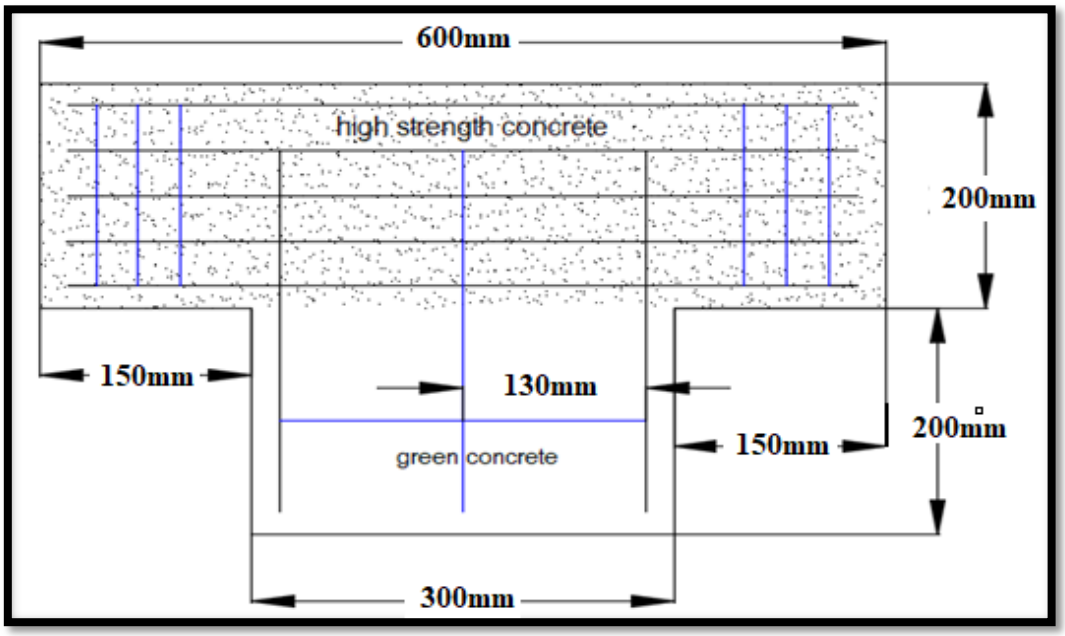

Figure 3. 10 Details of THSC pier specimen

Specimen No. 7 (HHSC)

In this case, pier behaviour was studied due to the effect of using high strength concrete (HSC) in casting pier cap and half part of the column, while the other part cast using GC mix as shown in Figure (3.11).

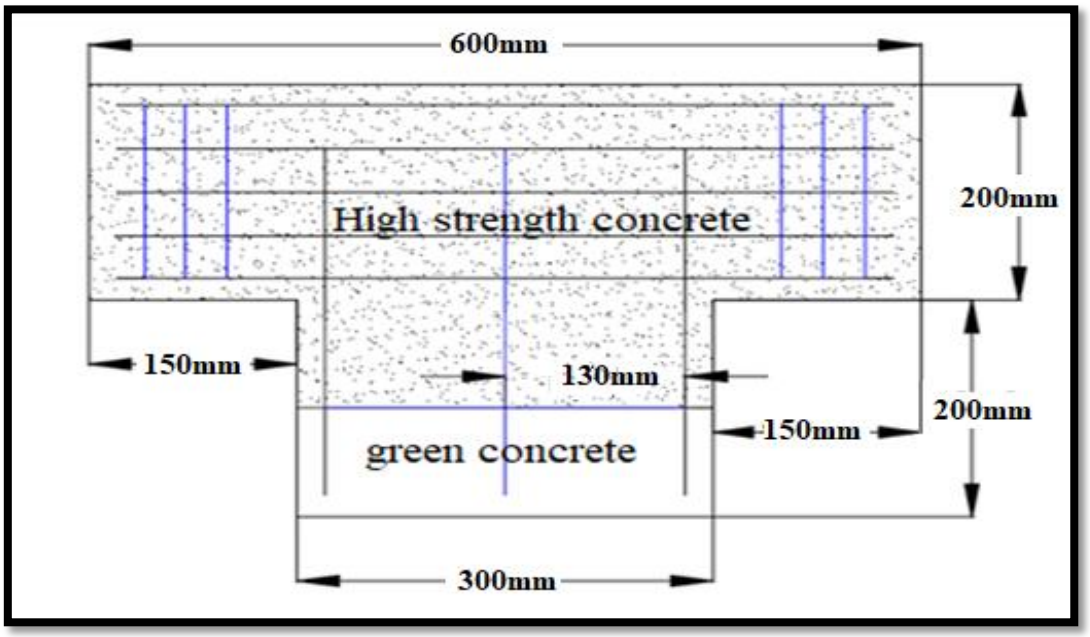

Figure 3. 11 Details of HHSC pier specimen

Specimen No. 8 (AHSC)

In this case, high strength concrete (HSC) was used for casting all pier specimen in addition to ordinary steel reinforcement as a reinforcement as shown in Figure (3.12).

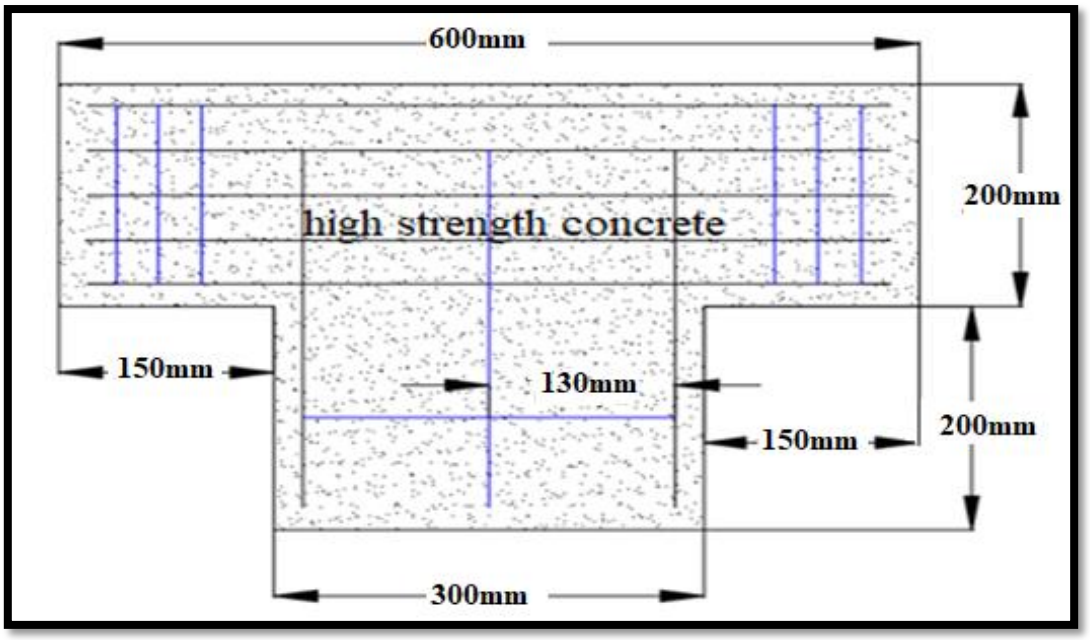

Figure 3. 4 Details of AHSC pier specimen

Specimen No. 9 (TCFRP)

Green concrete mix was used to cast this pier specimen with carbon fiber reinforced polymer (CFRP) bars with diameter of (Ø10 and Ø6) mm to be used for reinforcing all longitudinal reinforcement layers of the pier cap only as shown in Figure (3.13).

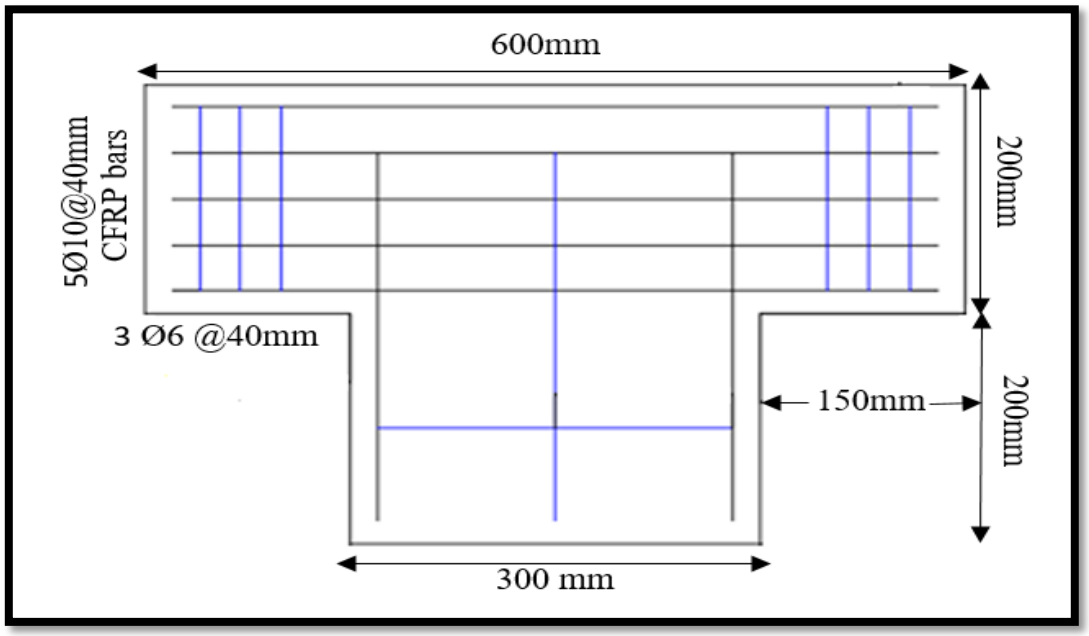

Figure 3. 5 Details of TCFRP pier specimen

Specimen No. 10 (T1CFRP)

This case studies the effect of CFRP bars used for reinforcing the two upper layers. Other layers were reinforced with ordinary steel reinforcement and cast with GC. The details of this specimen are shown in Figure (3.14).

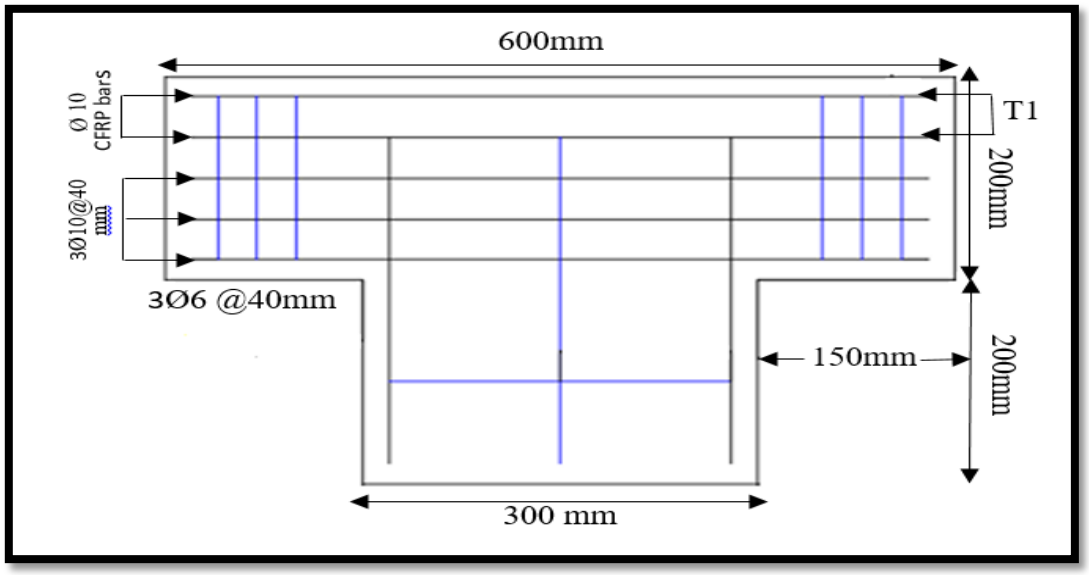

Figure 3. 14 Details of T1CFRP pier specimen

Specimen No. 11 (TGFRP)

This case was similar to study No. 9(TCFRP) with only one change, which is the use of GFRP bars instead of CFRP bars, as shown in Figure (3.15).

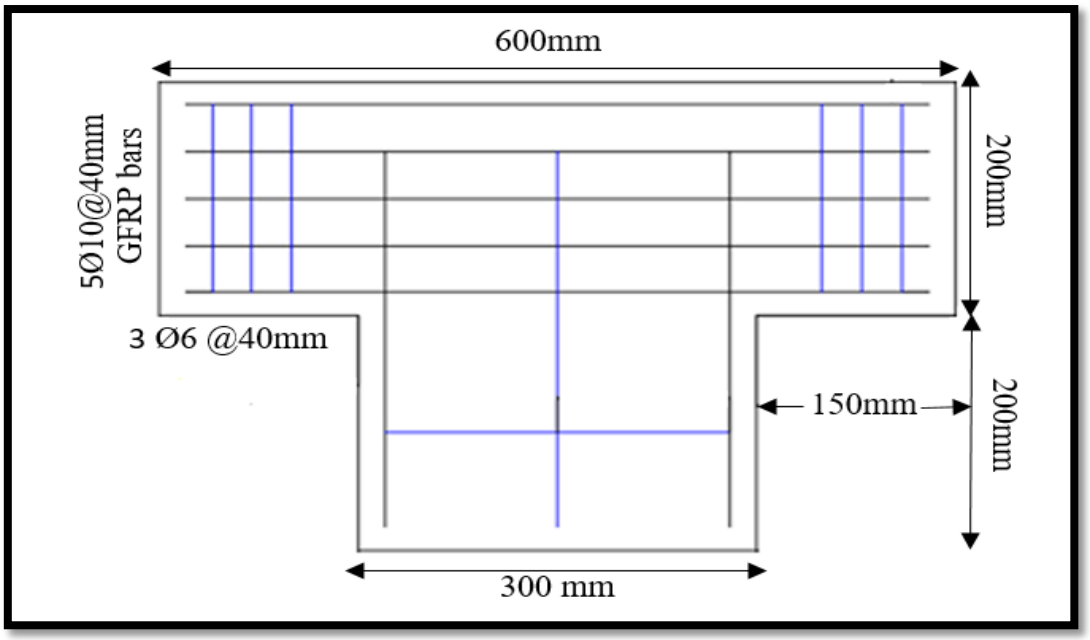

Figure 3. 6 Details of TGFRP pier specimen

Specimen No. 12 (T1GFRP)

Study No. 12 was similar to study No. 10 (T1CFRP) except using GFRP bars instead of CFRP bars as shown in Figure (3.16).

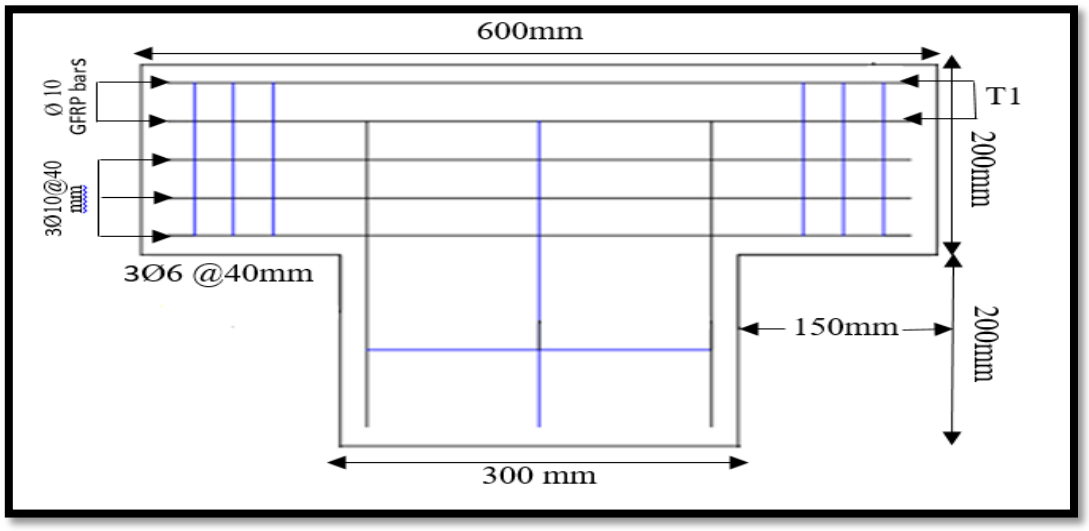

Figure 3. 7 Details of T1GFRP pier specimen

Specimen No. 13 (SGFRP)

This case studies the effect of GFRP stirrups when they are used for vertical reinforcement at pier cap and ordinary steel reinforcement for longitudinal reinforcement. This case cast with GC as shown in Figure (3.17).

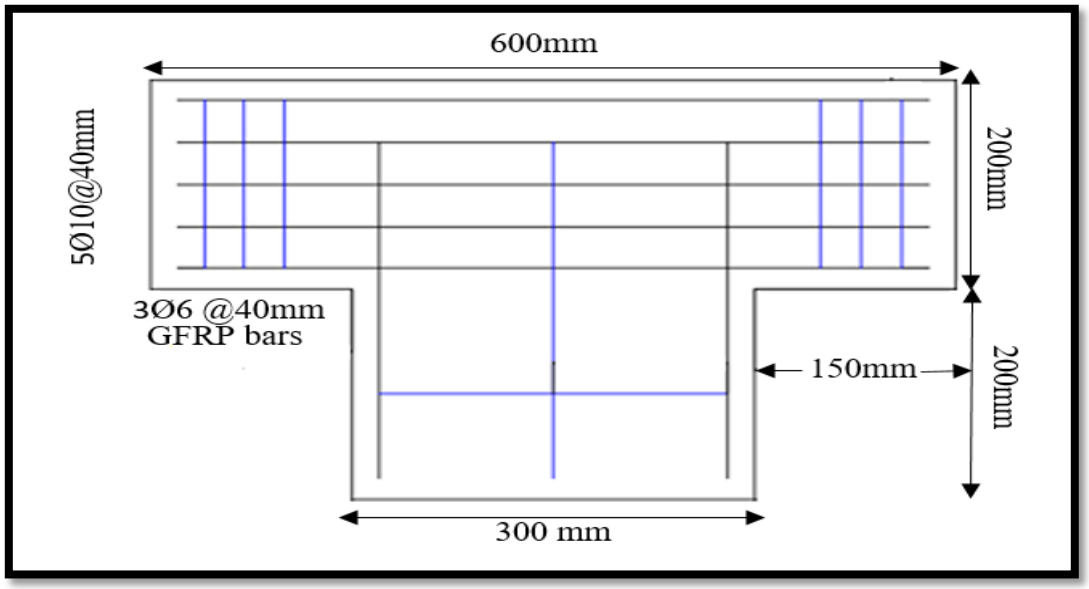

Figure 3. 8 Details of SGFRP pier specimen

3.6 Fabrication of Plywood Molds and Steel Reinforcement Cages

Eight plywood moulds were fabricated for casting all the models. The thickness of plywood moulds was 18 mm for each side. The moulds consist of bottom and side pieces connected together by small bolts in order to be easy for using again. Plates (3.5) to (3.8) shows the moulds that were used to cast specimens as well as the reinforcement cage of the piers.

Plate 3. 5 The plywood molds

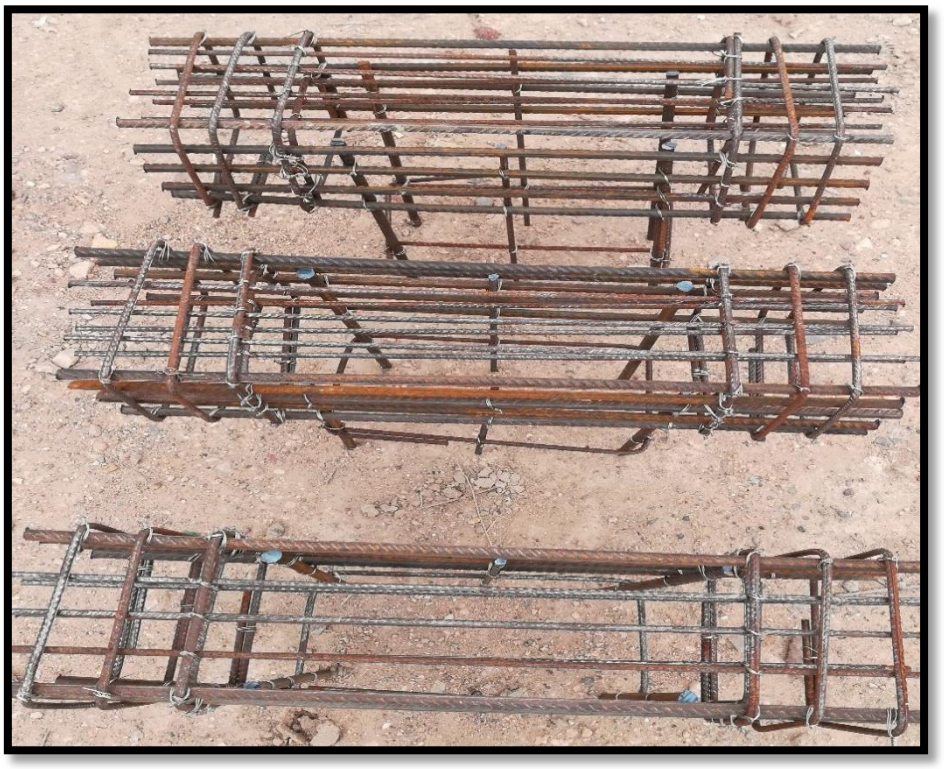

Plate 3. 6 Steel reinforcement cage of pier specimens

Plate 3. 7 Glass fiber reinforcement cage of pier specimens

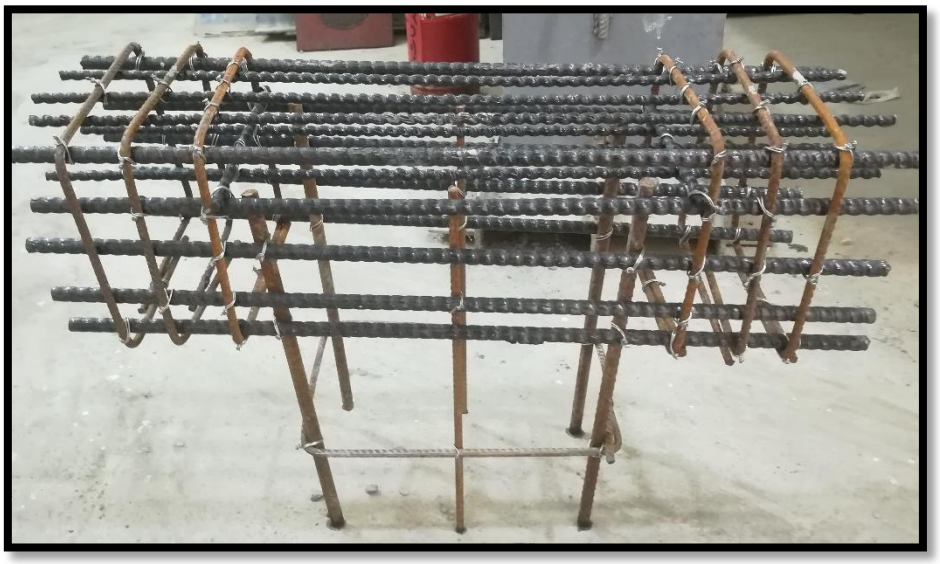

Plate 3. 8 Carbon fiber reinforcement cage of pier specimens

3.7 Concrete Casting and Curing

Normal (NC) and high strength concrete (HSC) were used to cast the pier specimens. The mix proportion was carried out by weight (1 cement: 1.4 sand: 2.2 gravel) with a w/c ratio of (0.43) for NC and (1 cement: 0.97 sand: 1.23 gravel) with a w/c ratio of (0.38) for high HSC. The mixes have been cast into the cylinders, and piers mould with three sequential layers until fully filled. The internal surfaces of the wooden moulds were previously oiled to prevent adhesion of the concrete after hardening. After filling the cylinder and piers specimens, their surfaces were smoothed with a trowel. All samples were allowed to cure for 24 hours. For casting HSC and specimens with ordinary steel fiber, a plate of plywood was used to separate HSC or steel fiber from the GC for specimens that partially use GC (see plate (3.9)). After a curing period of 24-hours, all samples were de-moulded. The samples were then stored in curing tanks filled with water until the time of testing.

Plate 3. 9 Separating of various mixes in the mold

Plate 3. 10 Casting of pier specimens

3.8 Testing of Fresh and Hardened Concrete

3.8.1 Slump Test

The workability of the fresh concrete mixes was measured by the slump test before casting these mixes in the moulds. This test was conducted according to ASTM C143/C143M-05a standard test method for a slump of hydraulic cement concrete, see Plate (3.11).

Plate 3. 11 Slump flow test

3.8.2 Compressive Strength Test

For the hardened concrete, the compressive strength test was carried out according to ASTM C39/C39M-05 standard test method for compressive strength of cylindrical concrete specimens using a digital testing machine of 2000 kN maximum capacity available in the laboratory of the civil engineering department, (see Plate 3.12). Three cylinders of 100 mm in diameter and 200 mm in length were tested for each mix at each age (7, 14 and 28) days to determinate the compressive strength. Thin plywood was placed on the upper and lower faces of the specimen during the test specimens. The load was applied approximately at a constant rate and failure load was recorded to the nearest 1 kN. Table (3.12) shows the results of the compressive strength and slump test for the selected trail mixes.

Table 3. 12 Compressive Strength and Slump Values for Trail Mixes

Type of Mixes	Average Compressive Strength(MPa)		
	7 days	14 days	28 days
NC	19	26.5	30
25%RCA	23	25.7	29.4
50%RCA	20.8	25.3	28.5
75%RCA	17.3	22.9	25.7
100%RCA	17.7	19.6	21
H S C	30.4	38.7	46.2

Plate 3. 12 Compressive strength test machine

3.8.3 Splitting Tensile Strength Test

The splitting tensile strength was carried out according to ASTM C496 M-2004 specification. Eight cylinders of 100 mm in diameter and 200 mm in height were used. The specimens were tested at the age of 28 days after water curing. Thin plywood was placed on the upper and lower faces of the specimen. The test was performed using a hydraulic compression machine ELE of (2000 kN) capacity, at a rate of 2.4 kN/sec until the failure occurs. The following equation was used for calculating of splitting tensile strength.

$$f_{sp} = \frac{2P}{\pi dl} \quad \text{..... (3.1)}$$

where:

f_{sp}: Splitting tensile strength, (MPa)

P: Maximum applied load indicated by the testing machine, (N)

d: Cylinder diameter, (mm)

l: Cylinder length, (mm)

3.8.4 Hardened Density Test

This test covers the findings of density in hardened concrete according to (ASTM C642-97). The specimens were tested at the age of 28 days. A total number of (12) cylinders of (100×200) mm were tested by determining the mass of the specimen and drying in an oven at a temperature of 100 to 110°C for not less than 24 hr. Then, after final drying, cooling, and determination of mass, the specimens were immersed in water at approximately 21°C for not less than 48 hrs, or until two successive values of mass of the surface-dried sample at intervals of 24 hr, show an increase in mass of less than 0.5 % of the larger value. The surface-dry of the specimen can be done by removing surface

moisture by a piece of absorbing clothes and then determining the mass. By using the values for mass determined by the procedures described, the density can be determined by the equation below. The average of three specimens was taken.

Bulk density, dry = $\frac{A}{C-D} \times \rho = g_1$ ……..…..(3.2)

Bulk density after immersion =$\frac{B}{C-D} \times \rho$ ……...……..…..(3.3)

Apparent density = $\frac{A}{A-D} \times \rho = g_2$ …….……..(3.4)

where:

A = mass of oven-dried sample in air, g

B = mass of surface-dry sample in the air after immersion, g

C = mass of surface-dry sample in the air after immersion and boiling, g

D = apparent mass of sample in the water after immersion and boiling, g

g_1= bulk density, g/cm^3 and; g_2= apparent density, g/cm^3

ρ = density of water = 1 g/cm^3

3.8.5 Modulus of Elasticity

The static modulus of elasticity test was carried out on cylinders of 100×200 mm dimensions according to the ASTM C469-02. The significance of this test is to provide the stress-strain relationship. For each mix, the average value of three-cylinder specimens has been taken from recording the values from the test. The load was applied by using a testing machine of 2000 kN capacity and a strain gauge was attached to the specimen as shown in Plate (3.13). The testing machine and the strain gauge (LVDT) were connected to a computer. The modulus of elasticity test for each cylinder specimens can be calculated using equation (3.6).

Ec= (S_2-S_1)/(Є$_2$-0.00005)……..……(3.6)

where :

Ec: modulus of elasticity in (MPa)

S_2= stress corresponding to 40% of the ultimate load, in (MPa).

S_1= stress corresponding to a longitudinal strain, ϵ_1, of (0.000050), in (MPa), and ϵ_2= longitudinal strain at stress S_2.

Plate 3. 13 Modulus of elasticity test

3.9 Test Setup and Instrumentation

All piers were tested up to failure using a hydraulic testing machine with 1000 kN ultimate capacity. Ten of pier specimens was tested at the laboratory of the department of civil engineering in kerbalaa university because it agree with the load condition ,the another three of them test at university of kuffa at laboratory of civil engineering department, as shown in Plate (3.14).

Plate 3. 14 Hydraulic esting machine of concrete piers

3.9.1 Deflection Measurements

The deflection corresponding to the applied load was measured at every load step by a dial gauge of accuracy 0.01 mm installed at the right and left mid-span of the cantilever part of pier cap as shown in Figure (3.18).

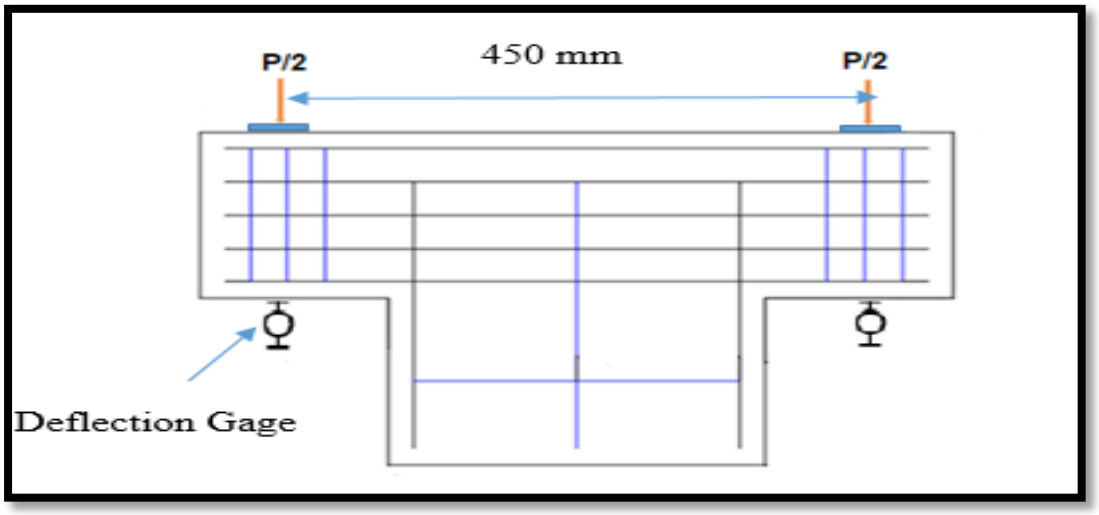

Figure 3. 9 The Layout of points loads and the deflection gages for pier specimens

3.9.2 Crack Width

Concrete can only resist small tensile strain before it cracks. As these cracks do not form at equal spacing, crack widths may vary in size and particular care was taken to measure the crack widths at all load stages. In order to have a consistent means of measuring crack widths, a microscope with an accuracy of 0.05 mm was used to determine the width of cracks as shown in Plate (3.15).

Plate 3. 15 Microscope used in the present study.

3.10 Testing Procedure

After the curing of samples had completed (after 28 days), the pier specimens were removed from water basins. Then, it was cleaned and painted by white color in order to clarify cracks and distinguishing the failure modes. The load was applied at two points of steel plates (200×60×6 mm) under the rigid rode with 75 mm from each side of the center in the longitudinal direction of the pier cap as shown in Figure

(3.18) and plate (3.15). The load was applied progressively up to the failure of the pier or when the deflection increases at constant load. The increment of the load was about 30 kN. At each load addition, notes of crack development on the concrete piers were traced. Also, the first visible cracking load, reading of dial gauges, and crack width were documented.

Chapter Four

Chapter Four
Experimental Results and Discussion

4.1 Introduction

This chapter displays the experimental test results of the behavior of reinforced concrete piers specimens. The mechanical properties of various concrete mixes are also presented in this chapter. Such properties included the effect of recycled concrete aggregate (RCA) that was used in producing the green concrete (GC), the effect of recycled steel fibers (RSF) on the mechanical properties of green concrete (GC) samples, the effect of high strength concrete (HSC) mix on piers specimens behavior, and the effect of two types of fiber reinforced polymer (FRP) bars on the behaviors of pier specimens. The effects of these variables were studied and discussed in terms of the first crack, crack width, load-deflection behaviour, and the ultimate load capacity.

4.2 Mechanical Properties of Concrete

The mechanical properties of concrete samples tested in this study included compressive strength, splitting tensile strength, and modulus of elasticity. The average values of the three samples were recorded to represent each mechanical property at each age.

4.2.1 Compressive Strength Results

The compressive strength, as one of the most important properties of hardened concrete, is in general, the characteristic material value for the classification of concrete in many codes. Standard cylinders of size 200 mm in height and 100 mm in diameter were utilized at ages of 7, 14, 28 days. Three cylinders are tested at each age for the sake of compressive strength determination for different types of concrete (normal concrete (NC), green concrete (GC), green high strength concrete (HSC) and green

concrete with 2% volumetric ratio of recycled steel fibers (RSF)). The compressive test results are given in Table (4.1) and drawn in Figure. (4.1).

Table 4. 1 Compressive Strength Results

Mix symbol	Compressive Strength (MPa)		
	7 days	14 days	28 days
NC	19.4	23.7	29.5
GC	17.9	26.3	29.1
RSF	18.7	23.6	35.0
HSC	32.1	38.7	47.2

It can be seen from the compressive strength values of different mixes that the GC mix has normally the lowest values, which could be due to the higher air content. However, its value was structurally acceptable and was nearly close to NC mix value. The compressive strength increased to a higher value due to the use of recycled steel fiber (RSF) (see Table (4.1). The failure modes of the tested compressive cylinders are shown in Plate (4.1).

(NC) (GC) (RSF) (HSC)

Plate 4. 1Compression failure modes of different concrete specimens

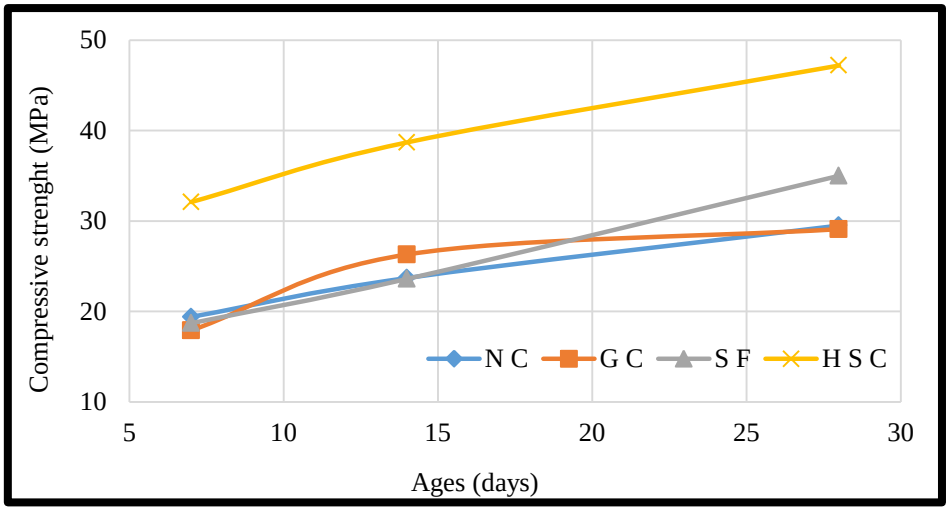

Figure 4. 1 Compressive strength development at dfferent ages

It is worth to mention that GC exhibited 28 days compressive strength value that was very close to NC by (6.7%). However, these values increase to (+14.7%) for RSF mix. While for HSC, the increase above the compressive strength of NC was about (30%) at the age of 28 days.

4.2.2 Splitting Tensile Strength

The splitting tensile strength governs the cracking behaviour and affects other properties, such as durability of concrete. In this research, the splitting tensile strength of concrete was measured following the procedure described in chapter three. The results of tests at ages (7, 14, and 28) days are given in Table (4 .2). The rate of development of tensile strength between 7 and 14 days was 11 %, 16.8 % 20 % and 13.7 % for NC, GC, RSF, and HSC mix respectively. Plate (4.2) shows the failure modes of these concrete specimens.

Table 4. 2 Splitting Tensile Strength Results

Mix symbol	Splitting Tensile Strength(MPa)		
	7 days	14 days	28 days
NC	2.76	3.06	3.47
GC	2.49	2.91	3.25
RSF	2.97	3.58	3.98
HSC	3.72	4.23	4.52

Plate 4. 2Failure splitting modes of different concrete specimens

4.2.3 Modulus of Elasticity Test Results

The modulus of elasticity was tested for each mix using the average value of three samples of cylinders with the dimensions of 100 mm in diameter and 200 mm in height. The vertical displacement has been measured when the load applied by the compressive state. Table (4.3) shows the value of modulus of elasticity for each mix. The results showed that the modulus of elasticity for NC was higher than GC by about 4.8%. For RSF, the modulus of elasticity was greater than those of GC by 13.6%. It was also observed that there is an increase in the modulus of elasticity by 32.6% when using HSC in comparison with GC.

Table 4. 3 Modulus of Elasticity Results

Mix Designation	Modulus of Elasticity (GPa) (28)days
NC	26.5
GC	25.3
RSF	28.7
HSC	33.5

4.3. Hardened Density

The air-dry density was tested for each mix (NC, GC, RSF, HSC) using the average of three samples as described in chapter three. The results are presented in Table (4.4).

Table 4. 4 Results of the Density of Different Concrete Mixes

Mix Notation	Date of Test (days)	Density g/cm^3
NC	7	2.307
	14	2.438
	28	2.485
GC	7	2.315
	14	2.371
	28	2.343
RSF	7	2.325
	14	2.359
	28	2.343
HSC	7	2.449
	14	2.450
	28	2.412

4.4 Experimental Results of Pier Models

In this research, there were five parameters to be studied by pier models as follows:

Case study 1 investigates the effect of replacement 50% natural coarse aggregate (NA) by recycled coarse aggregate (RCA) to produce green concrete (GC) using the same reinforcement as reference (control) pier model.

Case study 2 considers the effect of recycled steel fibers (RSF) that were added to GC mix at 2% volumetric ratio in the pier cap only (TRSF), pier cap and half of the column pier (HRSF), and whole pier specimen (ARSF). All piers have identical reinforcement pattern and were similar to the reference pier specimen NC.

Case study 3 examines the effect of green high strength concrete (HSC) on structural pier behavior in which such concrete would be used at pier cap only and green concrete at column pier (**THSC**), in pier cap and half of the column pier (**HHSC**), and in the whole pier (**AHSC**). Pattern and distribution of steel reinforcement were similar to the reference model.

Case study 4 inspects the influence of CFRP bars on the overall structural behaviour of the reinforced concrete pier specimen. Two piers specimens reinforced with CFRP bars with (Ø10 and Ø 6 mm) in diameter in which one of them uses CFRP bars for all layers of pier cap (longitudinal reinforcement) in specimen **TCFRP** while the other has used CFRP bars at only the top two layers in the specimen (**T1CFRP**). **Case study 5** studies the influence of GFRP bars (Ø10 and Ø6 mm) in diameter on the overall behaviour of the reinforced concrete pier specimen. Three pier specimens use this type of reinforcement in which two of them use the bars as the main reinforcement and the third one uses

GFRP for stirrups reinforcement only. The specimen **TGFRP** pier uses GFRP bars for all layers of pier cap, while the specimen **T1GFRP** pier uses GFRP bars at the top two layers only. Indeed, the last specimen (**SGFRP**) uses Ø6mm GFRP bars for stirrups pier cap only.

4.4.1 Cracks and Failure Loads

The cracks have been monitored during testing all pier models to get a good comparison in cracking behavior as illustrated in Table (4.5).

Table 4. 5 Failure Load, First Crack Load, First Crack Width, and Maximum Crack Width for Tested Pier Specimens

Pier symbol	Ultimate Load Wu (KN)	First Crack in Tension Face		Wi*/Wu %	Crack Width (70% Wu) (Service Load) (mm)	Maximum Crack Width (mm)
		Load (KN)	Width (mm)			
NC	538	200	0.1	37.17	1.22	2.3
GC	525	180	0.1	34.29	1.7	3.5
TRSF	550	238	0.08	43.27	1.4	2.3
HRSF	557	276	0.09	49.55	1.35	2.35
ARSF	572	292	0.08	51.05	1.32	2.2
THSC	680.7	320	0.1	47.01	1.51	3.65
HHSC	700	351	0.1	50.14	1.23	3.6
AHSC	718	354.6	0.09	49.39	1.2	3.5
TCFRP	561	265	0.09	47.24	1.3	2.5
TGFRP	489.9	181	0.11	36.95	2.4	4
T1CFRP	548	243	0.09	44.34	1.5	2.7
T1GFRP	502	175	0.1	34.86	1.9	3.2
SGFRP	530	168	0.13	31.70	2.8	5.5

*wi= first cracking load

The ultimate load was recorded when the deflection started with increasing at the constant load. For NC pier specimen the results showed

that the failure was occurred by splitting the concrete cover. For GC pier specimen, the failure was also occurred by splitting the concrete cover, however, the maximum load was less than that for NC. The cracks were also lower due to the effect of the existing recycled steel fiber (RSF) in the mix. This effect was noticed in the piers TRSF, HRSF, and ARSF. The effect of HSC mix was noticed in all piers that were cast with such concrete type, which were THSC, HHSC, and AHSC. It was also observed that using HSC mix caused an increase in the maximum capacity and a decrease in the deflection. The use of CFRP bars at pier cap increased the capacity of specimens reinforced with this type of reinforcement, as well as a decrease in the deflection under various loads. Indeed, it has been noticed that the use of GFRP bars at the pier cap had a marginal effect on the capacity of the specimen. However, the use of GFRP bars as stirrups with steel reinforcement in the pier cap found to have a limited influence on the ultimate load and the deflection.

4.4.2 General Behavior and Crack Patterns

The general behaviours of the tested pier models were different according to its case parameter and the early stages of loading. The behavior was generally within the inelastic ranges, which shows linear deformations. Thereafter, the behavior has been changed with the increase in load until the first crack appears at the piers face at about 31.7% to 51% of the ultimate load as can be seen in Table (4.5). The numbers and widths of cracks generally increased and distributed downward with the load increase. The parametric study of the behaviour of reinforced concrete piers in term of first crack load, crack width, ultimate load, load-deflection curves, cracks pattern, and failure modes will be presented and discussed in the next sections. The crack patterns for all pier models tested are shown in Plate (4.3).

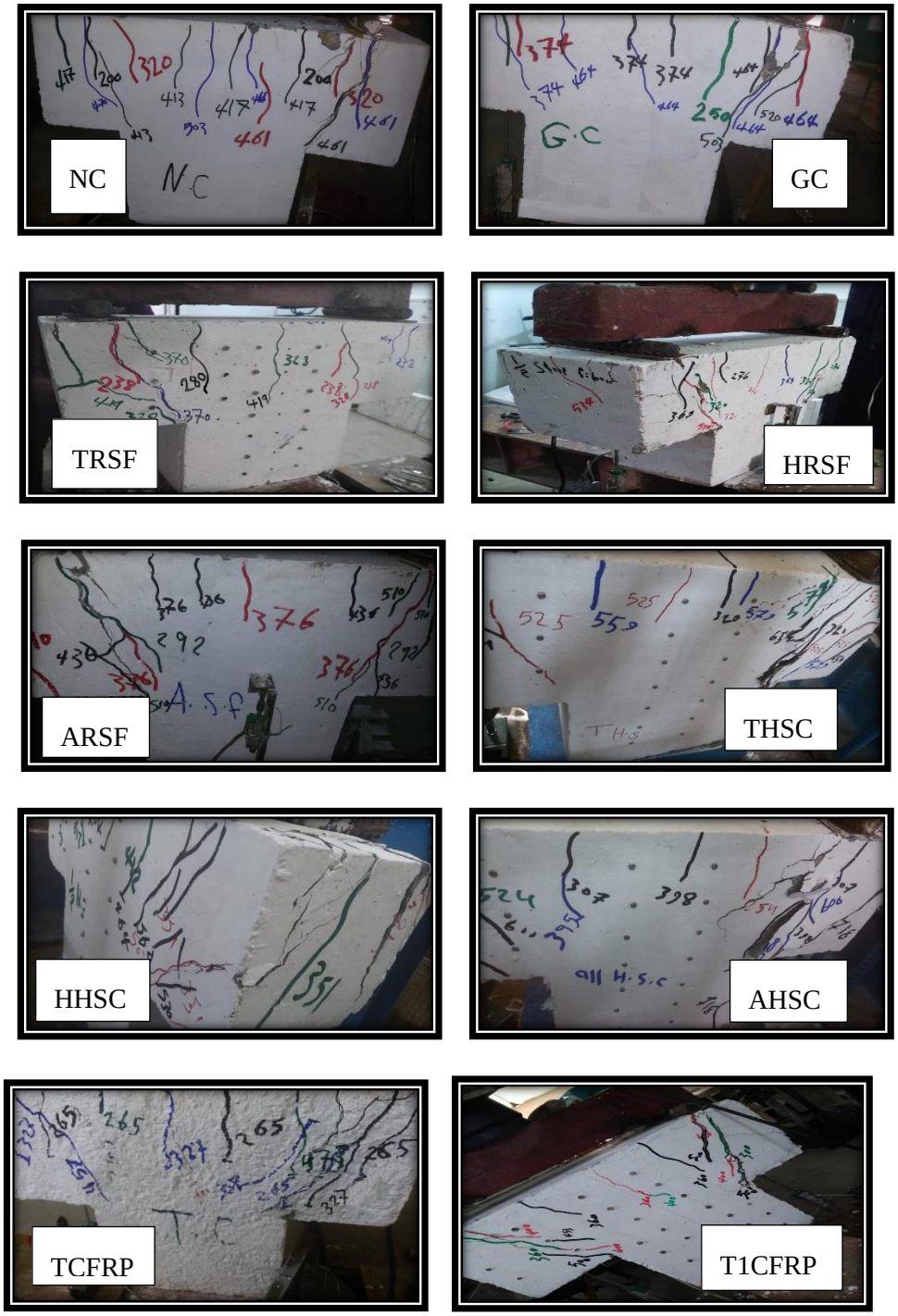

Plate 4. 3**Crack Patterns at the Failure Stage For Various Tested Pier Models**

Plate 4. 3: Continued

4.4.3 Crack Width

The propagation of cracks has been noticed and the crack width was recorded for each 30 kN of specimens loading. This monitoring was continued until reaching the ultimate loads. Table (4.5) shows the maximum crack width at failure as well as at 70% of the ultimate load. For reference pier (NC), the first crack was recorded at a load of 200 kN with 0.1 mm wide flexural crack, which was closed to the middle of pier cap propagated from the top surface. At service load (70% of the ultimate load), this pier recorded a crack width of 1.22 mm at a load of 417 kN and the first crack widened to 1.33 mm. Further loading to nearly 530 kN resulted in further cracks with a maximum crack width of 2.3 mm.

Pier GC recorded the first crack at 180 kN with a crack width of 0.1 mm, a maximum crack width of 3.5 mm at 520 kN, and crack width of 1.7 mm at the service load.

For pier TRSF, the first crack width was 0.08 mm to be developed to reach 1.4 mm at the service load with a maximum crack width of 2.3 mm. The first crack width was 0.09 mm and 0.8 mm for HRSF and ARSF with

a maximum crack width of 2.35 mm and 2.2 mm respectively. From these results, it can be noticed that the use of recycled steel fiber minimized the maximum crack width, resulting in increasing the durability of reinforced concrete piers.

Piers that cast using high strength concrete (HSC) have a first crack width of (0.1 mm, 0.1 mm, and 0.09 mm) for THSC, HHSC, and AHSC respectively. Moreover, at 70% of ultimate load, the crack width developed to reach a value of (1.51 mm, 1.23 mm, and 1.2 mm) as well as a maximum crack width of (3.65 mm, 3.60 mm, 3.50 mm) respectively. On the other hand, the first crack width was 0.09 mm for TCFRP and T1CFRP. Then,

cracks were propagated to reach a value of (1.3 mm and 1.5 mm) at the service load respectively.

Piers reinforced with GFRP showed a little effect on the first crack width and maximum crack width as well. Results showed that the first crack width was (1.11 mm, 1.10 mm, and 1.30 mm) for TGFRP, T1GFRP, and SGFRP piers respectively.

4.5.Ultimate Load and Failure Mode

For all pier specimens, the ultimate load was recorded when the deflection started with increasing at the constant load. The deflection was recorded by using several dial gauges placed under each pier specimen at the center of the two cantilever parts of the pier cap. Another dial gauge was placed at the center of the pier face to measure the column deflection but neglected it is reading due to its small value that approaching zero. Table (4.6) gives the value of the recorded ultimate load, deflection and failure modes for each pier specimen.

Table 4. 6 Ultimate Load, Deflection and Failure Mode for Tested Pier Specimens

Pier Symbol	Ultimate load (kN)	Deflection (mm)			Failure mode
		Dial gauge 1	Dial gauge 2	Average	
NC	538	6.5	6.68	6.59	Splitting of concrete covers
GC	525	6.76	8.86	7.81	Splitting of concrete covers
TRSF	550	5.12	5.88	5.5	Direct shear
HRSF	557	5.29	5.55	5.42	Direct shear
ARSF	572	4.81	5.73	5.27	Direct shear
THSC	681	5.41	3.51	4.46	Splitting of concrete covers
HHSC	700	4.14	4.62	4.38	Direct shear
AHSC	718	3.82	3.98	3.9	Direct shear and Splitting of concrete covers
TCFRP	561	4.78	5.7	5.24	Direct shear
TGFRP	490	7.3	7.82	7.56	Direct shear
T1CFRP	548	5.42	5.62	5.52	Direct shear
T1GFRP	502	7.65	7.91	7.78	Splitting of concrete covers
SGFRP	530	4.87	5.95	5.41	Splitting of concrete covers

It is clear from Table (4.6) that the failure mode of NC pier was a splitting of the concrete covers. For GC specimen, the failure was also by splitting of concrete covers, however, the maximum load was less than

that of NC specimen due to use a recycled aggregate that has mortar adhered to the aggregate. For piers cast with GC in addition to recycled steel fiber, the ultimate load increased while the deflection was decreased. The cracks width was less because of the effect of steel fiber in the RSF mix, which can be noticed in piers TRSF, HRSF, and ARSF. This could be due to the fibers existence that improves the flexural strength of the mix. The mode of failure for these piers was by direct shear when the deflection increased with a constant load. It is also noticed that failure types varied from one pier to another in HSC piers. For THSC pier, the failure was by splitting of concrete covers. While HHSC pier failed by direct shear at a load of (700 kN). Pier AHSC failed suddenly by direct shear and splitting of concrete cover at load (718kN).

The effect of CFRP bars was noticed in piers TCFRP and T1CFRP. It was observed that failure mode was by direct shear, while piers with GFRP bars in TGFRP, T1GFRP, and SGFRP failed by direct shear and splitting of concrete cover for TGFRP, T1GFRP and SGFRP piers respectively. The shear failure is initiated by a major diagonal crack, which extended horizontally at the level of the GFRP bars indicating a bond failure.

4.6 Load-Deflection Curves for Various Pier Models

The load-deflection curves for all tested piers specimens including the reference pier (NC) and other piers, which will be illustrated succinctly in this section.

4.6.1 Load-Deflection Behavior of NC Pier

The ultimate load of the NC pier was recorded at 538 kN when the deflection started with increasing at the constant load. This failure occurred by splitting of concrete cover.

4.6.2 Load-Deflection Behavior of GC Pier

The experimental results of GC pier with 50% replacement ratio of recycled coarse aggregate showed that the ultimate load of the GC pier was less than those of normal concrete NC pier by about 2.4%. It was also found that the deflection of GC pier at the ultimate load was greater by 18.5% than NC. Figure (4.2) shows the load-deflection curves of NC and GC piers.

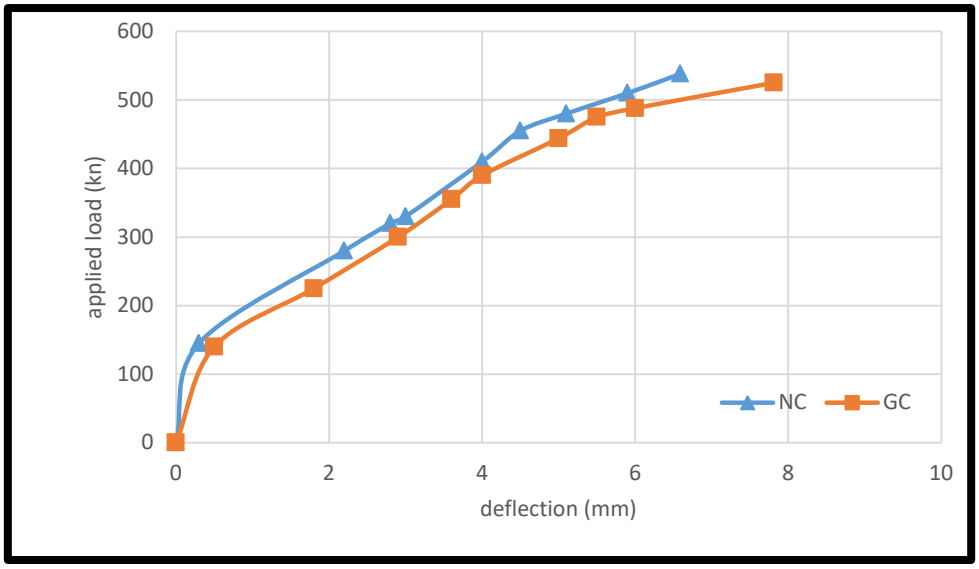

Figure 4. 2 Load-Deflection Relation of NC and GC Specimens

4.5.3 Load-Deflection Behavior of RSF Piers

Recycle steel fiber was added to the green concrete mix with 2% vol. ratio to improve the mechanical properties of concrete such as compressive and tensile strengths. The experimental results showed that adding RSF to the mix has improved the overall behaviour of piers. For (TRSF) pier ultimate load was increased by 4.76% in comparison with GC, and a decrease of deflection by 29.58% in comparison with GC. Increasing RSF from pier cap to part of column pier for HRSF pier led to improving the ultimate load by about 1.27% and decrease deflection by about 1.48%. Adding RSF for all pier for the specimen (ARSF) led to increasing the ultimate load by 8.95% from (GC). and by 4% and 2.69%

from (TRSF) and (HRSF) respectively. For deflection adding RSF for all pier for the specimen (ARSF) led to decrease deflection by about 32.52% from (GC) and (4.18%, 2.77%) from (TRSF) and (HRSF) respectively. This increase in the ultimate load of models is due to the addition of recycled steel fibers which significantly improves many of the engineering properties of mortar and concrete, notably impact strength and toughness. Flexural strength, tensile strength and the ability to resist cracking are also enhanced.

Figure (4.3) show the effect of RSF on the load-deflection curves.

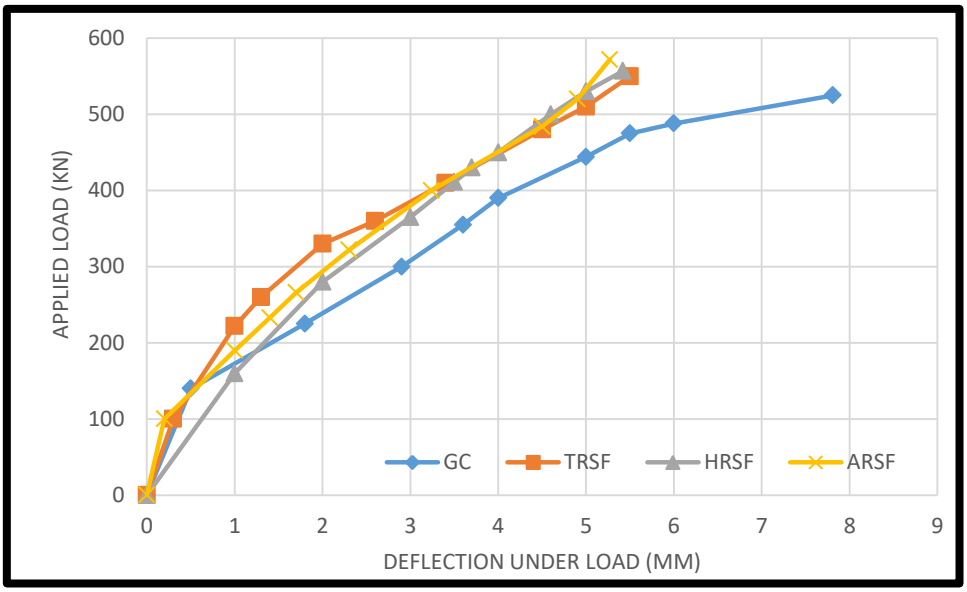

Figure 4. 3 Load- Deflection Behavior of RSF Specimen

4.6.4 Load-Deflection Behavior of HSC Piers

The use of high strength concrete (HSC) mix improved the mechanical properties of piers. For THSC pier with high strength concrete at pier cap only, the ultimate strength was greater than GC pier by 29.7%. Also, the deflection decreased by about 42.89% in comparison with GC. Furthermore, the using of HSC to the half-column pier (HHSC pier) increased the ultimate strength by about 33% when compared with GC pier. It has been also noticed that using high strength concrete for all

specimen (AHSC) increased the ultimate strength by 36.7% when compared with (GC). In addition, the use of high strength concrete for all pier specimen improved the ultimate strength by 5.48% and 2.57% greater than (THSC) and (HHSC) respectively. It is also noticed that the deflection decreased by about 12.56% from (THSC) and 10.96% from (HHSC). These results may be due to the effect of high strength mix with a lower amount of water to cement that led to higher rigidity and hardened concrete. Figure (4.4) show the load-deflection curve for (HSC) piers.

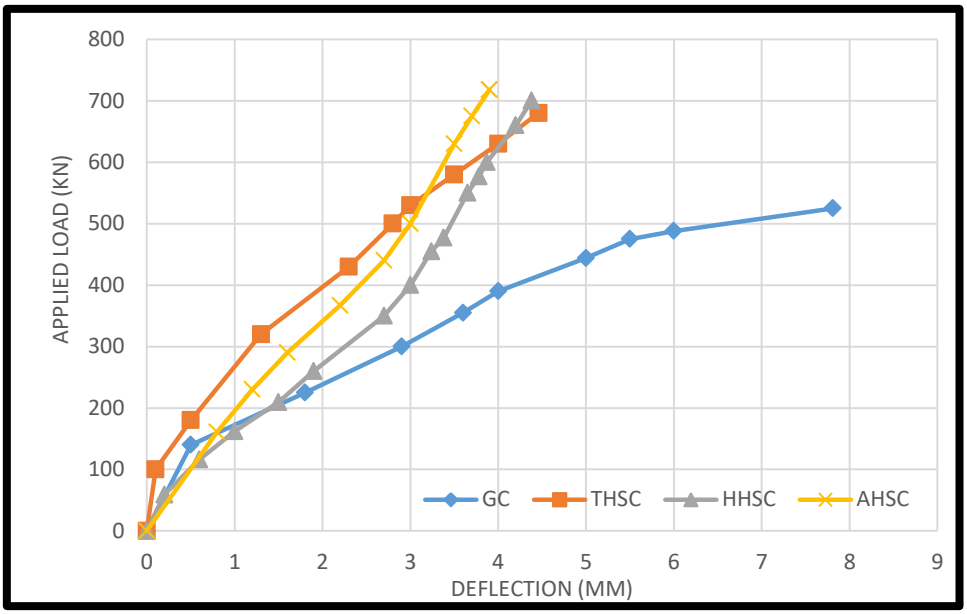

Figure 4. 4 Load-Deflection Relation of HSC Pier Specimens

4.6.5 Load-Deflection Behavior of CFRP Piers

The use of carbon fiber reinforced polymer to reinforce all layers of pier cap with steel reinforcement stirrups for TCFRP pier can increase the ultimate capacity by the rate of 6.86% in comparison with GC pier that reinforced with steel reinforcement. This increase in capacity due to the improvement in the performance of the structural member such as its load carrying capacity, and stiffness. It was also observed that at the ultimate load and the deflection decreased at a rate of 32.91% greater than (GC).

Furthermore, the use of CFRP bars at T1 (first two layers of reinforcement) for T1CFRP pier, found to have a positive effect on the ultimate strength by a per cent of 4.19% larger than (GC). It has been also noticed that the deflection decreased by 29.32% than (GC). From these results, it can be concluded that the use of CFRP bars for all pier cap layers reinforcement was more effective than T1 reinforcement only regarding the ultimate strength and deflection by about 2.56% for strength and 5.07% for deflection. Figure (4.5) show the effect of CFRP bars on the load-deflection curves. This reduction in deflection may be attributed to the increase of pier stiffness and rigidity.

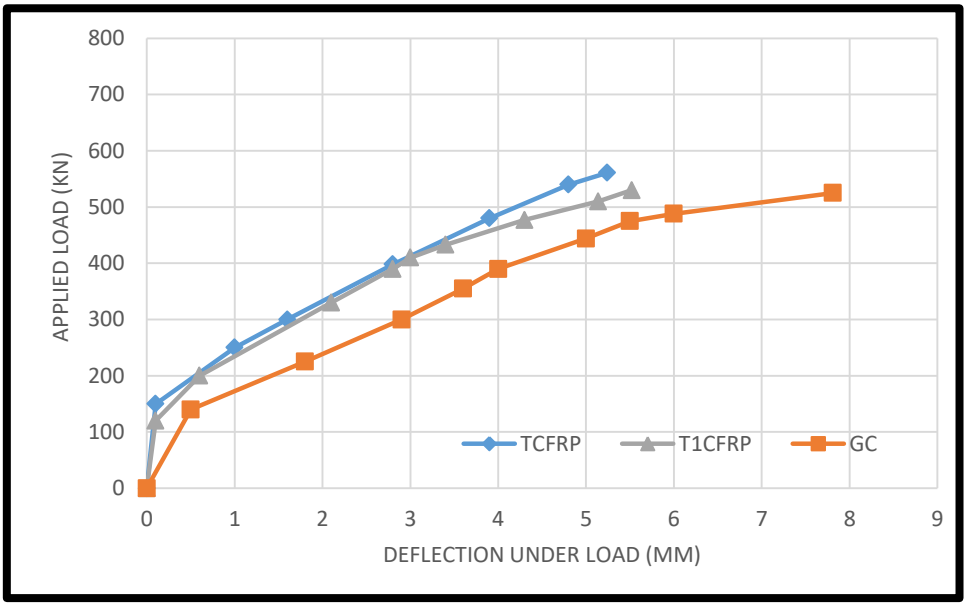

Figure 4. 5Load-Deflection Relation of CFRP Specimens pier

4.6.6 Load-Deflection Behavior of GFRP Piers

The results of reinforcing piers by glass fiber reinforced polymer (GFRP) showed that the ultimate load of the (TGFRP) and (T1GFRP) piers was lower than those for GC, which reinforced with steel reinforcement by about 6.69% and 4.38% respectively. This may be due to the reason that GFRP is anisotropic and nonhomogeneous nature, and the compressive

modulus is lower than the tensile one. The compressive strength and compressive modulus are around 50 per cent and 80 per cent of its tensile values respectively. GFRP bars are generally weak in transverse shear, and typical transverse shear strength ranges between (30 to 50 MPa). Bond stresses at the GFRP bar/concrete interface are transferred by the chemical bond (adhesion resistance of the interface), friction, and mechanical interlock due to the irregularity of the interface (Rinaldi, 2015). Also, it has been noticed that the deflection was larger than GC by a rate of 3.2% and 0.38% for (TGFRP) and (T1GFRP) respectively.

The last specimens that cast with green concrete and reinforced with steel reinforcement for all pier specimen except stirrups of pier cap in which GFRP bars were used. The ultimate strength of this pier was higher than (GC) specimen by 0.95% and the deflection was lower than (GC) by 30.73%, which means that GFRP bars work at shear better than flexural.

From these results, GFRP bars in compression neither increase the strength nor reduce the effects of concrete creep of GFRP reinforced concrete flexural members due to the limited compressive strength and modulus of GFRP bars. The behaviour of GFRP RC members was affected by the presence of reinforcement that does not yield and is considered to be liner-elastic up to failure as opposed to traditional RC structures, where failure is always controlled by crushing of the concrete. The Figure below shows the load-deflection curves of GFRP piers.

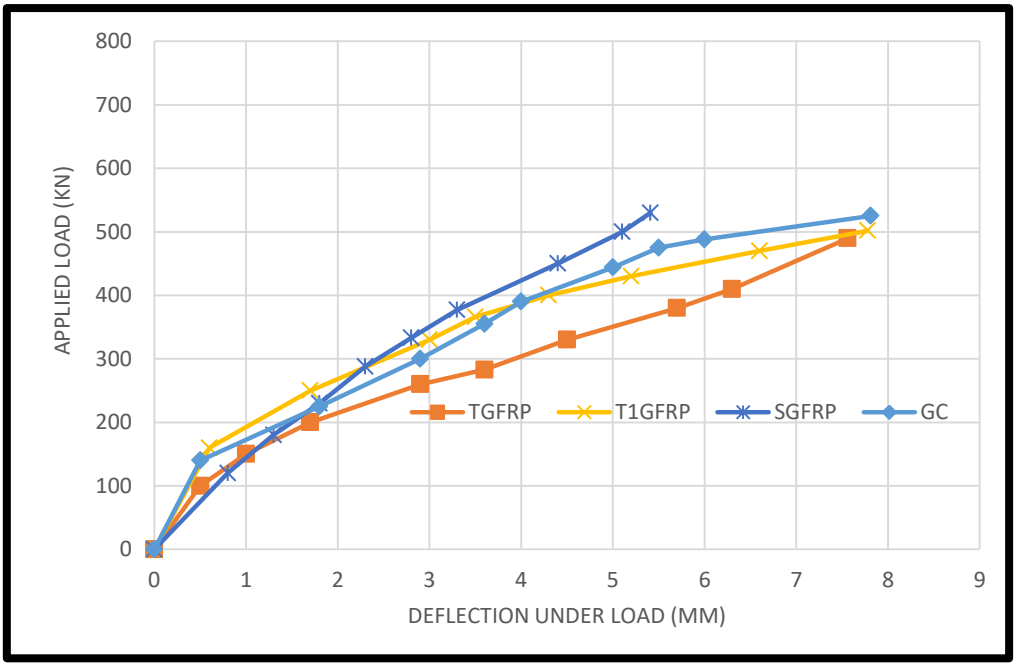

Figure 4. 6Load-Deflection Relation of GFRP Specimens pier

Chapter Five

Chapter Five
Numerical Application

5.1 Introduction

The finite element analysis method is largely used to obtain a solution for a large number of engineering problems. The origin of the modern finite element analysis method may be traced back to the early 1900 s. ANSYS program (version 17.2) was employed to satisfy this purpose. This chapter presented the modelling of pier models by ANSYS. The results included the behaviour of the load with respect to deflection and the distribution of cracks on the piers. This chapter also includes a comparison with the experimental results in term of load-deflection relationships.

5.2 Finite Element Material Modelling

Four pier models of different types of concrete (NC, GC, RSF, and HSC) have been represented using solid element (SOLID65) in ANSYS program. The SOLID65 element is defined by eight nodes having three translational degrees of freedom at each node. This element is capable of cracking in tension and crushing in compression. The geometry, location of nodes, and the system of the coordinate for this type of element are shown in Figure (5.1).

Three-dimensional bar element (LINK180) with three degrees of freedom was used for modelling steel reinforcement, CFRP and GFRP bars. Figure (5.2) shows the geometry and the location of nodes for this type of element.

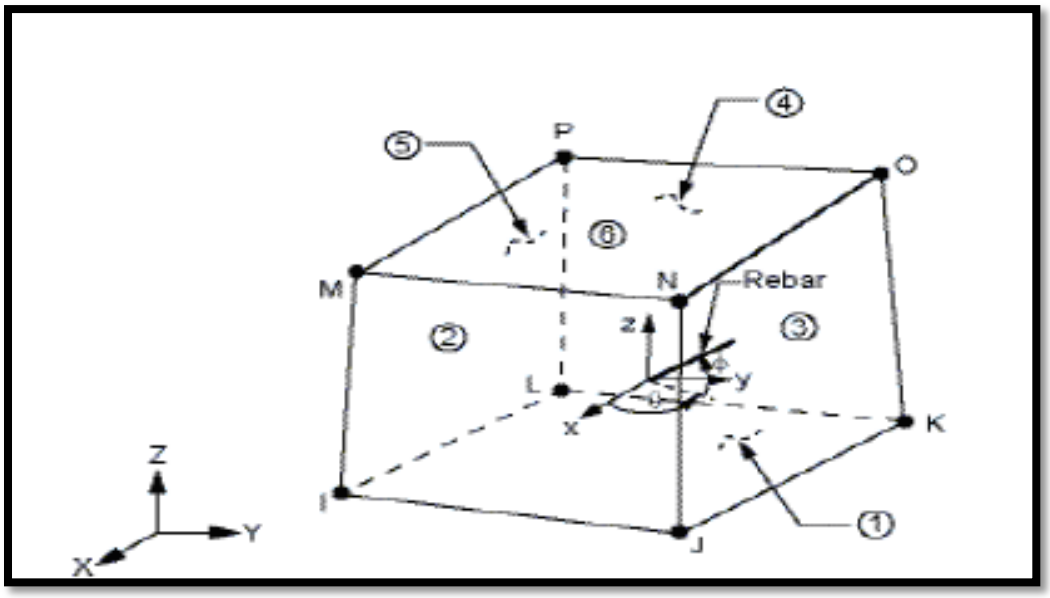

Figure 5. 1 Geometry of Element SOLID65

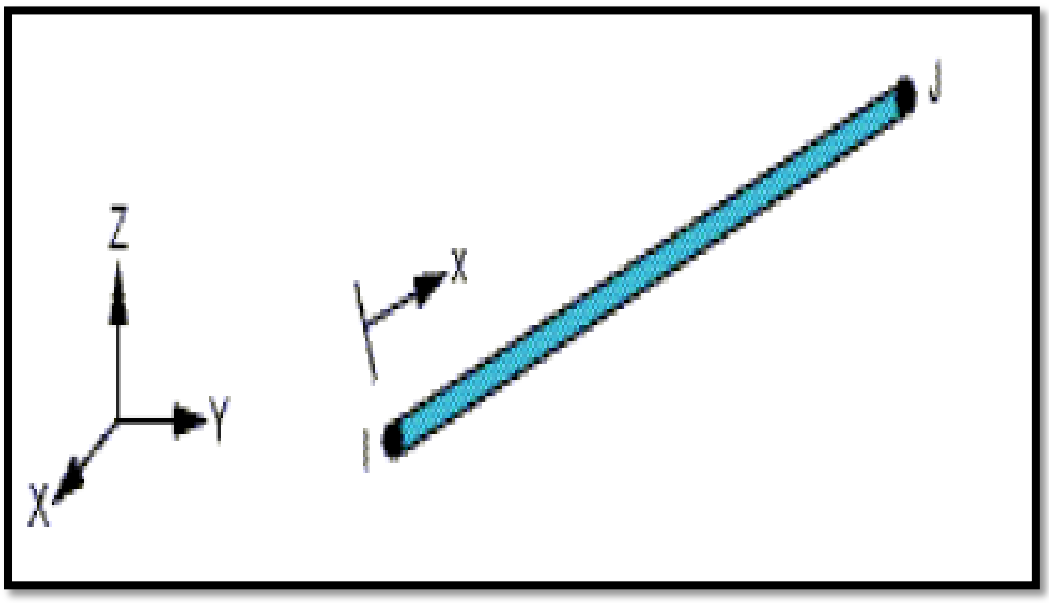

Figure 5. 2 Geometry of Element LINK 180

In order to represent steel plates used at loading and supporting points, three-dimensional brick elements (SOLID185) was also used to distribute the load in order to prevent the stress concentration problems. A schematic of the element is shown in Figure (5.3).

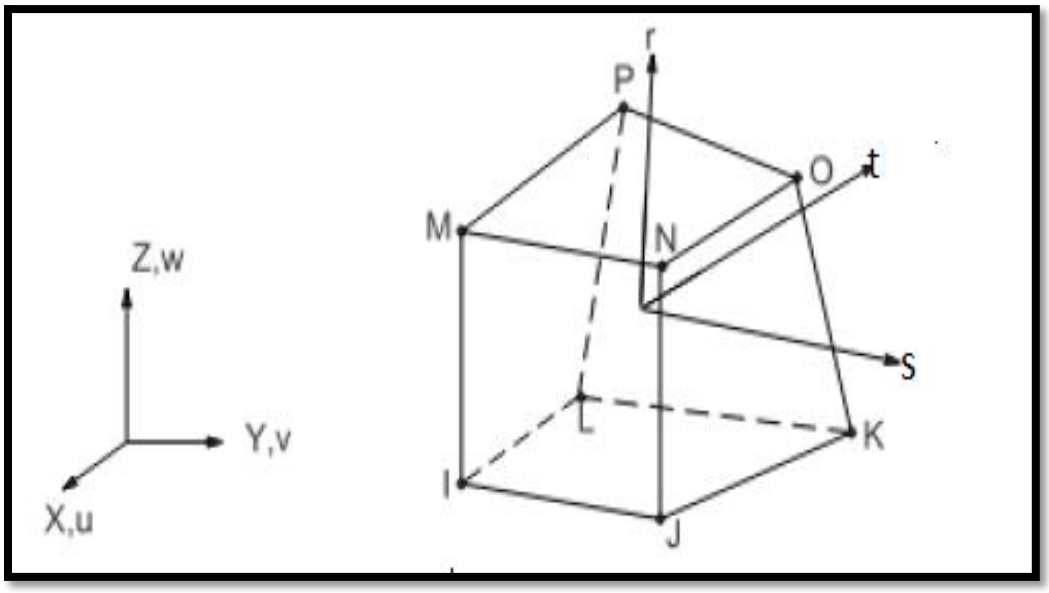

Figure 5. 3 Geometry of Element SOLID185

The main types of elements used for modelling the reinforced concrete piers are summarized in Table (5.1).

Table 5. 1 Types of the Elements used in ANSYS

Type of Material	Element in ANSYS
Concrete	SOLID 65
Steel plates	SOLID 185
Steel reinforcement, CFRP bars, and GFRP bars	LINK 180

5.3 Modeling of Reinforced Concrete Piers

In order to evaluate the results of the ANSYS program used to represent the behaviour of reinforced concrete piers, the same details of the tested piers mentioned in the experimental program in chapter three were used in the finite element modelling. The mesh modelling of concrete, steel plates, and reinforcement for piers are presented in Figure (5.4).

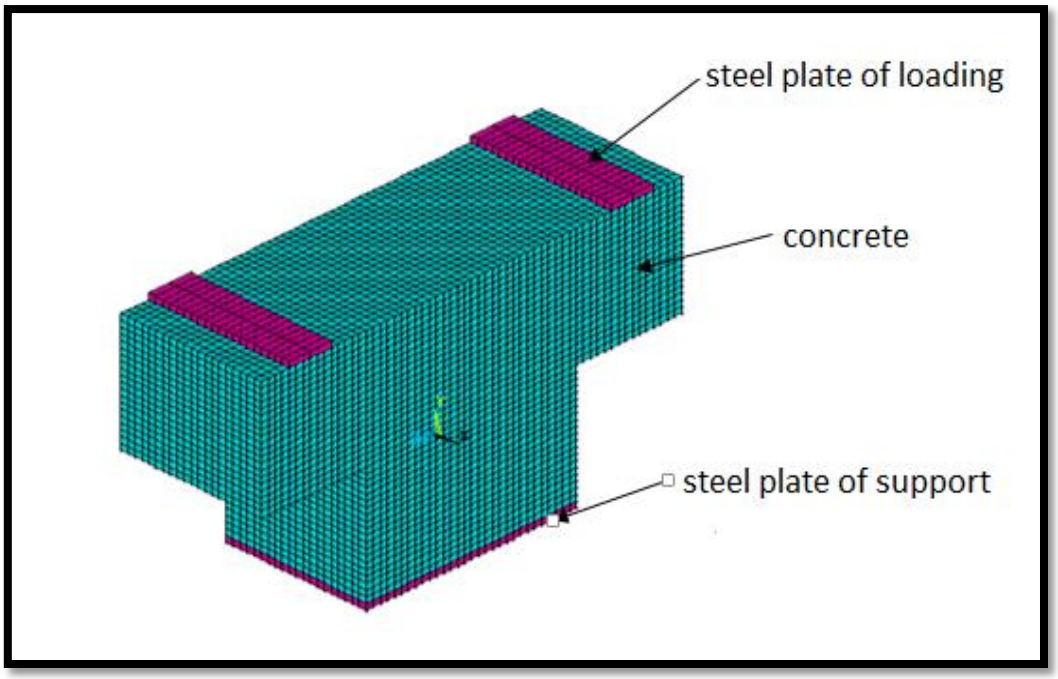

Figure 5. 4 Mesh Modeling of Concrete and Steel Plates for Pier Models

Figures (5.5) to (5.8) shows the modelling of other pier specimens that have been different properties of concrete to study the influence of each concrete material on the behaviour of each pier. They are (TRSF, HRSF, THSC, HHCS) specimens.

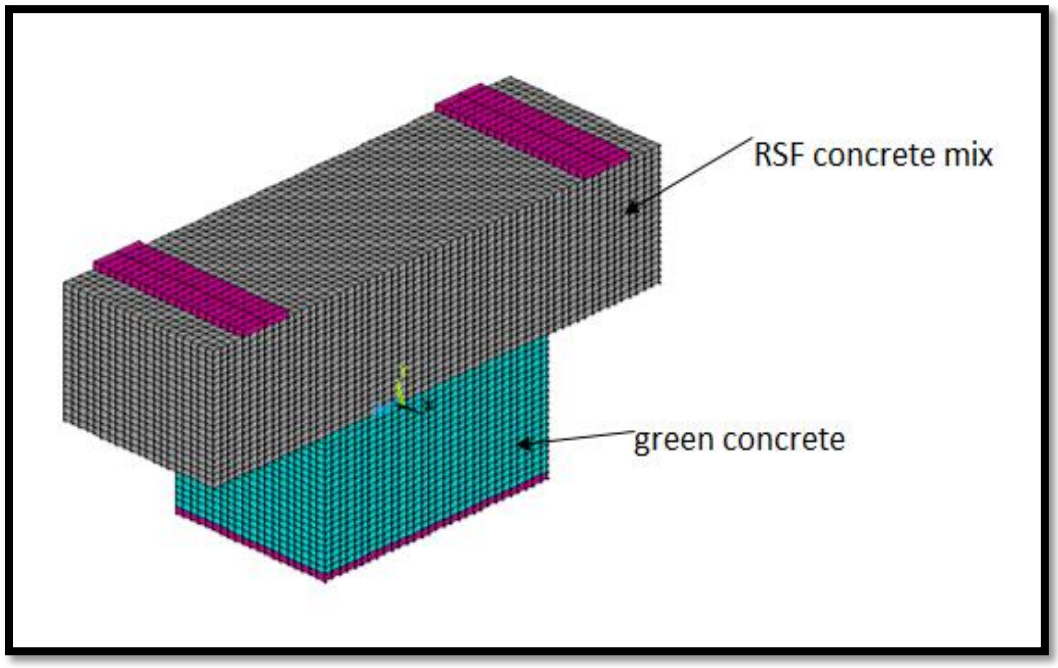

Figure 5. 5 Mesh Modeling for TRSF Pier specimen

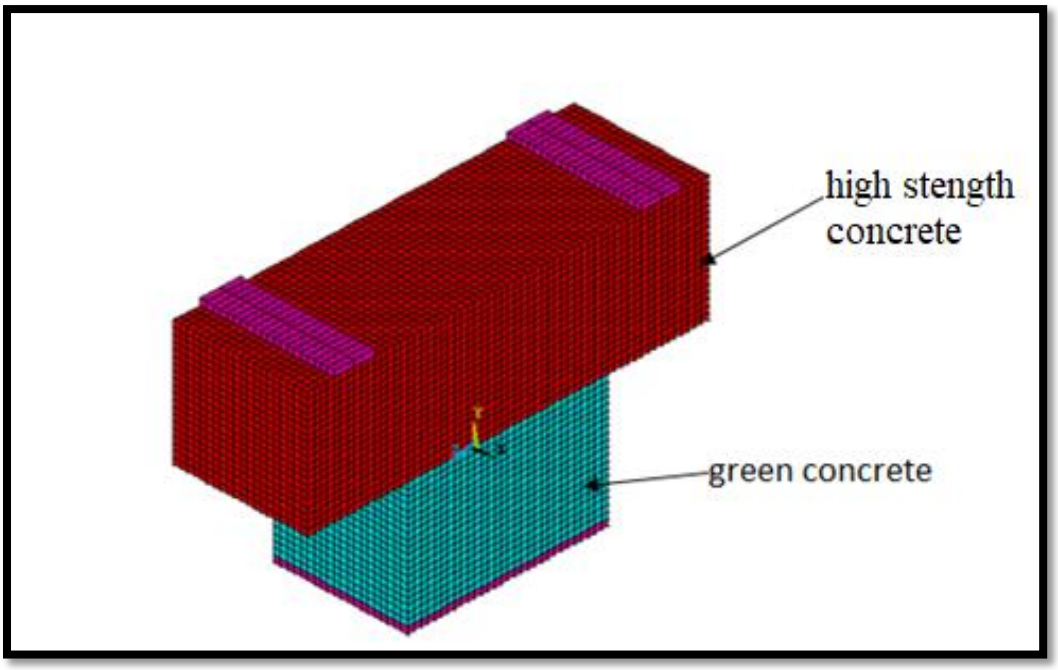

Figure 5. 6 Mesh Modeling for THSC Pier Specimen

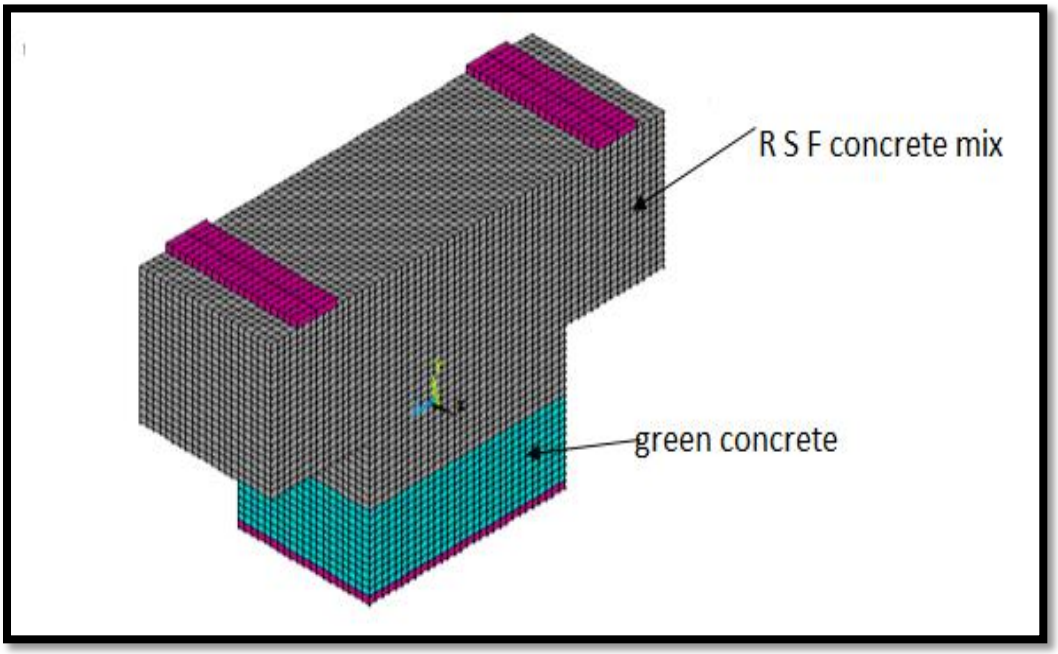

Figure 5. 7 Mesh Modeling for HRSF Pier Specimen

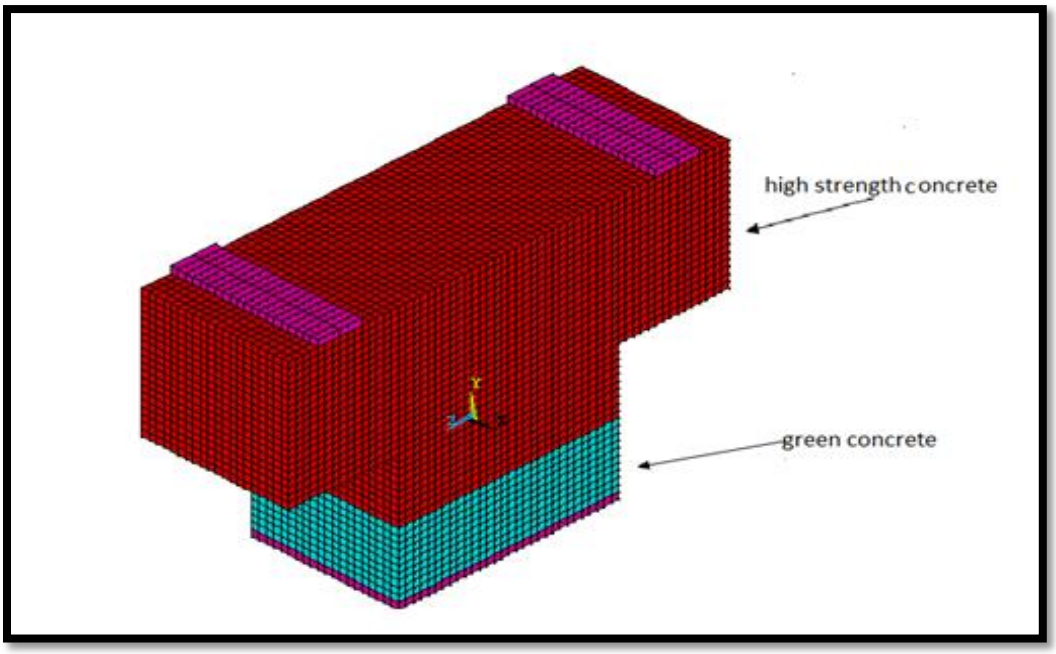

Figure 5. 8 Mesh Modeling for HHSC Pier Specimen

5.4 Loading and Boundary Conditions

As in the experimental work, the load was applied on each tested piers of two lines, these loads are represented by two steel plates of dimensions (200×60×6mm) located at the top face, which transforms the load to the piers. The total load has been distributed on nodes as shown in Figure (5.9). Displacement boundary conditions are required to constrain each model for getting a solution. The supports have been represented also by steel plates. The nodes were constrained in the X-direction, Y-direction, and Z-direction (Ux=0, Uy=0, Uz=0).

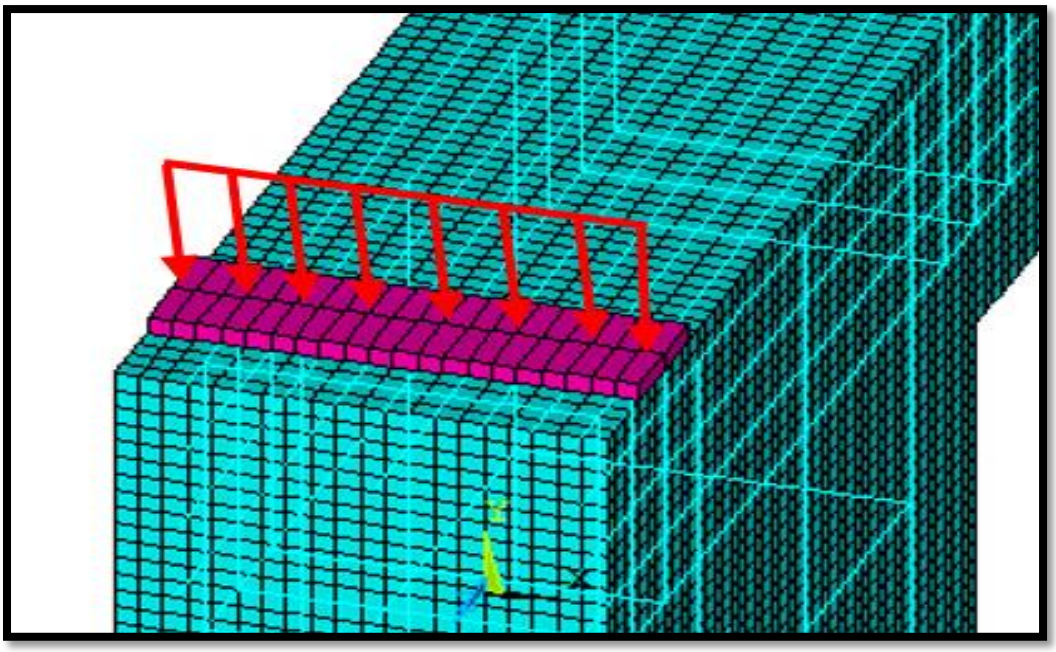

Figure 5. 9 Distribution of Applied Load on Nodes by Steel Plates

5.5 Verification Examples between Experimental and Numerical Results

The comparison between experimental and numerical results was made in term of load-deflection behaviour, crack patterns and ultimate strength and deflection.

5.5.1 Load-Deflection Behavior

A comparison between the numerical ultimate load obtained from ANSYS program, and the ultimate load obtained experimentally are presented in Table (5.2). The maximum differences in the ultimate load and the deflection reached up to (-6.72%) and (- 16.59%) respectively. The numerical ultimate load was recorded at the final step of loading after the solution has been finished when the convergence could not occur between the two successive values because the stress in steel reaches to the yield stress.

Table 5. 2 Numerical and Experimental Results of Ultimate Load and Deflection for Pier Specimens

Pier models notation	Ultimate load(Pu) kN			Deflection (mm)		
	Num.	Exp.	Δ%=(Num.-Exp.)/Exp.	Num.	Exp.	Δ%=(Num.-Exp.)/Exp.
NC	530.5	538	-1.39	6.7	6.59	1.67
GC	500	525	-4.76	8.23	7.81	5.38
TRSF	528	550	-4.00	4.87	5.5	-11.45
HRSF	540	557	-3.05	4.81	5.42	-11.25
ARSF	569.5	572	-0.44	4.76	5.27	-9.68
THSC	665	680.7	-2.31	3.72	4.46	-16.59
HHSC	680	700	-2.86	3.66	4.38	-16.44
AHSC	698.5	718	-2.72	3.5	3.9	-10.26
TCFRP	582	561	3.74	6.02	5.24	14.89
TGFRP	457	489.9	-6.72	8.46	7.56	11.90
T1CFRP	557	547	5.09	6.28	5.52	13.77
T1GFRP	470	502	-6.37	8.24	7.78	5.91
SGFRP	572	530	7.92	5.62	5.41	3.88
Average	-1.37			-1.4		

The deflection of each tested pier models has been measured at the point under the load and take the average value as the experimental test. The relation of the load-deflection curve has been figured for each increment of load and presented as follows.

Specimen No. 1 (NC)

For reference pier model NC the ultimate load of numerical analysis was lower than experimental results by (1.39%), while the deflection was greater than those of experimental result by about (1.67%). Figure (5.10) show the comparison between numerical and experimental results in term of load-deflection.

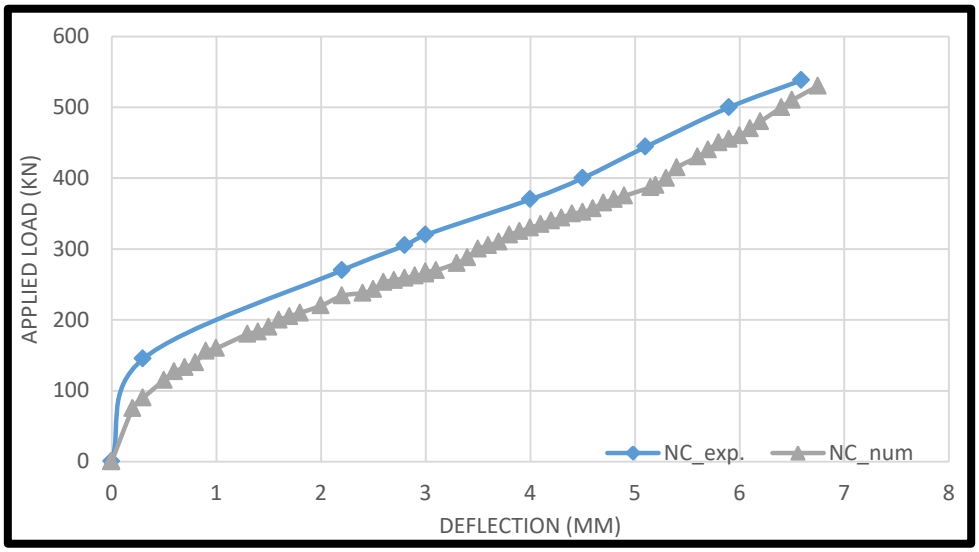

Figure 5. 10 Experimental and Numerical Load-Deflection Curves of NC Pier Model

Specimen No. 2 (GC)

Represent the green concrete pier model GC by ANSYS program to simulate its behaviour and compare with the experimental result. The result showed that the numerical ultimate load was lower than the experimental result by

4.74% while the deflection was greater than experimental by 5.38% as shown in Figure (5.11).

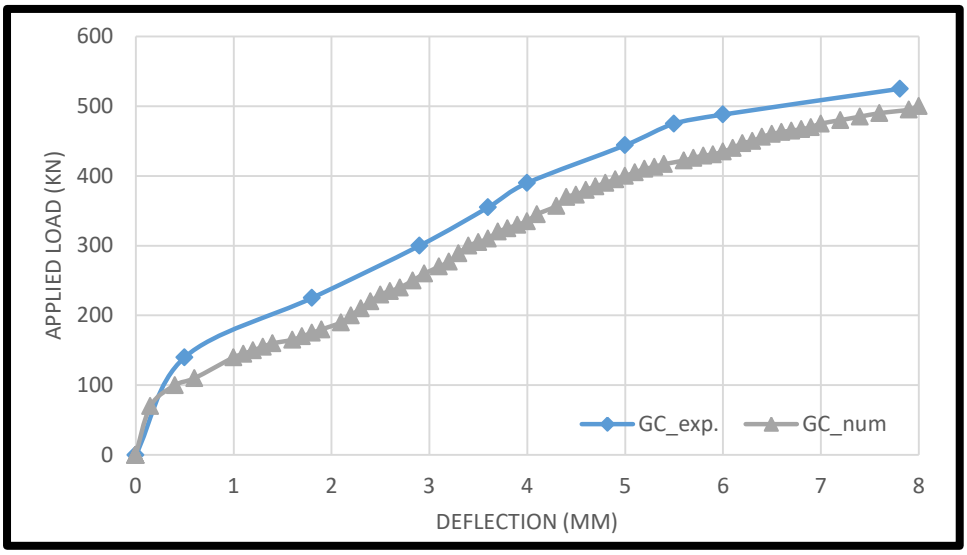

Figure 5. 11 Experimental and Numerical Load-Deflection Curves of GC Pier Model

Specimen No.3 (TRSF)

TRSF pier model represented in the ANSYS program. The results showed that the numerical ultimate load and deflection were lower than experimental results by4.0 %and 11.45 % respectively. Figure (5.12) shows a comparison between experimental and numerical load-deflection curves.

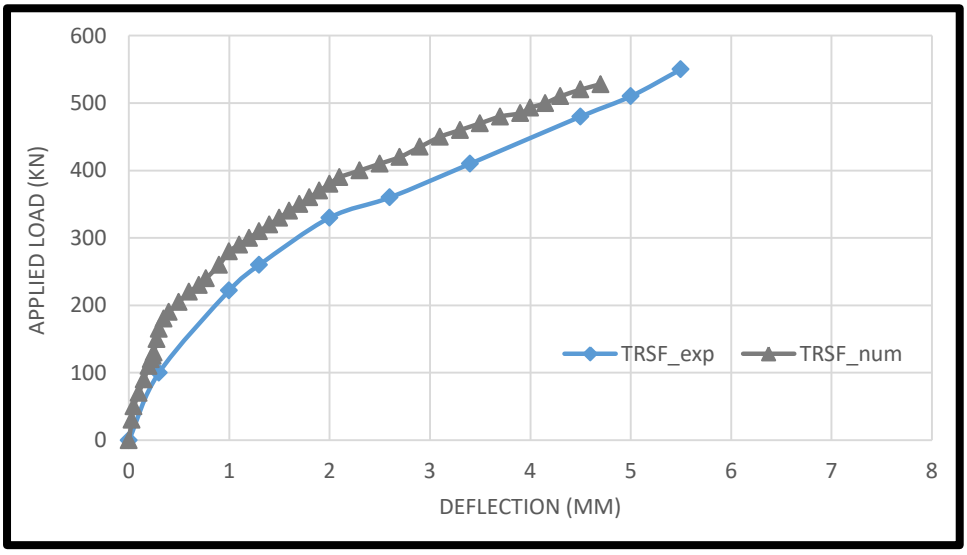

Figure (5. 12) Experimental and Numerical Load-Deflection Curves of TRSF Pier Model

Specimen No. 4 (HRSF)

HRSF pier model showed that the numerical ultimate load and deflection lower than experimental by (3.05 % and 11.25%) respectively. Figure (5.13) shows a comparison between experimental and numerical load-deflection curves.

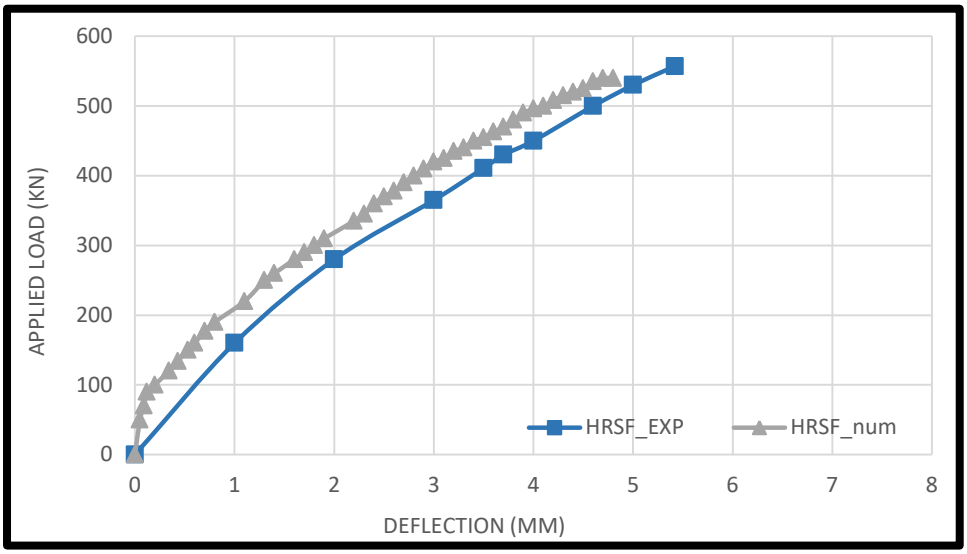

Figure 5. 13 Experimental and Numerical Load-Deflection Curves of HRSF Pier Model

Specimen No.5 (ARSF)

ARSF pier model reached 569.5 kN at ultimate load at the numerical analysis that was lower than experimental result by (0.44%), also the deflection was less than experimental by 9.68% as shown in Figure (5.14).

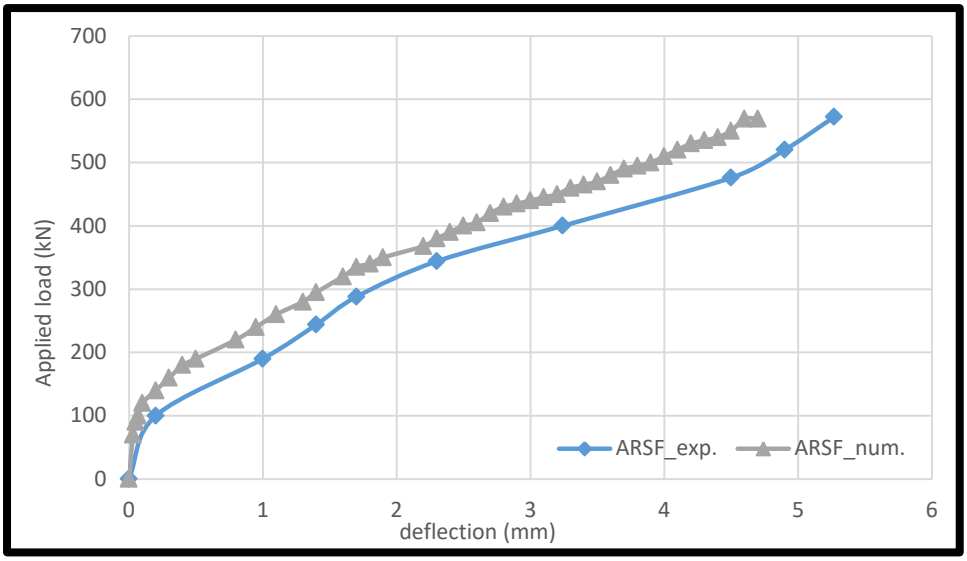

Figure 5. 14 Experimental and Numerical Load-Deflection Curves of ARSF Pier Model

Specimen No.6 (THSC)

THSC pier model exhibit ultimate load 665 kN and deflection of 3.72 mm that lower than experimental results by 2.31% and 16.59% for ultimate load and deflection respectively. Figure (5.15) presented a comparison between numerical and experimental results in term of load-deflection relationship.

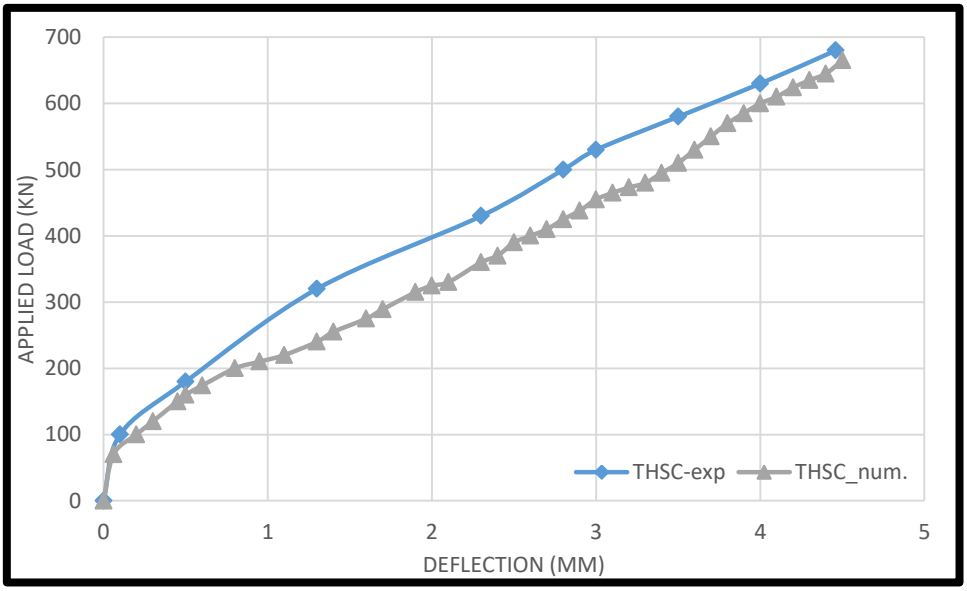

Figure 5. 15 Experimental and Numerical Load-Deflection Curves of THSC Pier Model

Specimen No.7 (HHSC)

The ultimate load for HHSC pier model as well as the deflection decreased by (2.86% and 16.44%) lower than the experimental result for ultimate load and deflection respectively. Figure (5.16) show the comparison between numerical and experimental result in term of load deflection-relationship.

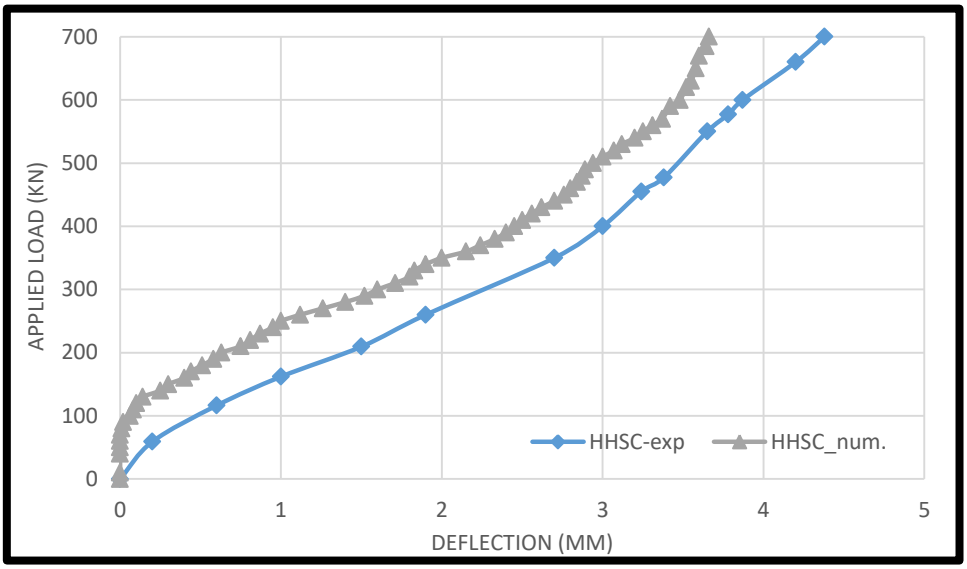

Figure 5. 16 Experimental and Numerical Load-Deflection Curves of HHSC Pier Model

Specimen No.8 (AHSC)

AHSC pier model was represented in the ANSYS program to simulate its behaviour. The result showed that the ultimate load and deflection were lower than experimental by (2.72 % and 10.26%) respectively as shown in Figure (5.17).

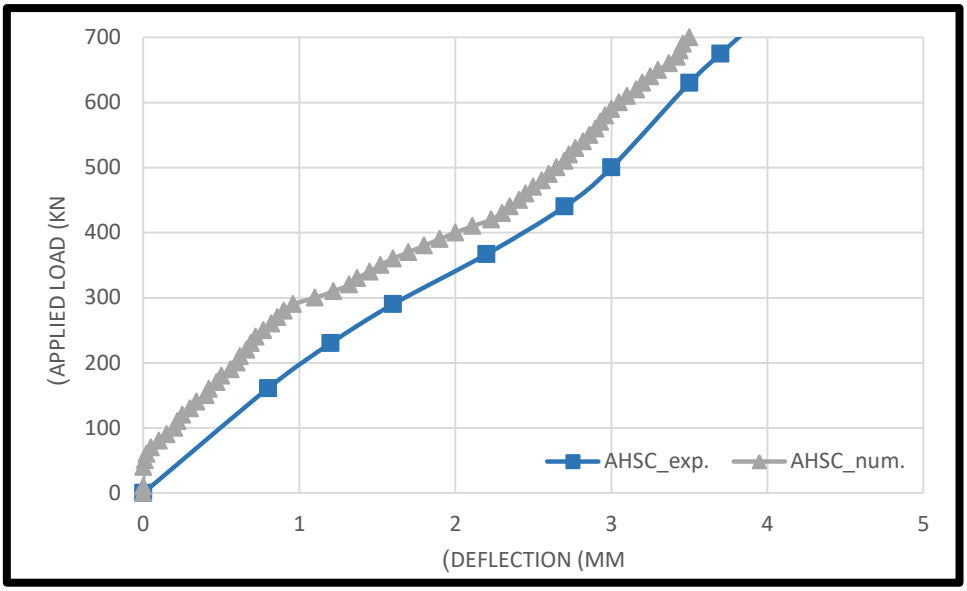

Figure 5. 17 Experimental and Numerical Load-Deflection Curves of AHSC Pier

Specimen No.9 (TCFRP)

TCFRP pier model exhibits ultimate load and deflection bigger than experimental result by (3.74% and 14.89%) respectively.

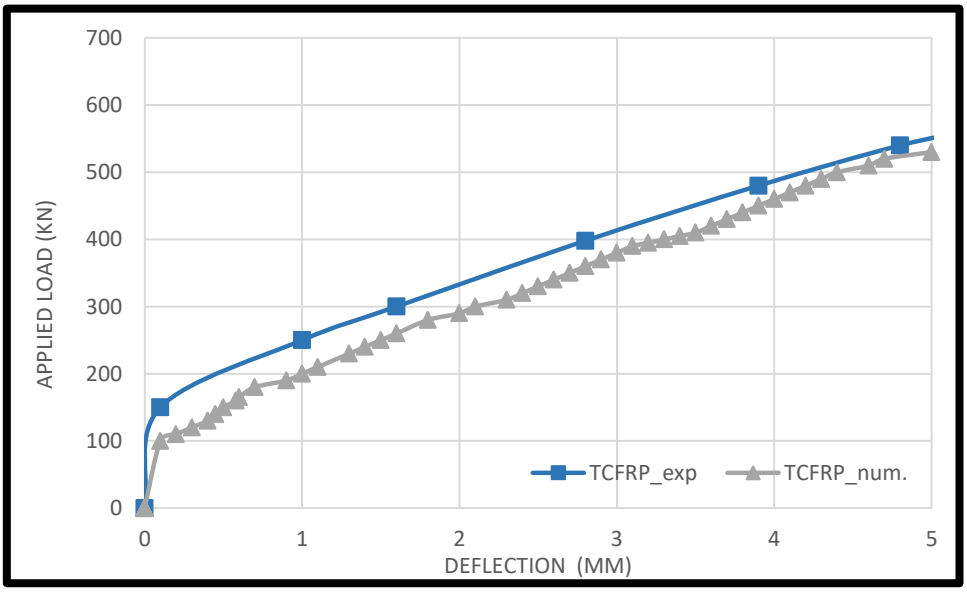

Figure 5. 18 Experimental and Numerical Load-Deflection Curves of TCFRP Pier Model

Specimen No.10 (T1CFRP)

T1CFRP pier model was represented in the ANSYS program to simulate its behaviour. The result shows that the ultimate load and deflection were bigger than experimental by (5.09 % and 13.77%) respectively. Figure (5.19) show the comparison between numerical and experimental result in term of load-deflection relationship.

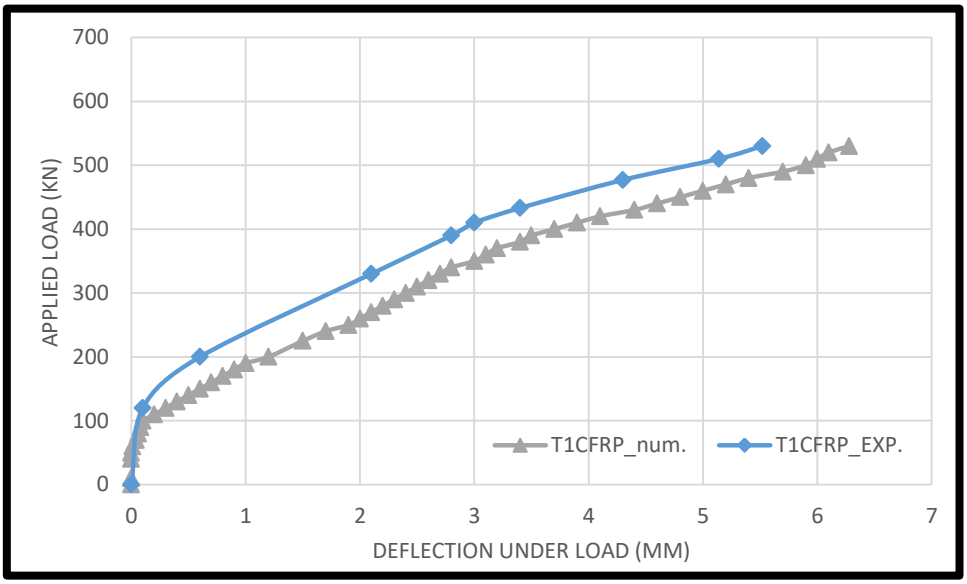

Figure 5. 19 Experimental and Numerical Load-Deflection Curves of T1CFRP Pier Model

Specimen No.11 (TGFRP)

TGFRP pier model reached 457 kN at ultimate load at the numerical analysis that lower than experimental result by (6.72%) with deflection of 8.46 mm that was bigger than experimental result by (11.9%) as shown in Figure (5.20).

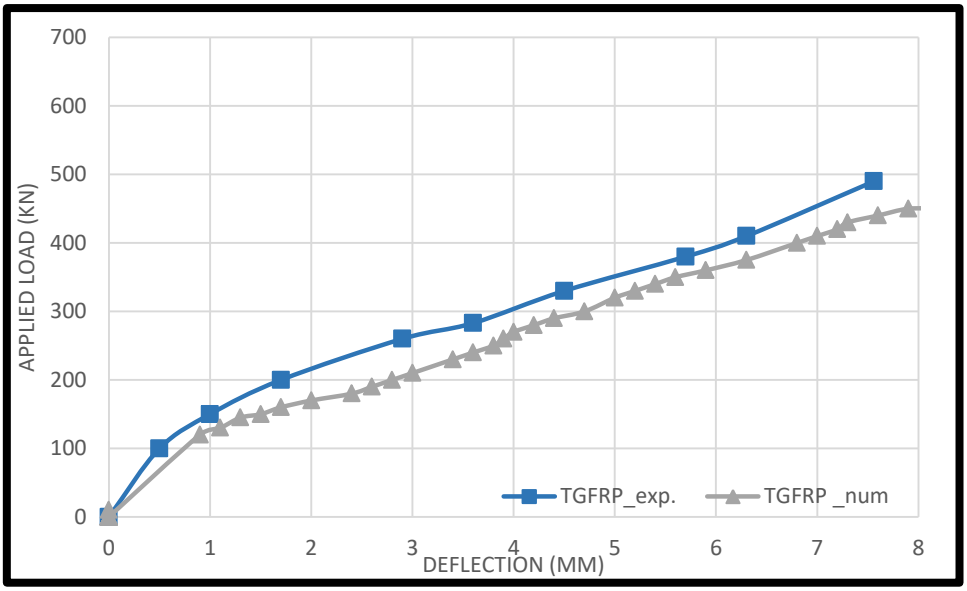

Figure 5. 20 Experimental and Numerical Load-Deflection Curves of TGFRP Pier Model

Specimen No.12(T1GFRP)

The ultimate load for T1GFRP pier model decreased by (6.37%), while the deflection was higher than experimental by (5.91%). Figure (5.21) show the comparison between numerical and experimental result in term of load-deflection relationship.

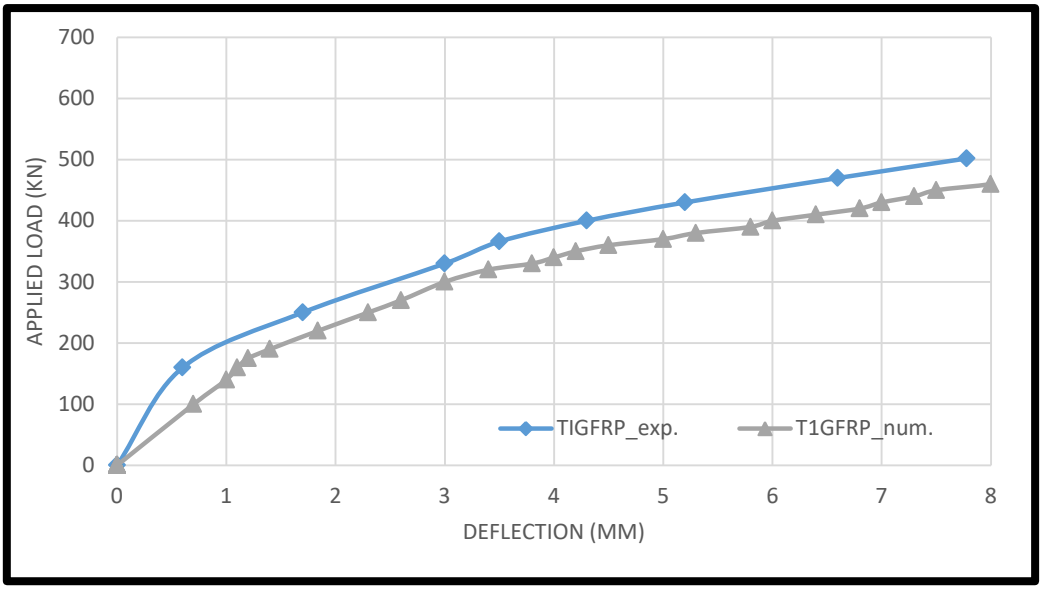

Figure 5. 21 Experimental and Numerical Load-Deflection Curves of T1GFRP Pier Model

Specimen No.13 (SGFRP)

The ultimate load for SGFRP pier model as well as the deflection increased by (7.92% and 3.88%) bigger than experimental result respectively. Figure (5.22) show the comparison between numerical and experimental result in term of load-deflection relationship.

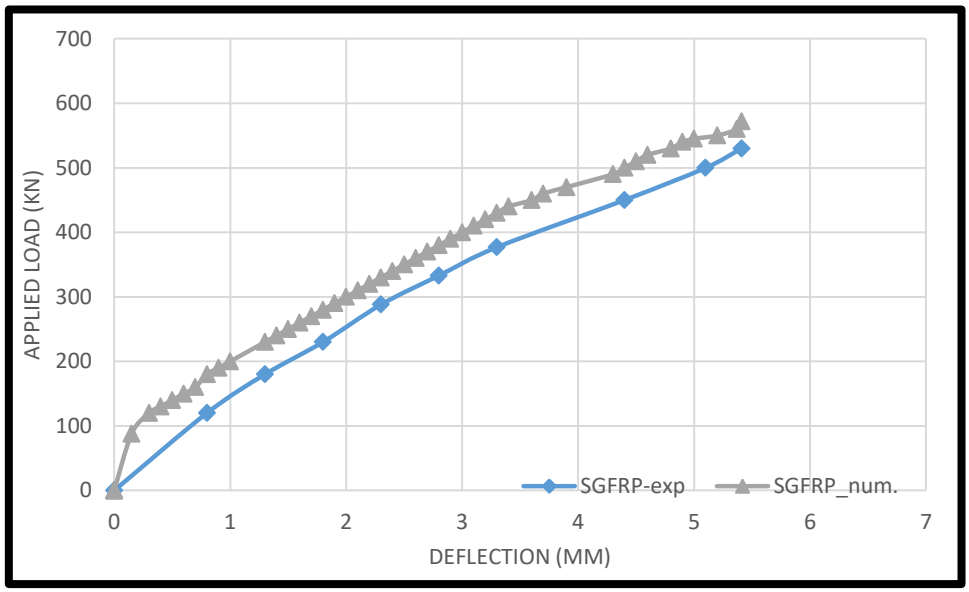

Figure 5. 22 Experimental and Numerical Load-Deflection Curves of SGFRP Pier Model

5.5.2 Cracks Propagation

One of the best characteristics of the ANSYS program gives the deflected shape at every step of the load increments, and the ability to provide the deflection at each node. Also, the ANSYS program has the ability to predict the crack pattern at any increment of loading. The red circles represent the first crack while the circles in green and blue represent the second and third cracks respectively. Figures (5.23) to (5.34) show the types of cracks formed in the pier models at the failure stage for all piers.

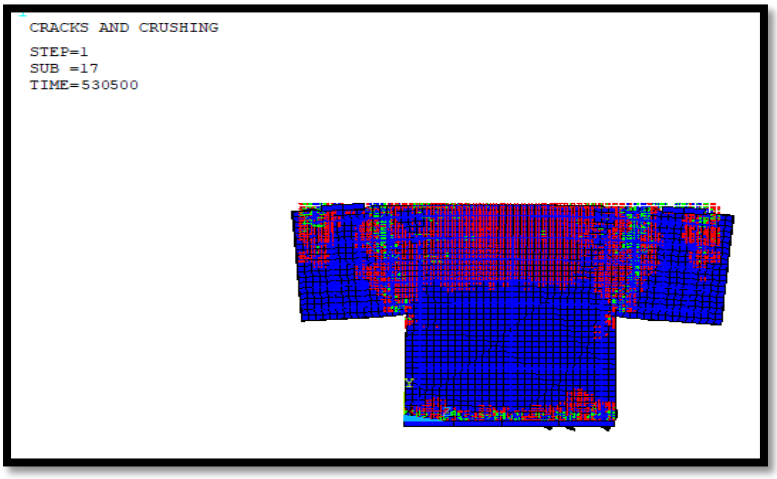

Figure 5. 23 Crack Patterns at the Ultimate Load of NC Pier Model

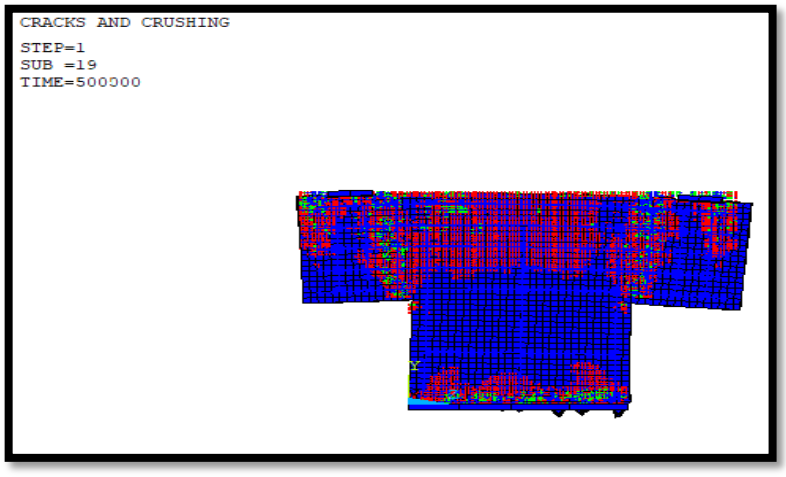

Figure 5. 24 Crack Patterns at the Ultimate Load of GC Pier Model

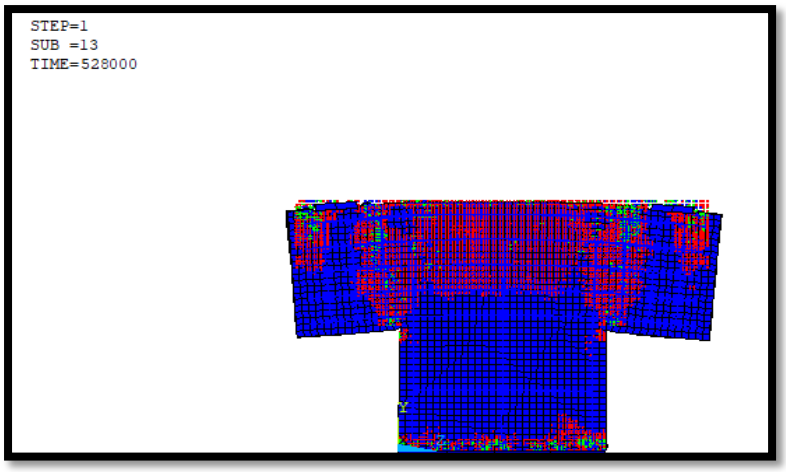

Figure 5. 25 Crack Patterns at the Ultimate Load of TRSF Pier Model

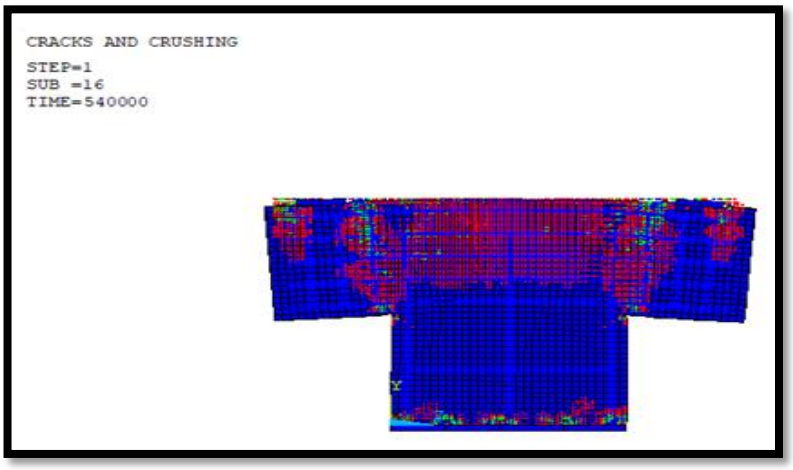

Figure 5. 26 Crack Patterns at the Ultimate Load of HRSF Pier Model

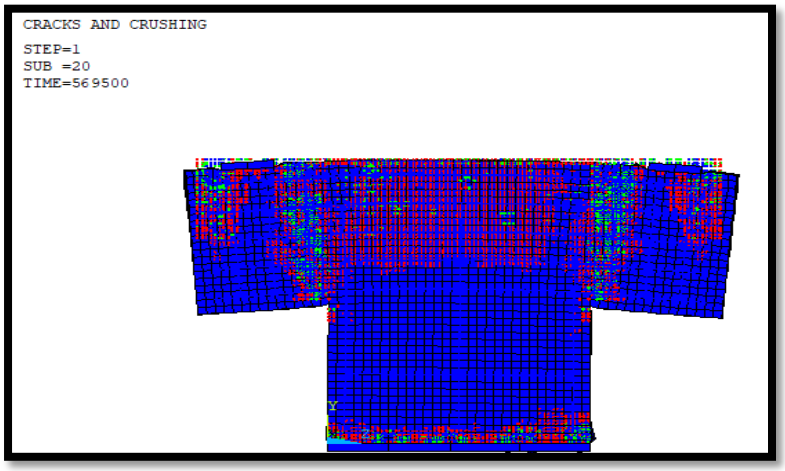

Figure 5. 27 Crack Patterns at the Ultimate Load of ARSF Pier Model

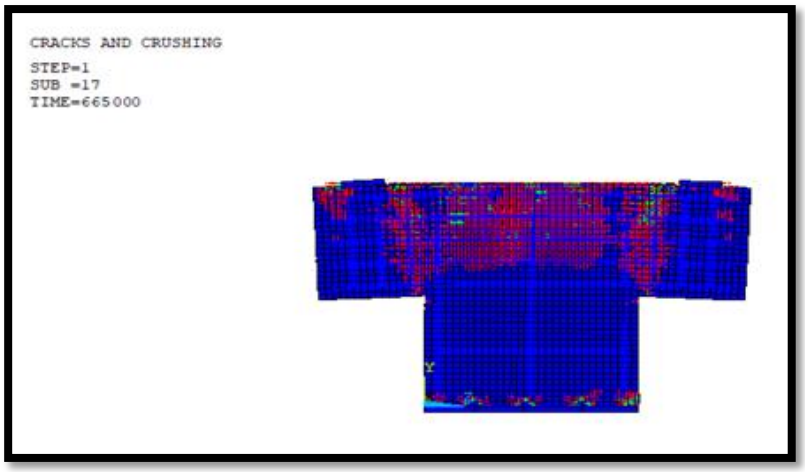

Figure 5. 28 Crack Patterns at the Ultimate Load of THSC Pier Model

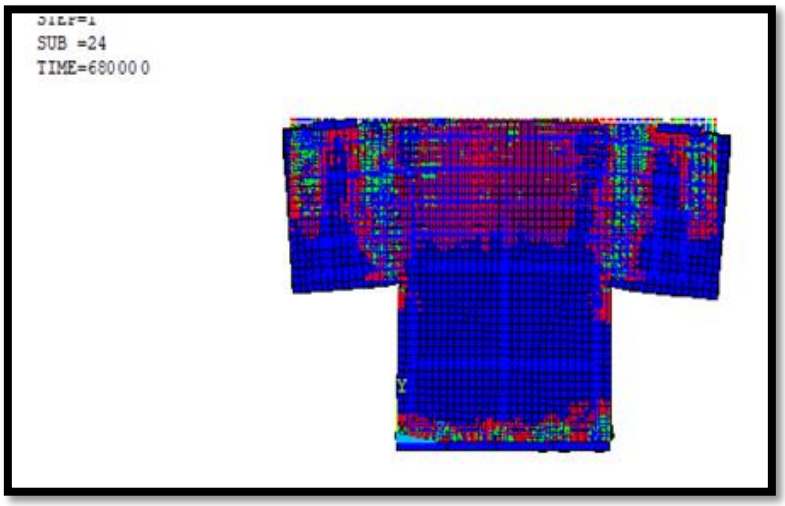

Figure 5. 29 Crack Patterns at the Ultimate Load of HHSC Pier Model

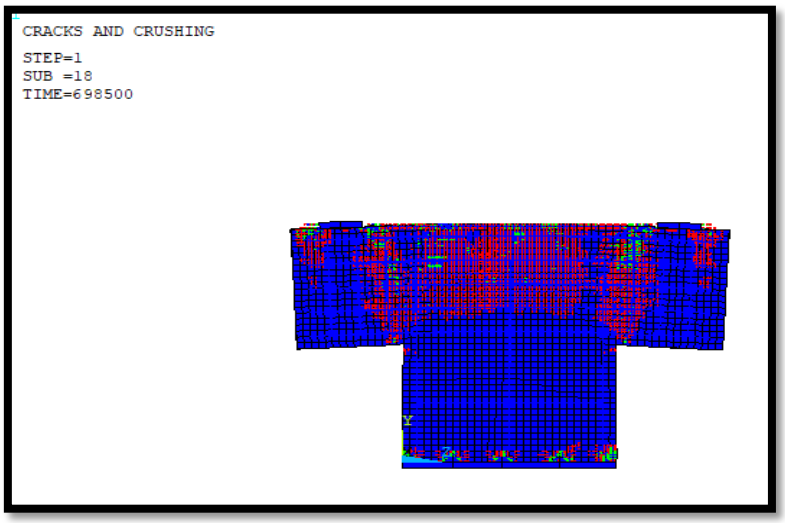

Figure 5. 30 Crack Patterns at the Ultimate Load of AHSC Pier Model

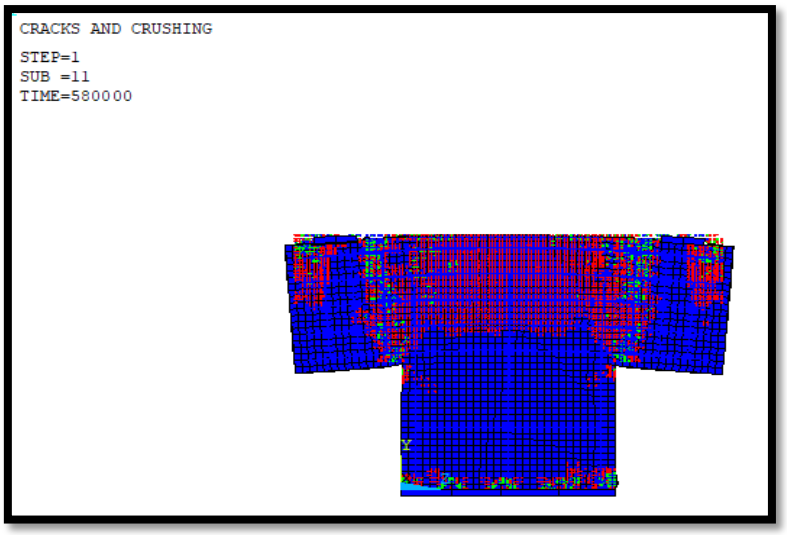

Figure 5. 31 Crack Patterns at the Ultimate Load of TCFRP Pier Model

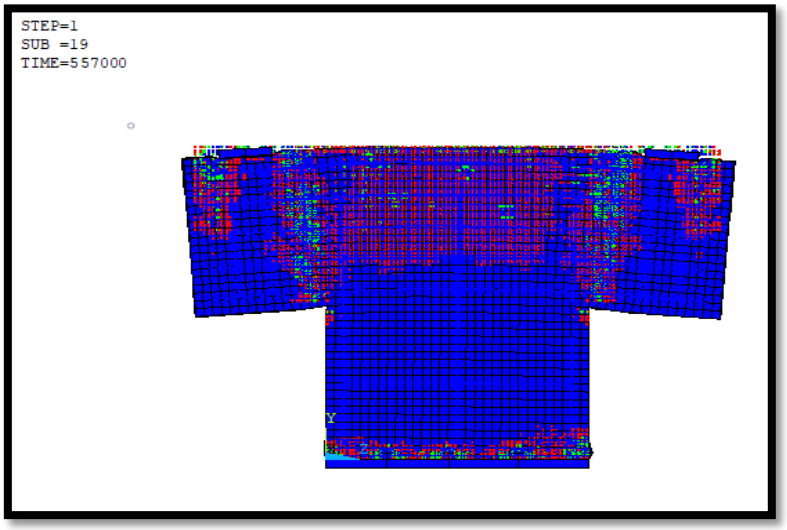

Figure 5. 32 Crack Patterns at the Ultimate Load of T1CFRP Pier Model

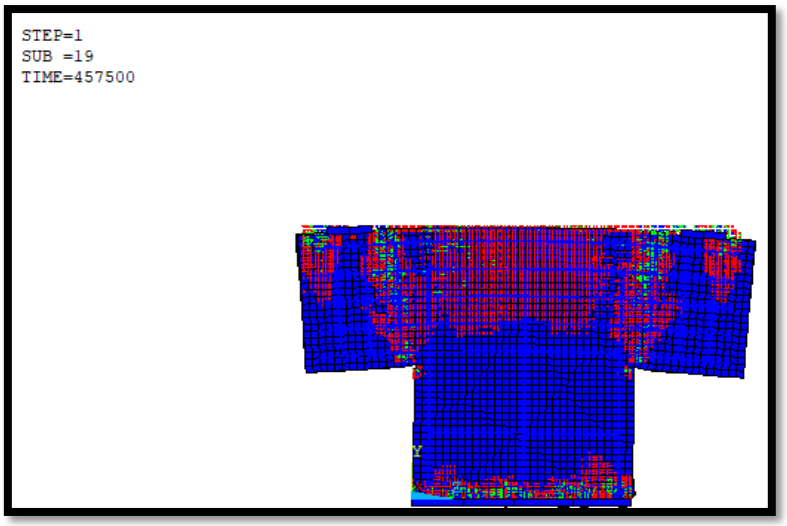

Figure 5. 33 Crack Patterns at the Ultimate Load of TGFRP Pier Model

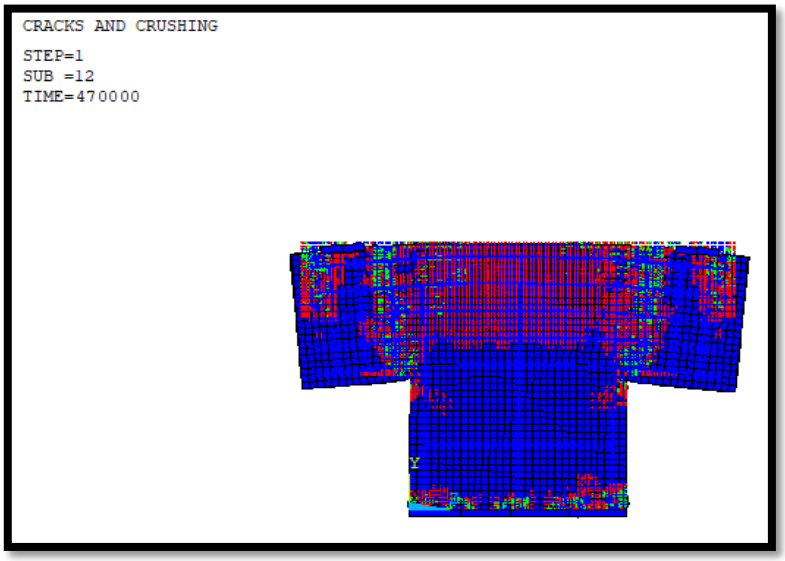

Figure 5. 34 Crack Patterns at the Ultimate Load of T1GFRP Pier Model

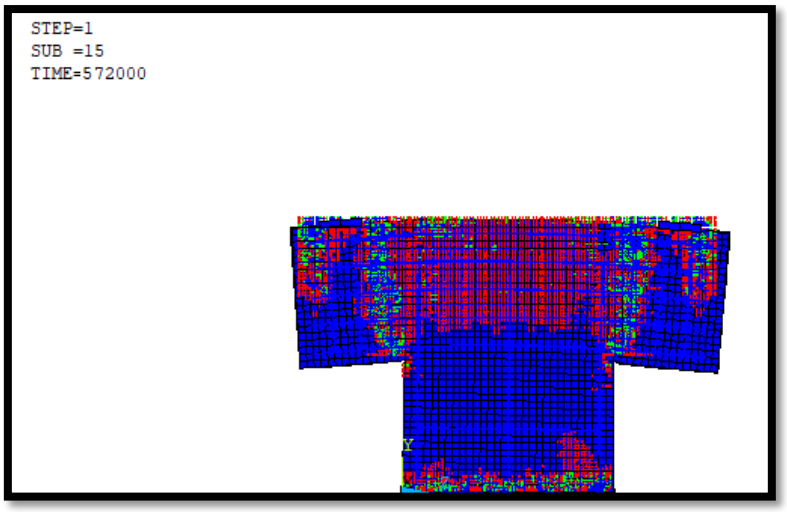

Figure 5. 35 Crack Patterns at the Ultimate Load of SGFRP Pier Model

Chapter Six

Chapter Six
Conclusions and Recommendations

6.1 Conclusions

Based on the experimental and numerical results of the reinforced concrete piers, several points have been concluded as follows:

1. The ultimate strength of the pier that is cast by using GC was less than that for normal pier NC (reference) by 2.4%. This small difference means that green concrete is effective for structural purpose use.

2. The deflection under the ultimate load of GC pier was 18.5% higher than those of NC pier.

3. It was observed that using recycled steel fiber with GC mix at the pier cap region led to an increase in the ultimate load by 4.76% against a decrease in the deflection by 29.58%.

4. Adding recycled steel fiber to pier cap and half of the pier column led to increasing the ultimate load by 4.76% and 6.1% and decreasing the deflection by 29.58 % and 30.6% when compared with GC pier. There was an increase of 1.27% in the ultimate load and a decrease of 1.45% in the deflection compared with the case of adding recycled steel fiber at pier cap only. Indeed, using recycled steel fiber in all pier increased the ultimate load by 8.95% and decreased the deflection by 32.52% when compared with GC results.

5. The use of high strength concrete (HSC) led to increasing the ultimate load by 29.7% when used at pier cap only (THSC), and 33% when used at pier cap and half of column (HHSC). For use HSC mix for all pier (AHSC), the ultimate load increased by 36.7% and the deflection decreased by 42.89%, 43.92, and 50.06% for (THSC, HHSC, and AHSC) respectively.

6. Use CFRP bars in the two top layers' reinforcement of pier led to improving the ultimate load by 4.19% and decreasing the deflection by 29.32%. However, using of CFRP at all layers of pier cap reinforcement increased the ultimate load by 6.86% and decreased the deflection by 32.9% as compared with the GC pier.

7. It was noticed that by replacement the steel reinforcement by GFRP bars at the top two layers and all layers of the pier cap decreased the ultimate load and increased the deflection by about 4.38%, 6.69% and 0.38%, 3.2% respectively as compared with GC pier.

8. The obtained results indicated that using GFRP stirrups reinforcement at the pier cap led to improving the specimen characteristics in term of ultimate load and deflection.

9. The ratio of numerical to the experimental ultimate strengths of pier specimens was 1.62 as an average value, where this ratio indicates an acceptable convergence between the experimental and numerical results for this study.

10. It was observed that the ratio of deflection of the numerical to the experimental results of specimens was 1.4 as an average value, where this value present that there is a slight difference between the experimental and numerical results.

11. Generally, the increase in the ultimate current capacity of all pier model is conjugated by an increase in the first crack load and a decrease in the crack width corresponding to the applied load.

6.2 Recommendations for Future Researches

For the purpose of more familiarity with the subject of the concrete pier and to take additional cases that have not been taken in the experimental

work and numerical application, the following recommendations are suggested:

1. Experimental investigation of the behavior of green concrete piers using broken brick instead of coarse aggregate in the mixture.

2. Experimental study on the green concrete in the casting of the rest of the structural members such as slabs and columns and testing the validity of such use.

3. The use of the remnants of the demolition of buildings complete, including bricks and concrete together to produce green concrete instead of pure concrete, so as to provide the remnants of construction more and the difficulty of obtaining the concrete of the demolition works independently and study its properties.

4. Extraction of scraps tires wire in a manner of drawing or any other method other than burning because the burn causes weakness in its properties.

5. Study the cost of production of green concrete to compare with natural concrete and high strength concrete.

6. Study the behavior of pier models under repeated load or impact load.

7. Investigate further parameters like the dimensions of pier cap and column and with different types of applied load like (dynamic, impact, or uniform load).

References

References

1) Abukersh, S. A. (2009) High quality recycled aggregate concrete. Edinburgh Napier University, UK.
2) American Association of State Highway and Transportation Officials (AASHTO LRFD Bridge Design), 2010, Abutments, Piers, and Walls, Design Specifications, Chapter 11..
3) Amorim, P., De Brito, J. and Evangelista, L. (2012) 'Concrete made with coarse concrete aggregate: Influence of curing on durability', ACI Materials Journal, 109(2), pp. 195–204.
4) Anderson, K. W. and Uhlmeyer, J. S. (2009) 'Use of Recycled Concrete Aggregate in PCCP : Literature Search', (June).
5) ASTM A615/A615M-15a, "Standard Specification for Deformed and Plain Billet-Steel Bars for Concrete Reinforcement," ASTM Int., 2015.
6) ASTM C39/C39M-05, "Standard Test Method for Compressive Strength of Cylindrical Concrete Specimens," ASTM Int., p. 8, 2004.
7) ASTM C496/C496M-04, "Standard Test Method for Splitting Tensile Strength of Cylindrical Concrete Specimens", Vol. 04.02, 2004, 5p.
8) ASTM/C143C143M 2005. Standard Test Method for Slump of Hydraulic-Cement Concrete. American Society for Testing and Materials.
9) A. Balsamo, G. P. Ludovico, A. Prota, G. Manfredi, and E.Cosenza, Composites for Structural Strengthening, Wiley Encyclopedia of Composites, 2nd edition, 2012.
10) Brothers, H. (2010) Carbon Fiber Reinforced Polymer (CFRP) Rebar Aslan 200/201.
11) Bambang Suhendro,2014,"Toward green concrete for better sustainable environment", 2nd International Conference on Sustainable Civil Engineering Structures and Construction Materials .
12) Buck, A. D. (1977) 'Recycled concrete as a source of aggregate', in Journal Proceedings, pp. 212–219.
13) Carolin, A. (2003) Carbon Fibre Reinforced Polymers for Strengthening of Structural Elements, Thesis. Luleå University of Technology.

14) Carrasquillo, R. L., Nilson, A. H. and Slate, F. O. (1981) 'Properties of High Strength Concrete Subjected to Short-Term Loads', in Journal Proceedings, pp. 171–178.
15) Chen, Wai-Fah, Duan, L. (2000) Bridge Engineering Handbook. Edited by L. D. Lian, Wai-Fah Chen. CRC Press LLC.
16) Chen, E. W., Duan, L. and Wang, J. (2000) '"Piers and Columns."', in Bridge Engineering Handbook. CRC Press LLC.
17) Denio, R., Yura, J. and Kreger, M. (1995) 'Behavior of reinforced concrete pier caps under concentrated bearing loads', Center for Transportation Research, University of Texas, 7(2).
18) Dewar, J. D. (1964) The indirect tensile strength of concrete of high compressive strength. Cement and Concrete Association.
19) Dhir, R. K., Henderson, N. A. and Limbachiya, M. C. (1998) Sustainable construction: Use of recycled concrete aggregate. Thomas Telford. Elnashai AS, Borzi B, Vlachos S. Deformation Based Vulnerability Functions for RC Bridges. Struc Engg Mech 2004;17(2):215-244.
20) Ferguson, P. M. (1964) Design Criteria for Overhanging Ends of Bent Caps - Bond and Shear. Univ., Center for Highway Research.
21) Francisco. D. B.(2015), "Comparison of Post-Tensioned Cast in Place Concrete and Steel-Concrete Composit Bent Caps"MSc. Thesis, University of TEXAS .
22) Fu, G. (2013) Bridge Design LRFD and LRFR. John Wiley & Sons, Inc.
23) Garber, S. et al. (2011) A Technology Deployment Plan for the Use of Recycled Concrete Aggregates in Concrete Paving Mixtures.
24) Gonzalez, G. and Moo-Young, H. K. (2004) 'Transportation Applications Of Recycled Concrete Aggregate FHWA State of the Practice National Iraqi Specification, No. 5/1984, "Portland Cement".
25) Iraqi Specification, No. 45/1984, "Aggregate from Natural Sources for Concrete and Construction".Review', (September), p. 47.
26) Lee, and Tae Hyung.(2016), Analytical Evaluation of Reinforced Concrete Pier and Cast-in-Steel-Shell Pile Connection Behavior considering Steel-Concrete Interface, Advances in Materials Science and Engineering,pp.14

27) Katz, A. (2004) ‘Treatments for the Improvement of Recycled Aggregate’, Journal of Materials in Civil Engineering, 16(6), pp. 597–603.
28) Kim, H. (2009) Crushed Returned Concrete Aggregate in New Concrete: Characterization, Performance, Modeling, Specification, and Application, Statewide Agricultural Land Use Baseline 2015. Maryland, College Park.
29) LI Juan, Zhao Xiang , WANG Haoqing, and CHENG Junlong, "Single Pier Bridge Lateral Stability Analysis in the Dynamic Load Conditions" ICTE 2013 © ASCE .
30) Limbachiya, M. C., Leelawat, T. and Dhir, R. K. (2000) ‘Use of recycled concrete aggregate in high-strength concrete’, Materials and Structures, 33(9), pp. 574–580.
31) Limbachiya, M., Meddah, M. S. and Ouchagour, Y. (2012) ‘Use of recycled concrete aggregate in fly-ash concrete’, Construction and Building Materials. Elsevier Ltd, 27(1), pp. 439–449.
32) MacGregor, J. . (1997) Reinforced Concrete: Mechanics & Design. 3 ed. Prentice Hall.
33) Milde, E. et al. (2005) Retrofitting Shear Cracks in Reinforced Concrete Pier Caps Using Carbon Fiber Reinforced Polymers, MinnDOT Final Report 2005-13.
34) Mirza, S. A. and Brant, W. (2009) ‘Chapter 5: Footing Design’, ACI Design Handbook, pp. 189–204.
35) Mjelde, D. G. (2013) Evaluation Of Recycled Concrete For Use As Aggregates In New Concrete Pavements. Washington State University.
36) Mörsch, E. (1909) ‘Concrete-Steel Construction,(Der Eisenbetonbau), English translation of the 3rd German edition’. McGraw-Hill Book Co., New York.
37) M. N. S. Hadi, “Behaviour of FRP strengthened concrete columnsunder eccentric compression loading,” Composite Structures,vol. 77, no. 1, pp. 92–96, 2007.
38) Naser, A. F. and Zonglin, W. (2011) ‘Damage inspection and performance evaluation of Jilin highway double-curved arch concrete bridge in China’, Structural Engineering and Mechanics. Techno-Press, 39(4), pp. 521–539.

39) Nitivattananon, V. and Borongan, G. (2007) '**Construction and Demolition Waste Management Current Practices in Asia**', Proceedings of the International Conference on Sustainable Solid Waste Management, 5-7 September, Chennai, India, (October), pp. 97–104.
40) Obla, K.H. (2009). "**What is Green Concrete** ?". The Indian Concrete Journal, April, 26-28.
41) Rao, Mc., Bhattacharyya, S. K. and Barai, S. V (2010) '**Influence of recycled aggregate on mechanical properties of concrete**', in 5th Civil Engineering Conference in the Asian Region and Australasian Structural Engineering Conference 2010, The Engineers Australia, p. 749.
42) Rinaldi, V. (2015),"**Design of GFRP Reinforcement for Concrete Bridge Structural Components**", MSc. Thesis, University of Miami, Florida.
43) Sami AI-Souf (1990),"**The Response of Reinforced Concrete**". MSc. Thesis, Departmellt of Civil Engineering and Applied mechanics University of McGill, Canada .
44) Schlaich, J., Schafer, K. and Jennewein, M. (1987) '**Toward a Consistent Design of Structural Concrete**', PCI Journal, 32(3), pp. 74–150.
45) Shayan, A. and Xu, A. (2003) '**Performance and properties of structural concrete made with recycled concrete aggregate**', Materials Journal, 100(5), pp. 371–380.
46) Smith, D. a. and Hendy, C. R. (2009) '**Design of the Dubai Metro light rail viaducts—substructure**', Proceedings of the ICE - Bridge Engineering, 162(2), pp. 63–74.
47) Standard, B. (2006) '**BS 8500-1 2006. Concrete-Complementary British Standard to BS EN 206-1. Part 1: Method of Specifying and Guidance for the Specifier'**. British Standards Institution London.
48) Tu, T. Y., Chen, Y. Y. and Hwang, C. L. (2006) '**Properties of HPC with recycled aggregates**', Cement and Concrete Research, 36(5), pp. 943–950.
49) Wen SH, Chung DDL.,"**A comparative study of steel fiber cement and carbon fiber cement as piezoresistive strain sensors**". Adv. Cem. Res 2003;15(3):119–28

50) Yong, P. C. and Teo, D. C. (2009) **'Utilisation of Recycled Aggregate as Coarse Aggregate in Concrete**', UNIMAS E-Journal of Civil Engineering, 1(1), pp. 1–6.

المستخلص

تتسبب التنمية الصناعية السريعة في حدوث مشكلات خطيرة في جميع أنحاء العالم ، كمشكلة استنفاد الموارد الطبيعية وإنشاء كمية هائلة من النفايات الناتجة عن أنشطة البناء والهدم. احدى الطرق للحد من هذه المشكلة ، هو استخدام الركام المعاد تدويره من الخرسانة القديمة (RCA) في إنتاج الخرسانة. الدراسة الحالية تتضمن جزءا عمليا واخر نظريا تطبيقيا لدراسة سلوك الجسور الخرسانية. تضمن العمل التجريبي اختباراً لثلاثة عشر ركيزة من الخرسانة المسلحة بأستحدام انواع مختلفة من الخلطات الخرسانية والتسليح. جميع النماذج لها نفس الأبعاد (عرض 200 مم ، وارتفاع 400 مم ، وطول إجمالي 600 مم) و أبعاد العمود (200 × 300 ملم) و 200 ملم للعمق. تضمنت المتغيرات للجانب العملي كلا من : نوع الخلطة الخرسانية ، باستخدام الركام الخرساني المعاد تدويره بنسة استبدال 50 ٪ بدلا من الخرسانة العادية ، واستخدام الالياف الفولاذية المعاد تدويرها بنسبة حجمية 2 ٪ التي اضيفت الى مناطق مختلفة من النموذج الخرساني وكما يلي : منطقة رأس الركيزه الجزء العلوي منها فقط ، رأس الركيزة مع نصف العمود ، وكل الركيزة .وكذلك تم استخدام مزيج الخرسانة عالية القوة في منطقة رأس الركيزة ، ورأس الركيزه مع نصف العمود ، وكذلك كل الركيزه. تضمنت الدراسة استخدام قضبان الكاربون والزجاج البوليميرية (CFRP bar) و (GFRP bar) لتسليح راس الركيزه فقط . تم تسليط الحمل بواسطة نقطتين ، وتم قياس الهطول تحت الحمل واخذ متوسط القيمة. أظهرت النتائج أن استخدام الخرسانة الخضراء بنسبة استبدال 50٪ يقلل من الحمل النهائي بنسبة 2.41٪ ويزيد الهطول بنسبة 18.5٪. يمكن زيادة القدرة الاستيعابية النهائية للركيزه التي استخدمت فيها الخرسانة الخضراء .لذلك أدى إضافة الألياف الفولاذية المعاد تدويرها إلى زيادة في الحمل النهائي وانخفاض الهطول وقد وجد أيضًا أن استخدام خليط الخرسانة عالي القوة في صب الركائز أدى إلى تحسين الحمل النهائي بنسبة تصل الى 36.76٪ للعينات ، مع انخفاض الهطول بنسبة قصوى مقارنة مع الركيزة التي استخدمت فيها الخرسانة الخضراء فقط.

تم تحسين الحمل النهائي أيضًا عن طريق تغيير نوع التسليح بأستخدام قضبان الكاربون البولميرية في الطبقة الاولى والثانية من تسليح رأس الركيزه وكذلك كل الطبقات أدى إلى زيادة الحمل النهائي بنسبة تصل 6.86٪ ، وانخفاض في الهطول مقارنة مع الركيزة التي استخدمت التسليح الفولاذي العادي .كما تم استخدام الياف الزجاج البوليميرية بنفس الترتيب الذي تم استخدامة لألياف الكاربون البوليميرية .حيث لوحظ انحفاض الحمل النهائي وازدياد الهطول مقارنة مع الركيزة GC .ايضا تم استخدام الياف الزجاج البوليميرية GFRP بقطر 6 مم في

تسليح الاترية الخاصة بمنطقة رأس الركيزه فقط حيث أدى إلى زيادة في الحمل النهائي بنسبة 0.95٪ وتقليل الهطول بنسبة 30.73٪.

بأستخدام طريقة تحليل العناصر المحدودة ثلاثية الأبعاد تم دراسة سلوك الركائز الخرسانية المسلحة. وذلك باستخدام برنامج ANSYS (الإصدار 17.2) لهذا الغرض. حيث تم افتراض ان هنالك ترابط كامل بين الخرسانة وحديد التسليح .تم تمثيل الخرسانة في البرنامج بالعنصرSOLID65 ، اما بالنسبة لحديد التسليح وقضبان الكاربون والزجاج البوليميرية LINK180، في حين تم تمثيل الصفائح الحديدية التي يسلط عبرها الحمل وتلك الخاصة بالاسناد بالعنصر SOLID185 وقد أظهرت نتائج التطبيق العددي درجة مقبولة من التباين مع النتائج التجريبية ، حيث كان الفرق الأقصى بين النتائج العددية والتجريبية في الحمل النهائي والهطول (-21.12٪) و (- 18.27٪) على التوالي.

جمهورية العراق
وزارة التعليم العالي والبحث العلمي
جامعة كربـــــــــــــلاء
كلية الهندســـــــــــــــة
قسم الهندســـــــــة المدنيـــــــــــة

سلوك الركائز الخرسانية المسلحة باستخدام الخرسانة الخضراء وأنواع مختلفة من التسليح

رسالة

مقدمة الى قسم الهندسة المدنية في كلية الهندسة/ جامعة كربلاء
وهي جزء من متطلبات نيل درجة الماجستير
في علوم الهندسة المدنية / البنى التحتية

من قبل

هاجر احمد سلمان

(بكالوريوس هندسة مدنية 2013)

بأشراف

أ.م.د. علي حميد ناصر

م.د. وجدي شبر صاحب

2019 م

1440 هـ